3.4.4. Method of the Analysis

The stability of the dam embankment was checked by the Slice method using slip-circle analysis. No particular explanations of the method are given, as it is an established, conventional method.

3.5. Stability Analysis of the Dam

3.5.1. Stability Analysis of the Upstream Face Slope

The stability analysis of the upstream face slope of the main dam was made of the three modes of sliding. The first one is the sliding lines passing through the rockfill zone only. The second one is the sliding lines passing through the rockfill and filter zones. And, the third one is the sliding lines passing through the rockfill, filter and core zones.

The analysis was made of the following seven cases under various loading conditions:

Case	Dam Face	Water Level at	Earthquake Effect (Kh = 0.15g)	
1	Upstream	HWL	Without	
2	Upstream	HWL		With
3	Upstream	LWL		With
4	Upstream	Abrupt drawdown from HWL to LWL	Without	
5	Upstream	Abrupt drawdown from HWL to LWL		With
6	Downstream	HWL	Without	
7	Downstream	HWL		With

(1) Stability Against Sliding Lines Passing Through Rockfill Zone Only

The loading conditions in Cases 1 through 3 are enough to be checked for the stability analysis against sliding lines passing through the rockfill zone only. The analysis on Cases 4 and 5 would result in the same end as on Cases 1 and 3.

The result of the analysis is as summarized below:

Safety Factor Against Sliding Lines Passing through Rockfill Zone Only

Case	Calculated Safety Factor: Rockfill Material ϕ=43°	Calculated Safety Factor: Rockfill Material ϕ=45°	Required Safety Factor
1	1.31	1.40	1.2
2	0.74 (0.069)	0.80 (0.087)	1.0
3	0.96 (0.13)	1.03	1.0

Note: The parenthesized figure represents the seismic coefficient shown in g with the safety factor assumed to be 1.0.

The safety factor against sliding under the loading conditions in Cases 2 and 3 is smaller than the required one. Indicated in a solid line on Fig.3.5.1 is the sliding line with the least safety factor.

Supposing there occurred an earthquake to cause sliding of front rock materials to the depth of the solid line as shown, the safety factor of such scooped slope against further sliding under static condition would be as given below:

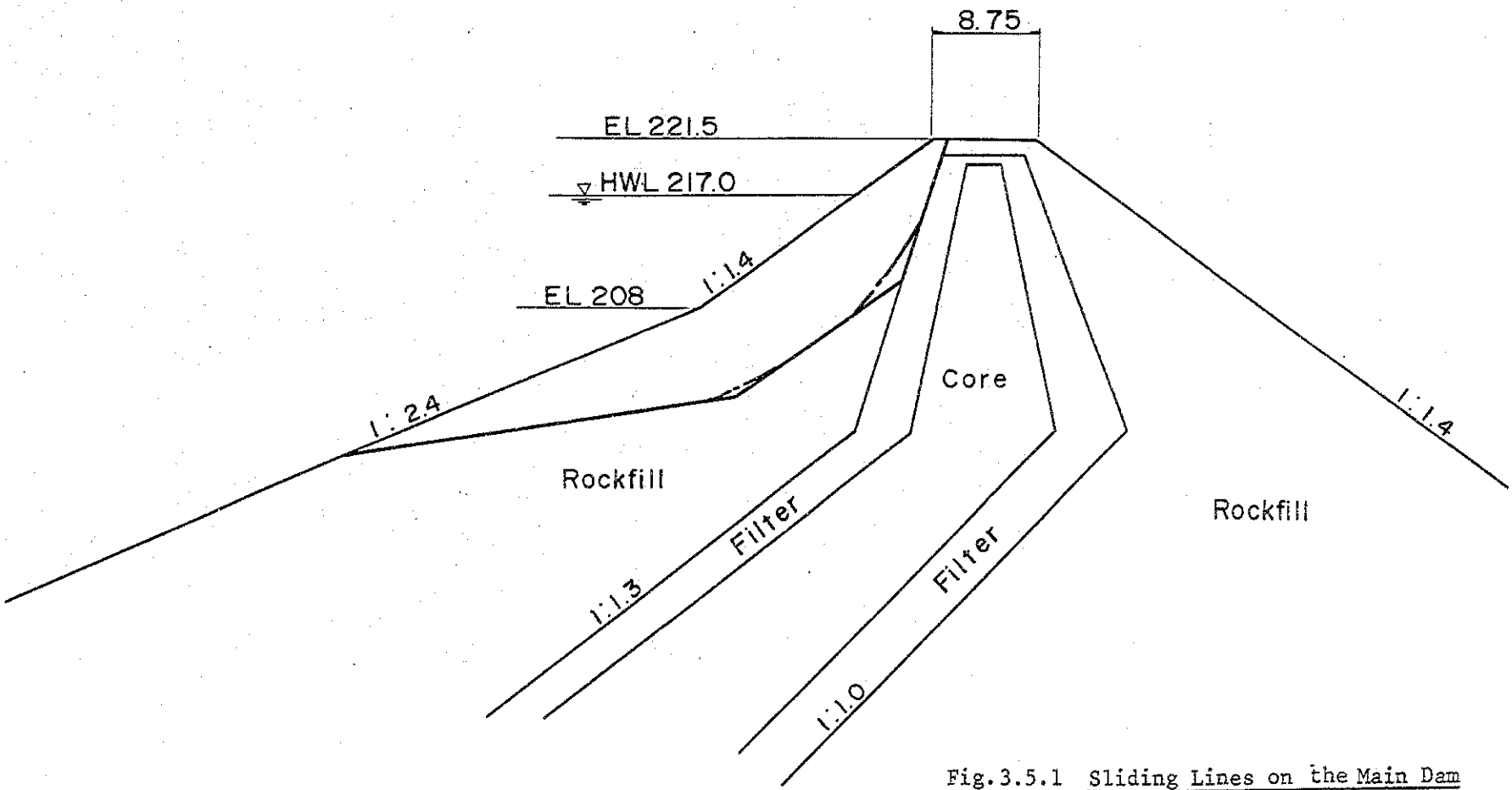

Fig.3.5.1 Sliding Lines on the Main Dam Upstream Face Slope, Passing Through Rockfill Zone

Case	Rockfill Materials ϕ=43°	ϕ=45°
1	-	-
2	1.00	1.00
3	1.31	-

As shown in the table, the dam with the upstream face slope being scooped by the earthquake would still be stable under static condition, and no catastrophic damage is likely to occur on the dam.

(2) Stability Against Sliding Lines Passing Through Rockfill and Filter Zones

Similarly to the foregoing subsection, the loading conditions in Cases 1 through 3 are enough to be checked for the stability analysis against sliding lines passing through the rockfill and filter zones. The result of the analysis is as summarized below:

Safety Factor Against Sliding Lines Passing Through Rockfill and Filter Zones
(Assuming that ϕ value of filter materials would be 35°)

Case	Calculated Safety Factor: Against Large Scale Sliding — Rockfill ϕ=43°	Against Large Scale Sliding — Rockfill ϕ=45°	Against Small Scale Sliding — Rockfill ϕ=43°	Against Small Scale Sliding — Rockfill ϕ=45°	Required Safety Factor
1	2.163	2.266	1.364	1.455	1.2
2	1.156	1.313	0.860 (0.10)	0.919 (0.12)	1.0
3	1.118	1.172	1.065	1.140	1.0

Note: The parenthesized figure represents the seismic coefficient shown in g with the safety factor assumed to be 1.0.

The large scale sliding as referred to herein represents the one that may produce a serious effect on the embankment (with a depth of some 10 m), and the small scale sliding is the one that affects a layer close to the surface and may have no serious effect on the dam stability.

As is seen in the table, there could occur no such large scale sliding that may affect the dam stability under static condition, but a local sliding may occur if an earthquake with Kh of 0.15 g happens when the reservoir water level is at HWL.

Supposing, unfortunately, there occurred an earthquake with Kh of 0.15 g and it caused embankment to slide as shown in Fig.3.5.2, the safety factor of such scooped slope against further sliding under static condition would be as shown below:

Safety Factor of the Scooped Slope Against Further Sliding

	Against Large Scale Sliding		Against Small Scale Sliding	
Case	Rockfill Material ϕ=43°	Rockfill Material ϕ=45°	Rockfill Material ϕ43°	Rockfill Material ϕ=45°
2	-	-	1.00	1.00

As is seen, the dam with the upstream face slope being scooped by a large Kh value earthquake would still be stable under static condition, and no catastrophic damage is likely to occur on the dam.

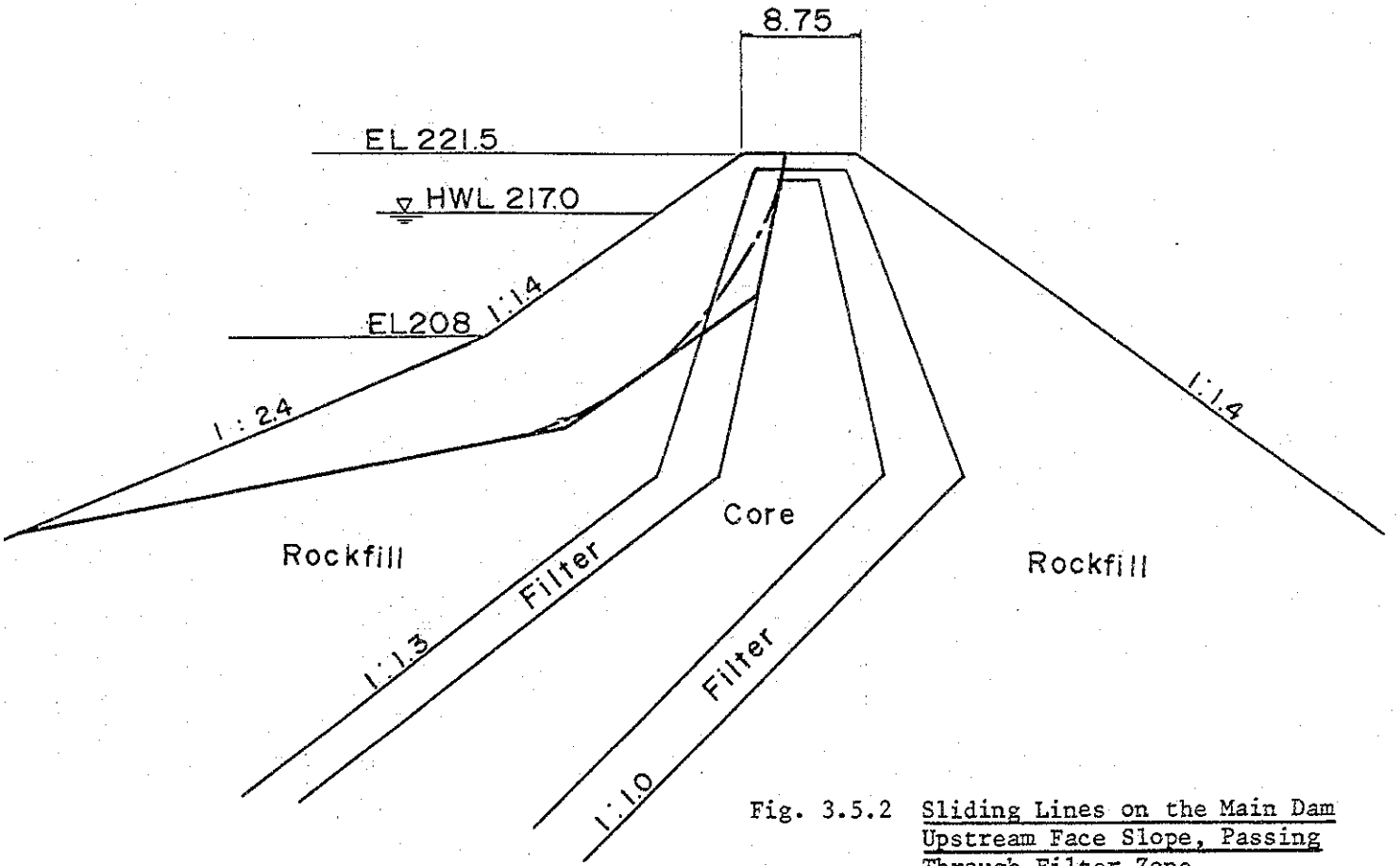

Fig. 3.5.2 Sliding Lines on the Main Dam Upstream Face Slope, Passing Through Filter Zone

(3) Stability Against Sliding Lines Passing Through Rockfill, Filter and Core Zones

The stability analysis against sliding lines passing through the core zone was made under the loading conditions in all five cases, because such sliding may cause pore pressures in the zone to act as an adverse effect on the dam stability. The result of the analysis is as shown below:

Cohesion of Core Materials Necessary to Keep the Required Safety Factor

Case	Rockfill Material ϕ=43° Core Material ϕ=20°	ϕ=25°	ϕ=30°	Rockfill Material ϕ=45° Core Material ϕ=20°	ϕ=25°	ϕ=30°
1	(1.49) 0	(1.69) 0	(1.90) 0	(1.54) 0	(1.74) 0	(1.95) 0
2	6.19	2.51	(1.03) 0	4.65	1.5	(1.06) 0
3	10.08	5.84	1.43	8.55	4.34	0.44
4	1.18	(1.29) 0	(1.45) 0	0.34	(1.33) 0	(1.49) 0
5	13.67	8.66	3.2	11.68	6.77	1.59

(Filter material ϕ = 35°)

The figures given in the table show the cohesion strength of core materials necessary to keep the required safety factor of the upstream face slope against sliding (1.2 under static condition and 1.0 under the loading conditions with the earthquake effect). The parenthesized figures show the safety factors, illustrating they are greater than the required safety factor even in case where the cohesion strength of core materials is zero.

Of the loading conditions for the stability analysis, Cases 4 and 5 (assuming an abrupt drawdown of the reservoir water level from HWL to LWL) are practically unlikely to occur, because of the considerably large surface area of the reservoir. The loading conditions were, therefore, classified into three groups as follows in summing up the result of the stability analysis:

Group I : Cases 1 through 3
Slope - Upstream face
Water Level - HWL or LWL

Group II : Cases 4 and 5
Slope - Upstream face
Water Level - Abrupt drawdown

Group III: Cases 6 and 7
Slope - Downstream face
Water Level - HWL

Plotted on Figs. 3.6.1 and 3.6.2 is the relation between the assumed internal friction angle (ϕ) of the core materials and the maximum value of cohesion (C) necessary to keep the required safety factor under various loading conditions of Groups I and II. In the Figures, ϕ values (°) are shown on the abscissa and C values (ton/m^2) on the ordinate.

Fig. 3.6.1 shows the relation in Cases 1 through 3 of Group I and Fig.3.6.2 shows the relation in Cases 4 and 5 of Group II.

Group III is to deal with the stability analysis of the downstream face slope. Since the core zone of the Angat dam is inclined to the upstream face, any sliding lines on the downstream face slope are unlikely to pass through the core zone, and, accordingly, the physical properties of the core zone have not directly to do with the safety factor against sliding.

On the Figures, C values of the assumed core materials are also plotted.

Fig. 3.6.1 Relation Between Ø and C Values of Core Materials Necessary to Keep the Required Safety Factor

(Loading Conditions - Group I)

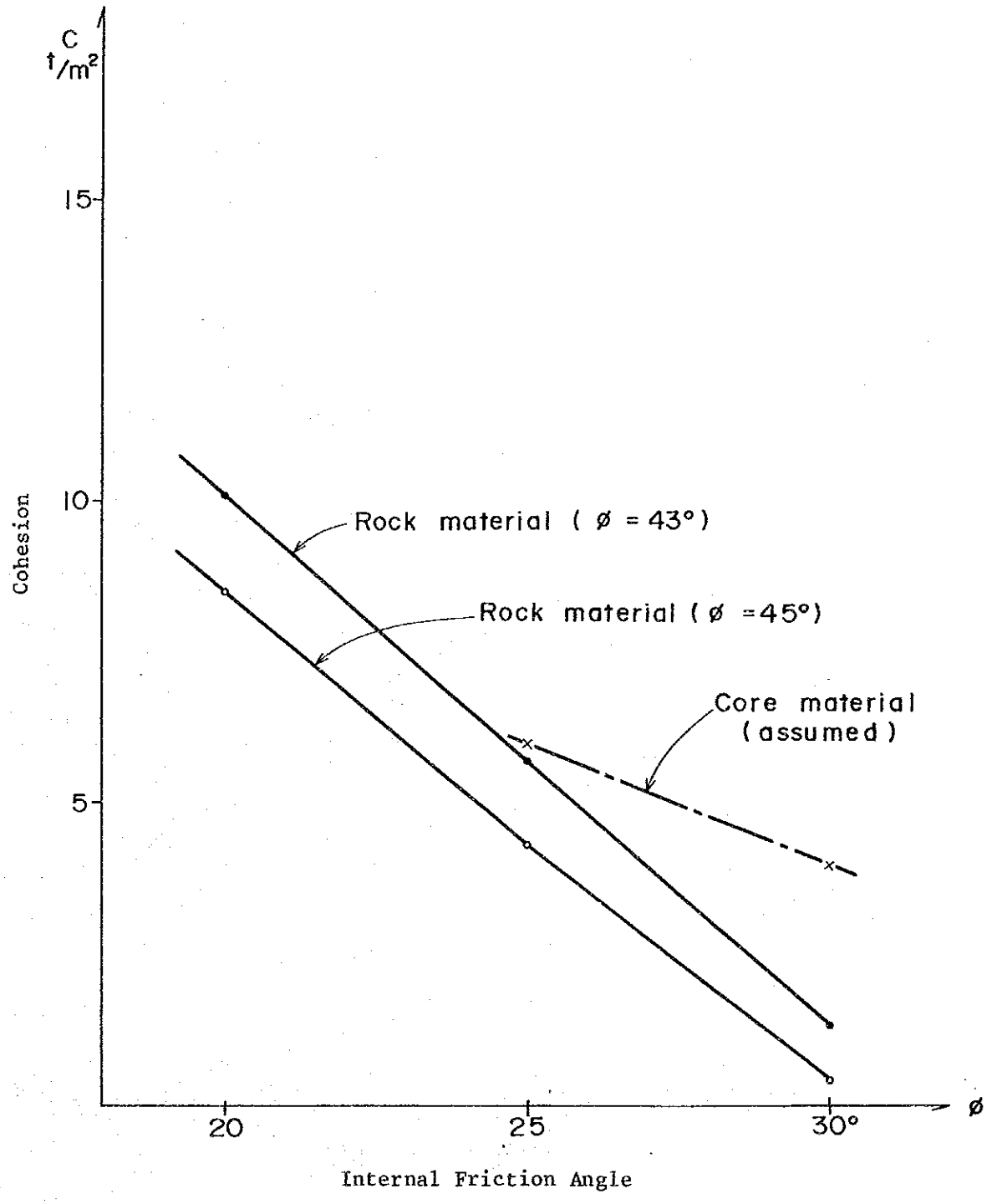

Fig. 3.6.2 Relation Between Ø and C Values of Core Materials Necessary to Keep the Required Safety Factor

(Loading Conditions - Group II)

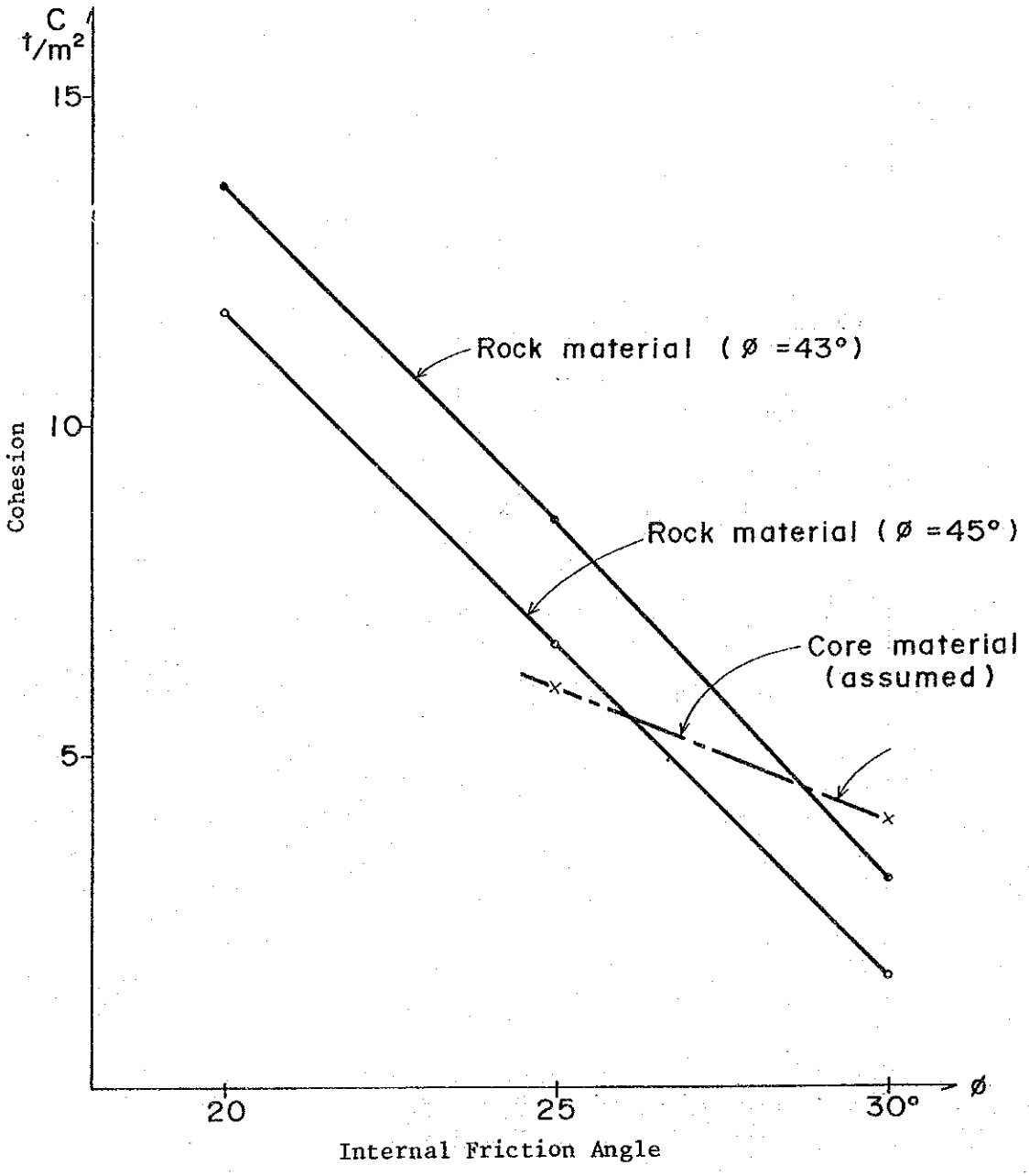

It is extremely difficult to identify the properties of the core materials in use for the Angat dam. A slight clue can be found from the report presented in November 1963 by N.V. Angeles, Material Engineer, NAPOCOR, to the World Power Conference and Congress on Large Dams, titled "Some Physical and Engineering Properties of Residual Soils in the Angat Dam Site", as it deals with the characteristics of overburdens of the dam foundation.

It is a matter of course that no such residual soils are used as the core materials for the Angat dam. The core materials must have been taken from the designated borrow site, and therefore, must in no case be worse in the physical properties than the residual soils as referred to in the report.

The physical properties of the residual soils are, according to the records of measurement, 25.15° in the internal friction angle (ϕ), and 2.2 ton/m^2 or 450 psf in the cohesion strength (C). For the stability analysis of the Binga dam, ϕ value of 23° and C value of 6 tons/m^2 are used as the physical properties of its core materials. For the stability analysis of the Ambuklao dam, ϕ value of 29° and C value of 3.77 tons/m^2 are used as the physical properties of its core materials under static condition, and ϕ value of 25° and C value of 6.45 tons/m^2 under loading conditions with the earthquake effect.

It can be assumed that the core materials used for the Angat dam would be of the physical properties of 25° - 30° in ϕ value and 4 - 6 tons/m^2 in C value, judging from the fact that the dam was built at a later date than the Binga and Ambuklao dams.

Based on the above discussion, the stability analysis was made on the assumption of two combinations of ϕ and C values, 25° and 6 tons/m^2 on one combination, and 30° and 4 tons/m^2 on the other.

The results of the analysis made under the Group I conditions (upstream face; water level at HWL or LWL) with and without the earthquake effect are as follows:

The case in which C value of the core materials necessary to keep the required safety factor becomes the largest would be under the Case 3 loading conditions (LWL with the earthquake effect). The required safety factor against sliding in this case would be 1.0.

If ϕ value of the rockfill materials is assumed at larger than 43°, while that of the core materials at larger than 25°, then the dam would be safe against sliding even under the Case 3 loading conditions (LWL with the earthquake effect).

Since it is a general practice to use the rockfill materials with ϕ value of larger than 43° and the core materials with ϕ value of nearly 30° for rockfill dams, it can be considered that the Angat dam would be safe against sliding for any loading conditions of Group I.

The results of the analysis made under the Group II conditions (upstream face; an abrupt reservoir drawdown from HWL to LWL) with or without the earthquake effect are as follows:

If ϕ value of the rockfill materials is in the range of 43° to 45°, and ϕ value of the core materials in the range of 25° to 30°, then, the safety factor against sliding would be greater than the required factor of 1.2 under static loading conditions without the earthquake effect.

If ϕ value of the rockfill materials is 43°, and ϕ value of the core materials is smaller than 29°, then, the safety factor against sliding would be less than the required factor of 1.0 under the loading conditions with the earthquake effect.

The loading condition of an abrupt reservoir drawdown from HWL to LWL is, however, practically unlikely for the Angat dam, because it has a considerably large reservoir surface area as mentioned above. It is not considered realistic that pore pressures in the core zone would remain unchanged during the drawdown. It is also considered unrealistic that the earthquake with such an extremely large seismic coefficient of 0.15 g would occur just at the time when the reservoir water level is down to LWL.

Therefore, the results of the analysis made under the Group II conditions should be dealt with as reference only.

3.5.2. Stability Analysis of the Downstream Face Slope

Group III is to analyze the safety factor against sliding on the downstream face of the dam.

The slope gradient of the downstream face of the dam from the crest to the bottom is uniformly 1:1.4. Hence, the stability of the downstream slope of the dam can be dealt with as that of an infinite slope.

The result of the analysis is as summarized below:

Safety Factor of the Downstream Face Slope Against Sliding

Earthquake Effect	Safety Factor: Rockfill Material ϕ=43°	Safety Factor: Rockfill Material ϕ=45°	ϕ Value to Keep Safety Factor at 1.0
Without	1.306	1.401	-
With	0.964 (0.13)	1.034	44°

Note: The parenthesized figure represents the seismic coefficient shown in g with the safety factor assumed to be 1.0.

Shown in Fig.3.7 is how safety factors of the downstream face slope against sliding may change by depth from the surface under loading conditions with an earthquake effect of Kh value 0.15 g, when assuming ϕ value of the rockfill materials is 43°.

As is seen in the Figure, the surface of the slope is worst in the safety factor against sliding, and deeper into the dam body, the higher the safety factor against sliding becomes. It should be noted, however, that the increase in the safety factors is very slow in pace from the slope surface (0.964) to the depth of 16.8 m (0.98).

Hence, it can be imagined that the surface layer of the slope with the least safety factor of 0.964 would first begin sliding, if there occurs an earthquake with Kh value of 0.15 g. If, unfortunately, such earthquake occurred, and it caused the embankment to slide to the depth of 16.8 m (SF=0.98), then the profile of the slope after sliding would be as illustrated in Fig.3.7. However, the stability analysis made on the scooped slope indicates that it would have a safety factor of 1.0 under static condition, implying that the dam is still stable against further sliding.

Fig. 3.7 Change By Depth in the Safety Factors Against Sliding of the Downstream Face Slope of the Main Dam During Earthquake (ø Value of Rockfill Materials Assumed at 43°)

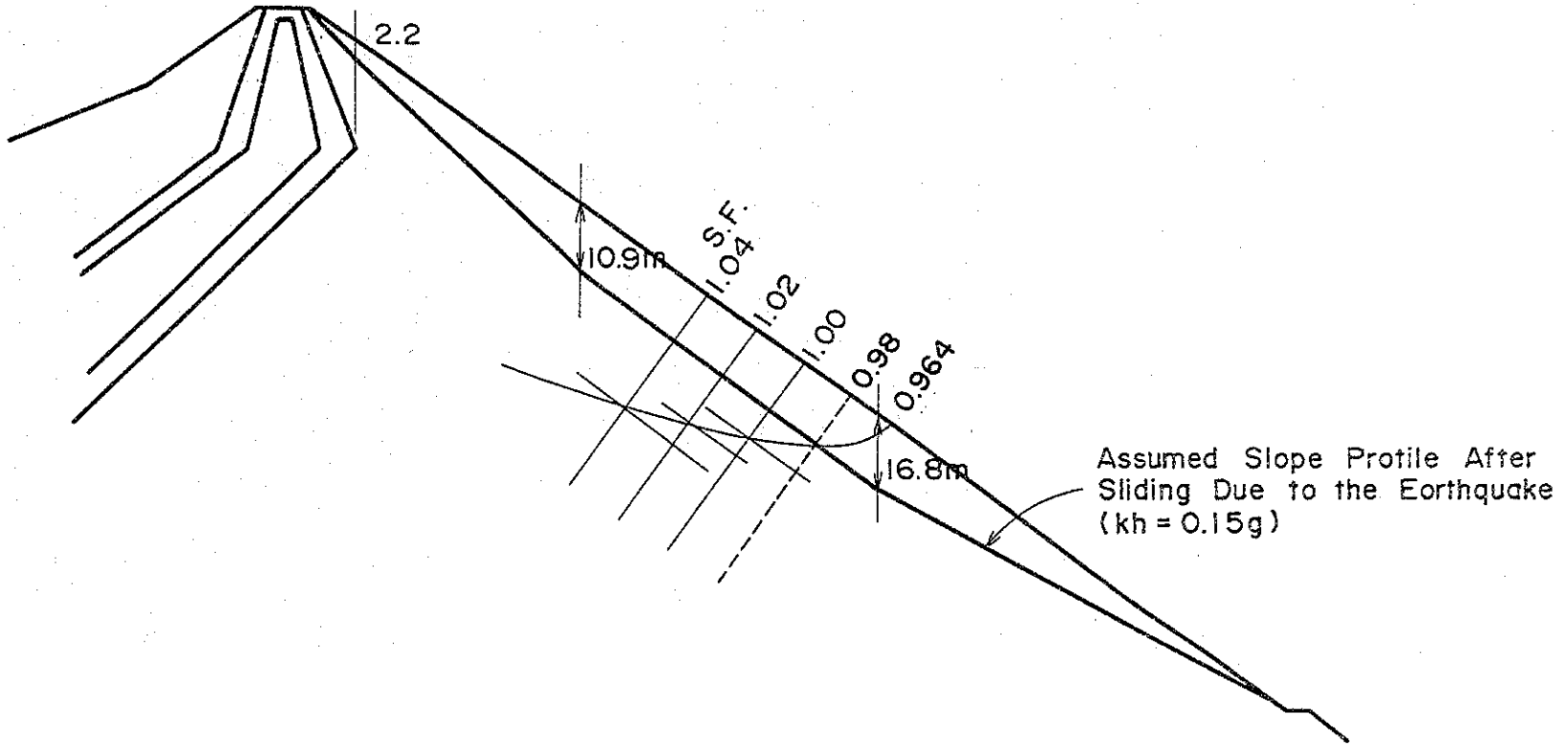

3.5.3. Stability of the Dam

As discussed above, if ϕ value of the rockfill materials is assumed to be 43°, same as used for the stability analysis of the Ambuklao and the Binga dams, there should be a possibility of sliding on the downstream face slope due to an earthquake with Kh of 0.15 g, in so far as the analysis is made in strict accordance with the principle of safety factors. In order to protect the downstream face slope from such sliding, it may be necessary to make the existing slope gradient gentler, i.e., from 1:1.4 (35.5° as an angle to elevation) to 1:1.46 (34.4°).

However, such sliding, if occurred, being limited only to the portion close to the surface of the downstream face slope, it does not mean that the dam is prone to any serious disruption.

The pertinent conclusion from the above analysis is that it is not necessary to do anything to the existing Angat dam structures until there occurs any large Kh earthquake, which unfortunately, causes any surface layer sliding on the downstream face. The dam stability may be maintained by rebuilding the embankment to change the slope gradient to 1:1.46, but this should be done only when such surface sliding should occur.

It is confirmed that any sliding on the upstream face slope of the dam due to an earthquake may not cause any substantial damages unless it is in such a large scale that the sliding lines would pass through the core zone. In fact, it is ascertained by the stability analysis that even an earthquake with Kh of 0.15 g, if happened, may not cause any sliding of such scale that it passes through the core zone.

Therefore, even if there occurred an earthquake and, unfortunately, it caused the embankment of the upstream face slope to slide to some extent, the dam could still be stable under static condition once the earthquake is over. Therefore,

any appropriate rehabilitation program should be worked out only when such damages should take place.

3.6. Stability Analysis of the Dyke

The stability analysis of the dyke was made of a cross section with the maximum height. The section used for the analysis is shown in Fig.3.3. As is seen in the Figure, the downstream face slope profile has undergone little change from that shown in the design drawing. This indicates that the downstream face slope has not suffered from any physical changes since it was built. The analysis of the upstream face slope was made of a section of the design drawing, as no measurement was possible due to a high water level of the reservoir at the time of the field survey for this Study.

3.6.1. Stability Analysis of the Upstream Face Slope

The stability analysis of the upstream face slope of the dyke was made of the three modes of sliding as was the case with the main dam. The first one is the sliding lines passing through the rockfill zone only. The second one is the sliding lines passing through the rockfill and filter zones. And, the last one is the sliding lines passing through rockfill, filter and core zones.

(1) Stability Against Sliding Lines Passing Through Rockfill Zone Only

The analysis was made under the loading conditions in Cases 1 through 3 out of seven cases as given in Subsection

3.5.1. The loading conditions in Cases 1 through 3 are enough to be checked for the stability analysis of the upstream face slope against sliding lines passing through the rockfill zone only. The result of the analysis is as summarized below:

Safety factor Against Sliding Lines Passing Through Rockfill Zone Only

Case	Calculated Safety Factor: Rockfill Material ϕ=43°	Calculated Safety Factor: Rockfill Material ϕ=45°	Required Safety Factor
1	1.31	1.40	1.2
2	0.74 (0.069)	0.80 (0.087)	1.0
3	0.96 (0.13)	1.03	1.0

Note: The parenthesized figure represents the seismic coefficient shown in g with the safety factor assumed to be 1.0.

Under the loading conditions in Cases 2 and 3 with the earthquake effect, the safety factor would be smaller than 1.0. Indicated in a solid line on Fig. 3.8.1 is the sliding line with the least safety factor.

Supposing there occurred an earthquake to cause sliding of rock materials to the depth of the solid line as shown, the safety factor of such scooped slope against further sliding under static condition would be as given below:

Safety Factor of the Scooped Slope Against Further Sliding

Case	Rockfill Materials ϕ=43°	Rockfill Materials ϕ=45°
1	-	-
2	1.00	1.00
3	1.31	-

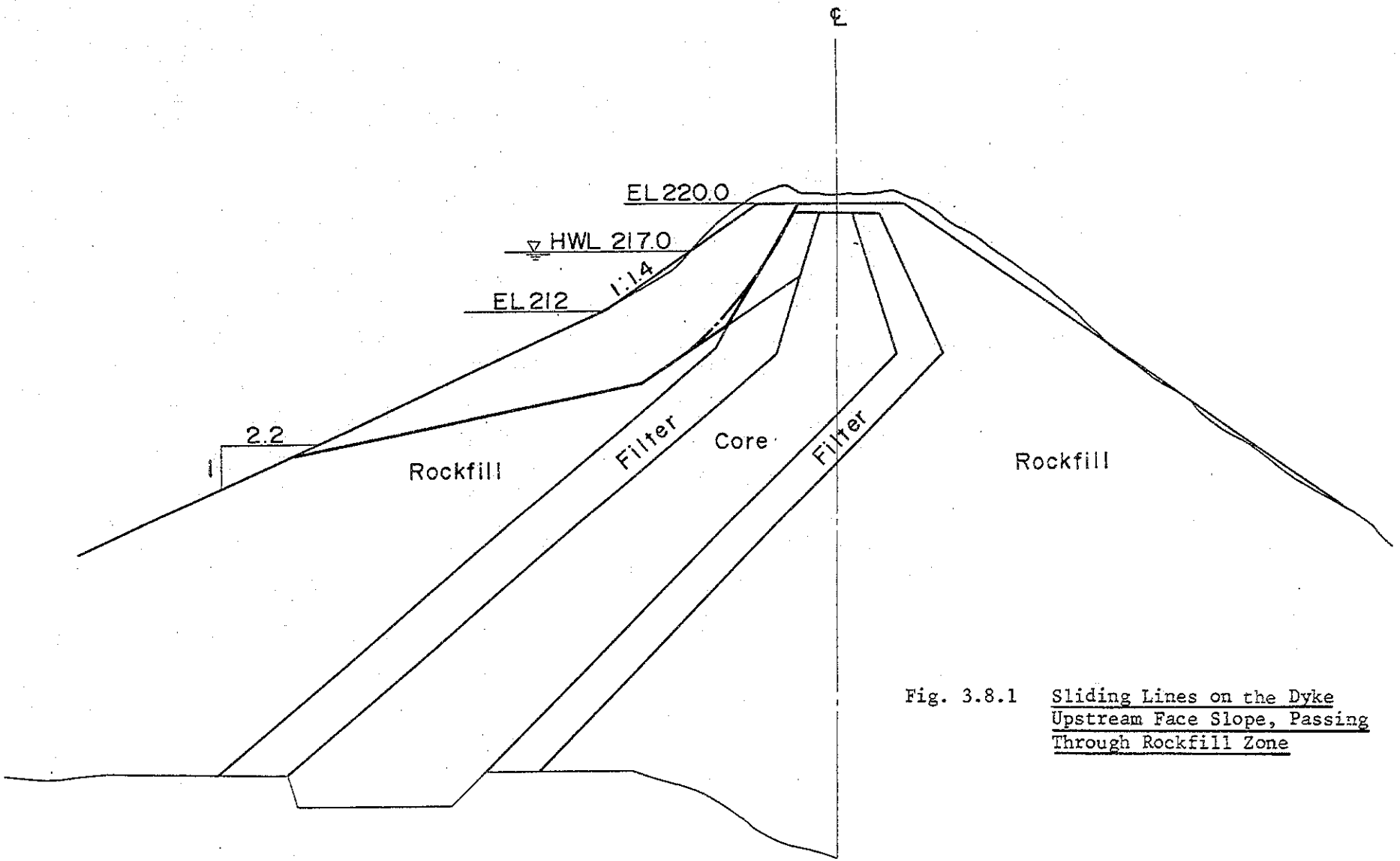

Fig. 3.8.1 Sliding Lines on the Dyke Upstream Face Slope, Passing Through Rockfill Zone

As is seen in the table, the dyke with the upstream face slope being damaged by the earthquake would still continue to be stable under static condition.

(2) Stability Against Sliding Lines Passing Through Rockfill and Filter Zones

Similarly to the foregoing subsection, the loading conditions in Cases 1 through 3 are enough to be checked for the stability analysis against sliding lines passing through the rockfill and filter zones. The result of the analysis is as summarized below:

Safety Factor Against Sliding Lines Passing Through Rockfill and Filter Zones

Case	Calculated Safety Factor: Against Large Scale Sliding — Rockfill Material ϕ=43°	Against Large Scale Sliding — Rockfill Material ϕ=45°	Against Small Scale Sliding — Rockfill Material ϕ=43°	Against Small Scale Sliding — Rockfill Material ϕ=45°	Required Safety Factor
1	1.78	1.86	1.53	1.61	1.2
2	1.01	1.06	0.97 (0.14)	1.02	1.0
3	1.12	1.23	1.21	1.29	1.0

Note: The parenthesized figure represents the seismic coefficient shown in g with the safety factor assumed to be 1.0.

As shown in the table, there could occur no such large scale sliding that may affect the stability of the dyke under static condition, but there may occur a local sliding, if an earthquake with Kh of 0.15 g happens when the reservoir water level is at HWL, in so far as the internal friction angle (ϕ) of rockfill materials is assumed to be 43°. Even in such case, the least safety

factor would be very close to 1.0, indicating that the upstream face slope of the dyke is stabler against sliding than that of the main dam.

Supposing, unfortunately, there occurred an earthquake with Kh of 0.15 g, and it caused a local sliding on the upstream face slope as shown in Fig. 3.8.2, the safety factor of such scooped slope against sliding under static condition would be as shown below:

Safety Factor of the Scooped Slope Against Further Sliding

Case	Against Large Scale Sliding		Against Small Scale Sliding	
	Rockfill Material ϕ=43°	Rockfill Material ϕ=45°	Rockfill Material ϕ=43°	Rockfill Material ϕ=45°
2	>1.0	>1.0	1.00	>1.0

Note: ϕ value of filter materials assumed to be 35°.

(3) Stability Against Sliding Lines Passing Through Rockfill, Filter and Core Zones

The stability analysis against sliding lines passing through the core zone was made under the loading conditions in all five cases. The result of the analysis is as shown below:

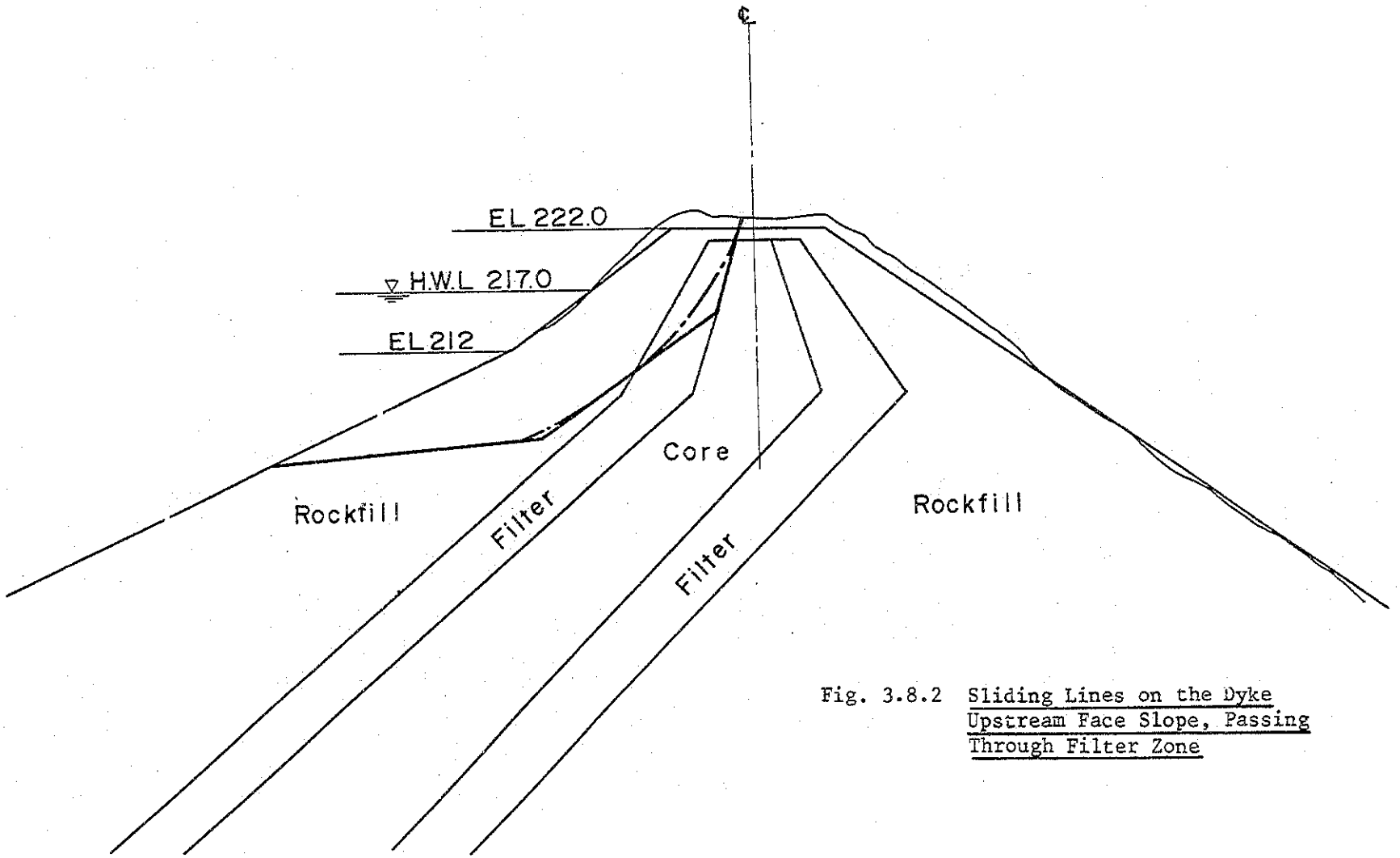

Fig. 3.8.2 Sliding Lines on the Dyke Upstream Face Slope, Passing Through Filter Zone

Safety Factor Against Sliding Lines Passing Through Rockfill, Filter and Core Zones
(ϕ Value of Rockfill Materials Assumed to be 43°)

Case	Against Large Scale Sliding: Core Material, ϕ=20°, C=8 t/m^2	Against Large Scale Sliding: Core Material, ϕ=30°, C=4 t/m^2	Against Small Scale Sliding: Core Material, ϕ=20°, C=8 t/m^2	Against Small Scale Sliding: Core Material, ϕ=30, C=4 t/m^2
1	1.81	1.81	1.67	1.67
2	1.02	1.02	1.06	1.06
3	1.23	1.21	1.29	1.29
4	1.79	1.63	1.62	1.63
5	1.20	1.18	1.29	1.29

As shown above, there could occur no such sliding that may pass through the core zone even under the loading conditions with the earthquake effect. This implies that the upstream face slope of the dyke is safe enough against sliding.

3.6.2. Stability Analysis of the Downstream Face Slope

The stability analysis of the downstream face slope of the dyke was made under the loading conditions in Cases 6 and 7. The result of the analysis is as summarized below:

Safety Factor of the Downstream Face Slope Against Sliding

Case	Rockfill Material ϕ=43°	Rockfill Material ϕ=45°	Seismic Coefficient (Kh)
6	1.31	1.40	0
7	1.00	1.07	0.15

The gradient of the downstream face slope of the dyke is 1:1.45, which is gentler than the corresponding gradient of 1:1.4 of the

main dam. This implies that the downstream face slope of the dyke is stabler against sliding than that of the main dam even under the loading conditions with the earthquake effect.

3.6.3. Stability of the Dyke

There is a possibility of sliding on the upstream face slope of the dyke since there are cases in which the safety factor against sliding may come down below 1.0 under the loading conditions accompanied with an earthquake with Kh of 0.15 g. However, such sliding, if occurred, should be limited only to the portion close to the surface or to the localized portion, and there could be no such sliding that may pass through the core zone. If, unfortunately, there occurred a sliding on the portion with the safety factor of smaller than 1.0, the dyke with the scooped slope could still have a safety factor of 1.0 under static condition, and no catastrophic damage is likely to occur.

The pertinent conclusion from the above analysis is that it is not necessary to do anything to the upstream face slope of the dyke until it is damaged by a large Kh earthquake. Any appropriate repair program should be worked out only when such damages should occur in actuality.

It was confirmed by the stability analysis that the downstream face slope of the dyke is stable under any loading conditions even with the earthquake effect.

4. LANDSLIDING AT THE EX-BATCHER PLANT SITE

4. Landsliding at the Ex-Batcher Plant Site

There was a heavy rainfall in this area in August 1986. This caused a large landslide at the ex-batcher plant site which was prepared for the Angat dam construction, and volumes of slidden earth and sand running into the Angat river blocked a smooth stream flow.

The Angat Power Station consists of a main plant and an auxiliary plant as shown in Fig.4.1. The tailrace outlet for the main plant being located downstream of the Ipo dam exclusively provided for water supply to Metro Manila, the discharged water from the outlet can not be available for the water supply. On the other hand, the tailrace outlet for the auxiliary plant being located immediately downstream of the plant, or upstream of the Ipo dam, the discharged water from the outlet runs wholly into the Ipo dam and is used for the water supply.

The blockage of a smooth stream flow of the Angat river took place downstream of the tailrace outlet for the auxiliary plant and upstream of the Ipo dam, and this caused problems for proper plant operation and the resultant difficulties for adequate water supply service to Metro Manila. Such situation remained unchanged until the deposited earth and sand were removed.

This is the general background for the impending need to take measures to protect the ex-batcher plant site against recurrence of landsliding.

4.1. Geological Survey in the Past

The geological survey hitherto conducted by NAPOCOR at the ex-batcher plant site was by means of boring investigation mainly on the foundation soils closer to the ground surface.

Shown in Fig.4.2 are the locations of the boring investigation conducted by NAPOCOR. The results of the boring investigation are

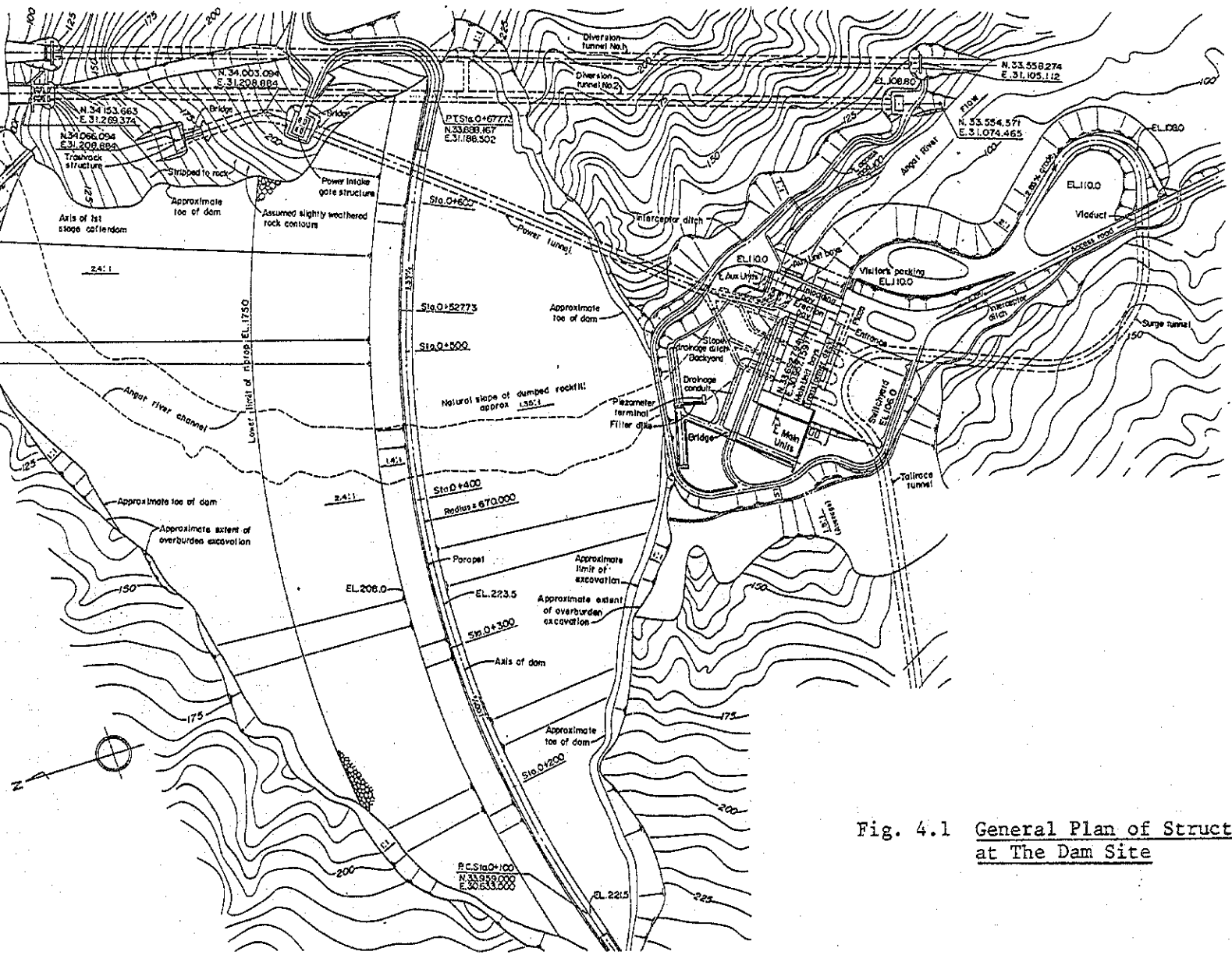

Fig. 4.1 General Plan of Structures at The Dam Site

Fig. 4.2 Location of Investigation Points

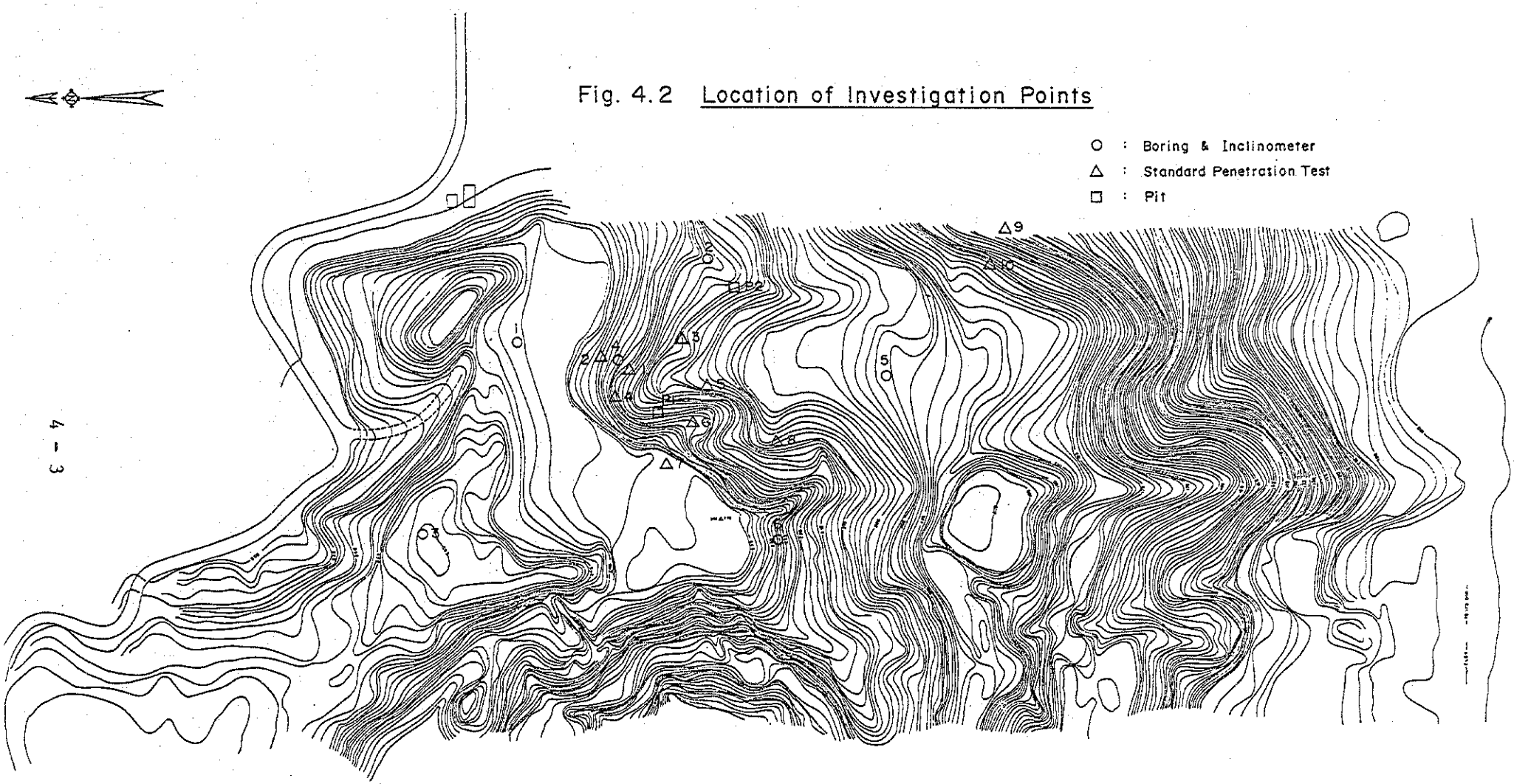

as shown in Table A4.1 and Fig.A4.1 as attached to the Appendix. The results indicate that penetration tests would have been suspended wherever they were confronted with any obstacles such as cobblestones.

4.2. Geological Survey for this Study

As the geological data available from the past geological survey were not good enough to seize the development of landsliding, it was decided to provide additional bore holes and install inclinometers to check whether landsliding is still in progress, and if so, to confirm the depth of the sliding plain.

Fig.4.2 shows the locations of bore holes for inclinometer measurement. The data have, however, not been available in time for the preparation of this Report, mainly because of some defects in the instruments.

Table 4.1. Additional Field Investigation at the Ex-Batcher Plant Site

Item	Unit	Quantity
Plane survey	m^2	151,000
Drilling		
Geological investigation	hole	6 (180 m)
Soil test		
Pit Sampling	pit	3
Test	set	3

4.3. Studies on Landsliding by Back Analyses

The characteristics of the slid materials can be estimated by back analyses based on the actual landsliding.

Fig. 4.3 is a topographic map (1/500 scale) prepared by the survey made this time on the ex-batcher plant site. From this map, it is easy to identify the exact location where the landslip did happen, but it is difficult to estimate the volume of slid materials because of lack of proper topographic maps of the site before landsliding.

As the alternative to such a map, an old topographic map was available from the as-built drawings prepared upon the completion of the Angat dam, and this was superposed on the map prepared this time to estimate the pre-slide topography, as shown in Fig.4.4.

As described in the Progress Report on the Study for the Angat Dam Rehabilitation Project, Jan. 1988, page 23, it is assumed from the result of field surveys in September 1987 that a landslide would have begun along the line "A" shown in Fig.4.5, and this would have caused a subsequent landslide to occur along the line "B" shown in the same Figure.

Fig. 4.6 shows the estimated sliding directions of the Aug. 1986 landslide, and Fig.4.7 shows longitudinal profiles along these sliding directions. It was assumed from these profiles that a topography as indicated in the dotted lines would have slidden to produce a topography as indicated in the solid lines. Assuming that the safety factor against sliding of this land would be equal to 1.0, it is possible to estimate the physical properties, cohesion(C) and internal friction angle (ϕ), of the mountain mass where the landslide actually occurred.

As is seen in these longitudinal profiles, the gradient of the mountain slope in and around the ex-batcher plant site changes rather suddenly at the elevations in the neighborhood of EL.180 m. It can therefore be assumed that there should be a distinction in the geotechnical condition between the elevations higher than EL.180 m and those lower than EL.180 m. Hence, the corresponding distinction was made in analyzing the possibility of landsliding in the following subsections.

Fig.4.3 Topographic Map of the Ex-batcher Plant Site
(Prepared in 1987)

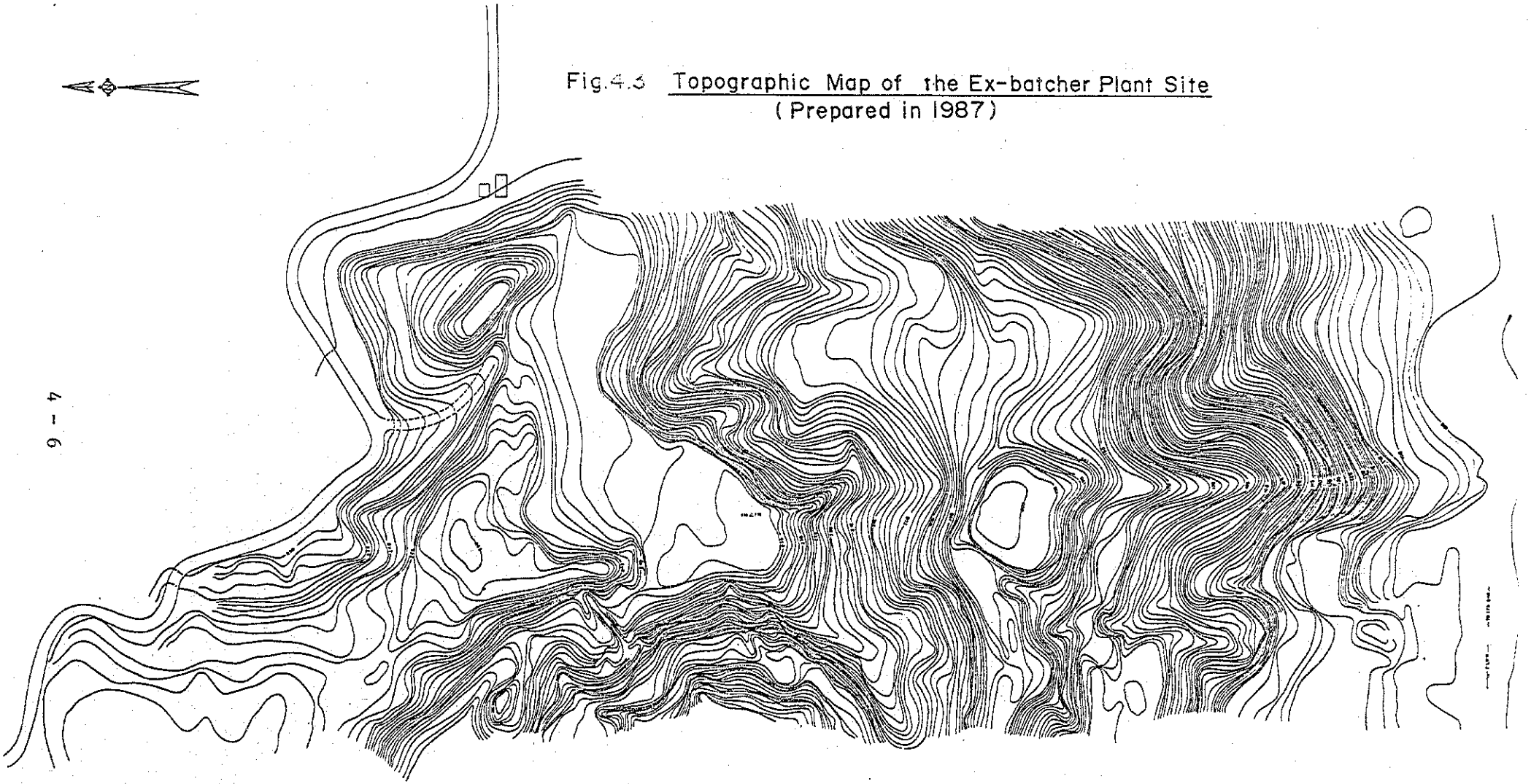

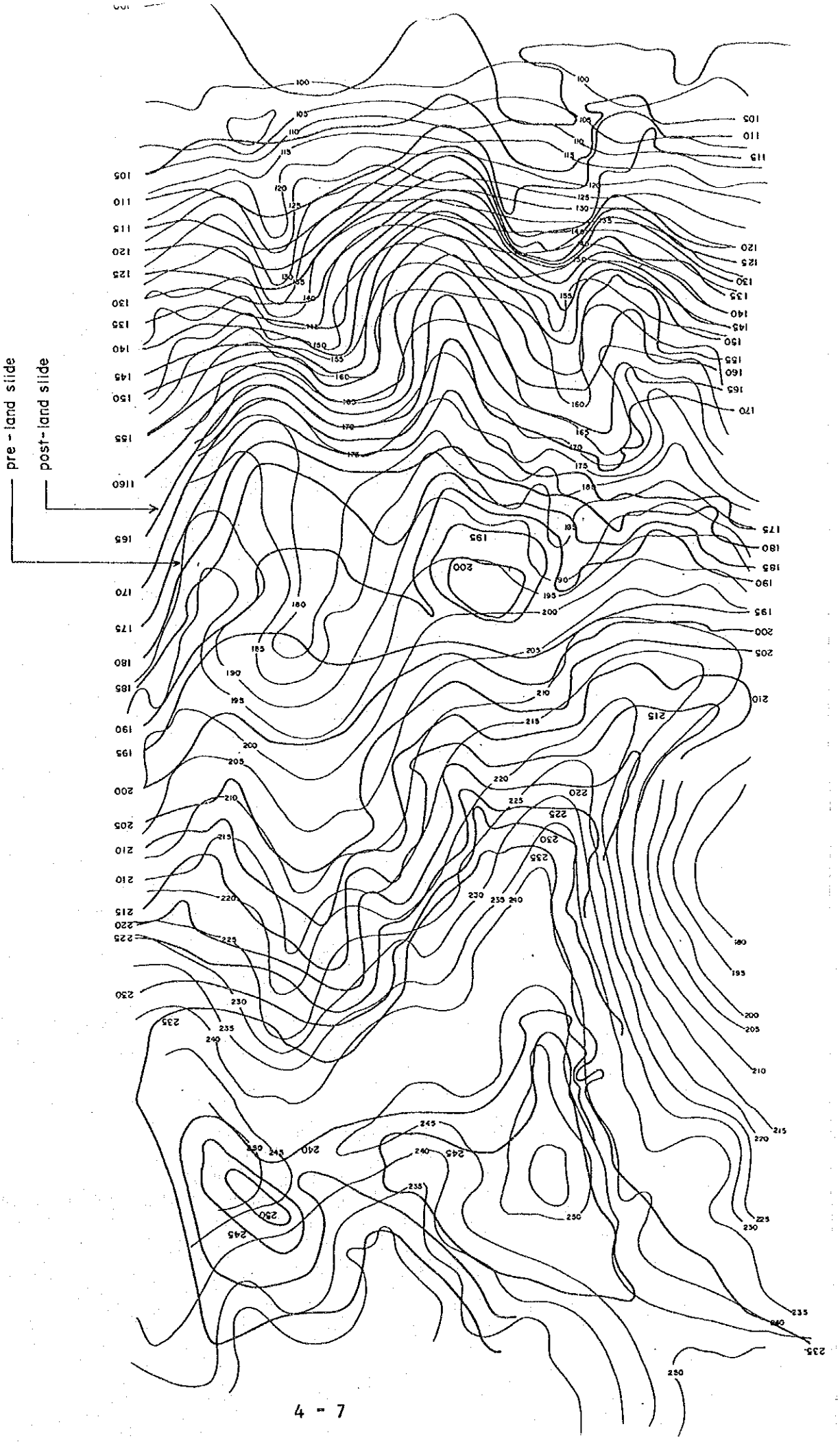

Fig. 4.4 PRE- AND POST-SLIDE TOPOGRAPHY OF THE EX-BATCHER PLANT SITE

Fig. 4.5 Movement of Earth at the 1986 Landslide

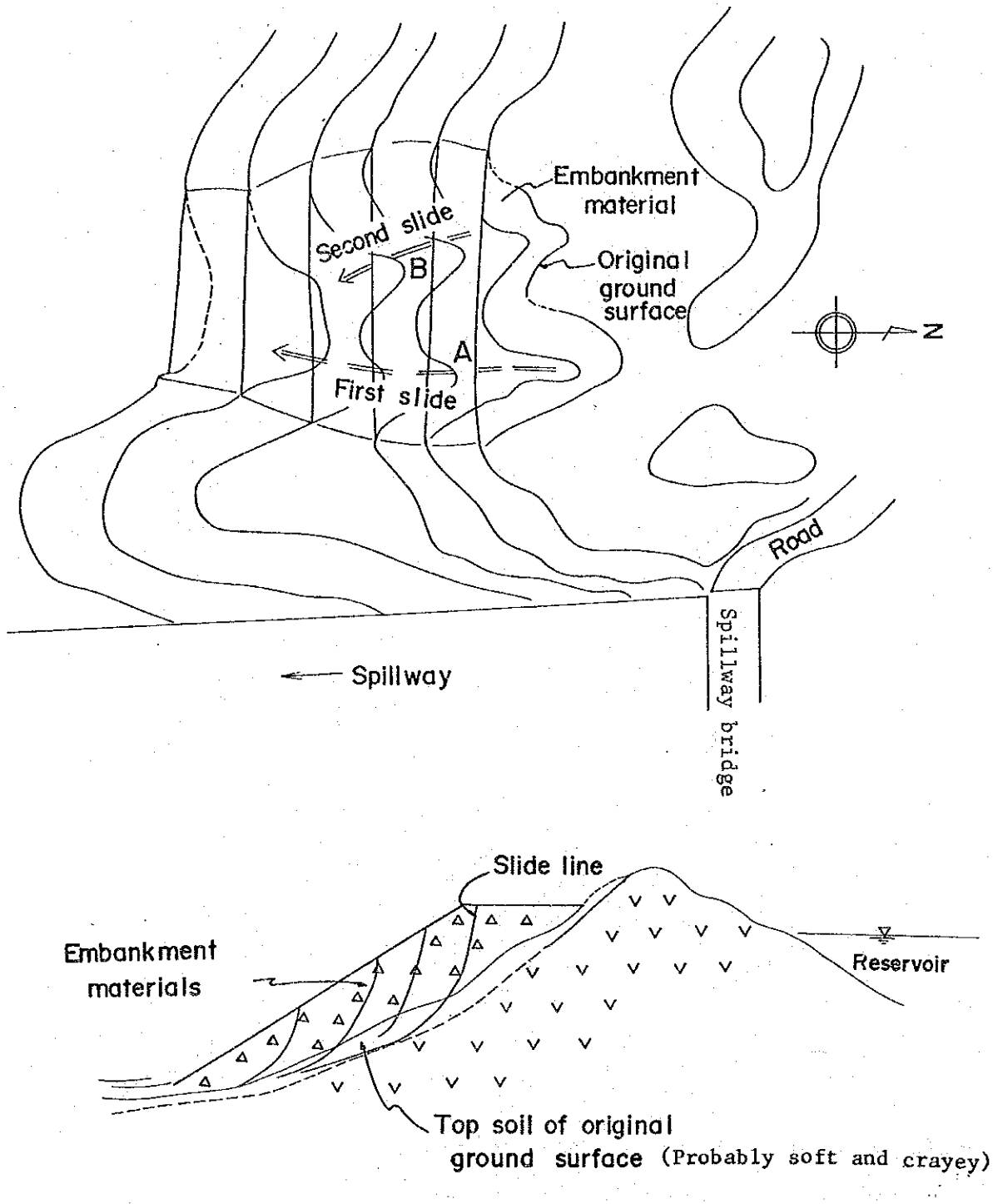

Fig. 4.6 ESTIMATED SLIDING DIRECTIONS OF AUG. 1986 LANDSLIDE

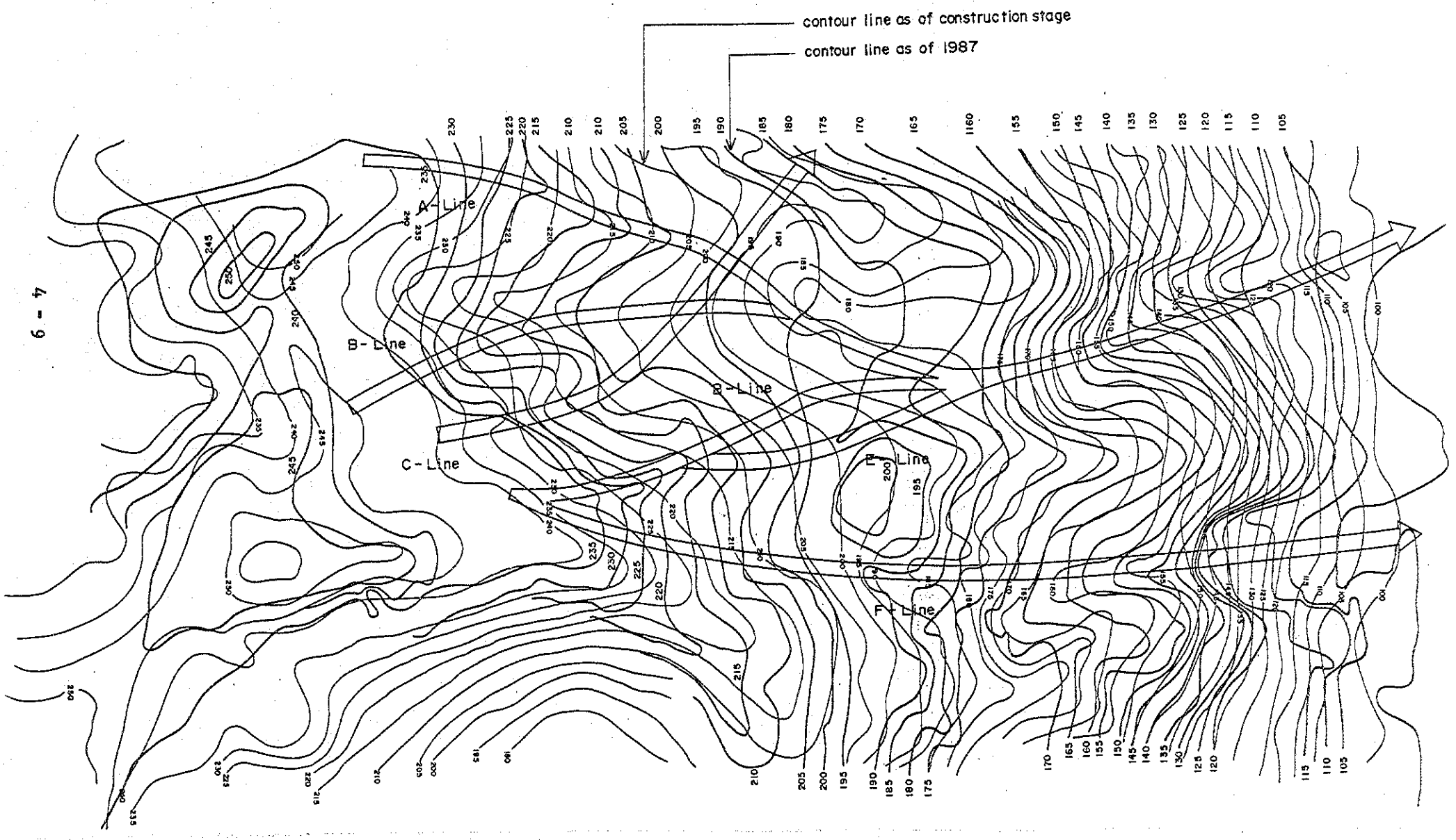

Fig. 4.7.1 LONGITUDINAL PROFILES ALONG THE ESTIMATED SLIDING LINES

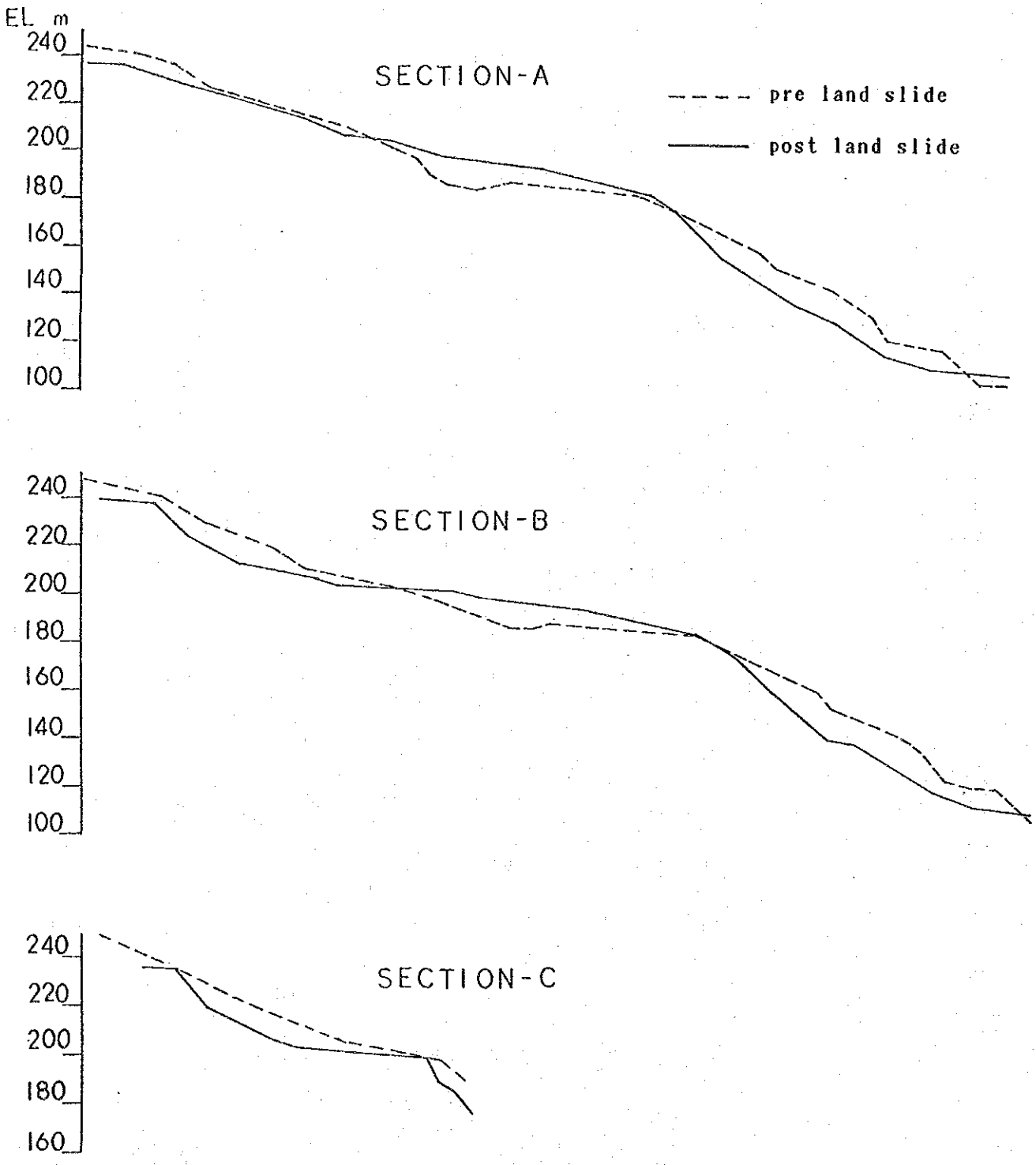

Fig. 4.7.2 LONGITUDINAL PROFILES ALONG THE ESTIMATED SLIDING LINES

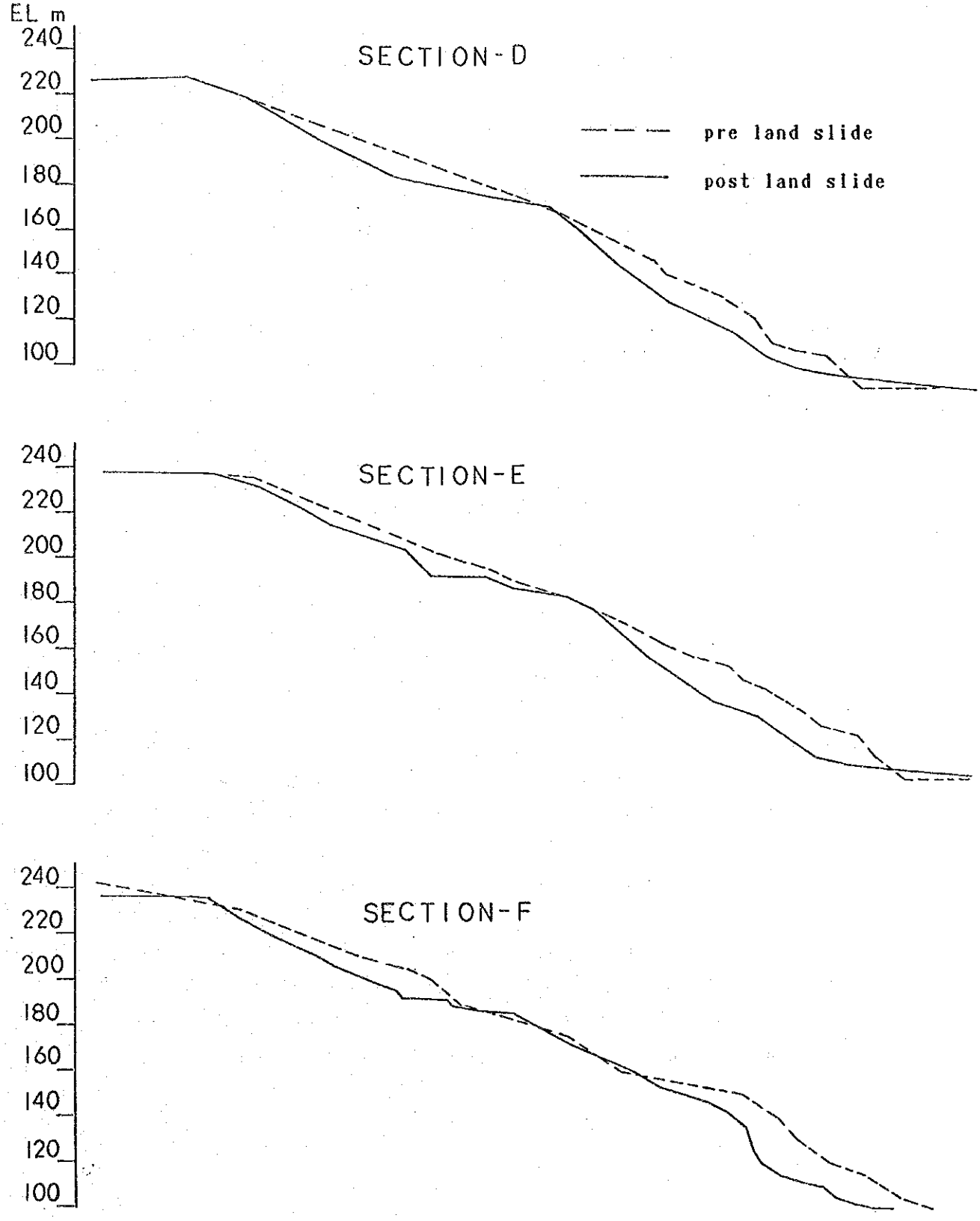

4.3.1. Characteristics of the Mountain Mass along Sliding Lines

Shown in Fig.4.8 is the relation between the cohesion (c) and the internal friction angle (ϕ) of the mountain mass to cause the landslide from the dotted-lined topography to the solid-lined topography on all longitudinal profiles shown in Fig.4.7, when the safety factor is assumed to be 1.0. The relation in the Figure is shown for two different cases, one is on the assumption that the landslide would have occurred in condition with no ground water, and the other is on the assumption that it would have occurred in condition with ground water up to the ground surface.

Tabulated in Table 4.2 is the value of C and ϕ of the mountain mass on each longitudinal profile obtained from the back analyses as mentioned above. Table 4.3 is a summary of these data.

4.3.2. Characteristics of the Mountain Mass Deeper than the Sliding Lines

In the foregoing subsection, the physical properties of the mountain mass were estimated from the back analyses on the basis of the actual sliding lines.

However, if the mountain mass is composed of the homogeneous and uniform soil material, these actual sliding lines may not necessarily mean the ones with the least safety factor against sliding.

As illustrated below, for instance, a line with the least safety factor against sliding may possibly be such the one shown as the dotted line, rather than the actual sliding line shown as the solid line, when assuming that the mountain mass would be composed of the homogeneous and uniform soil material.

Fig. 4.8 RELATION BETWEEN C AND ϕ VALUES OF THE MOUNTAIN MASS

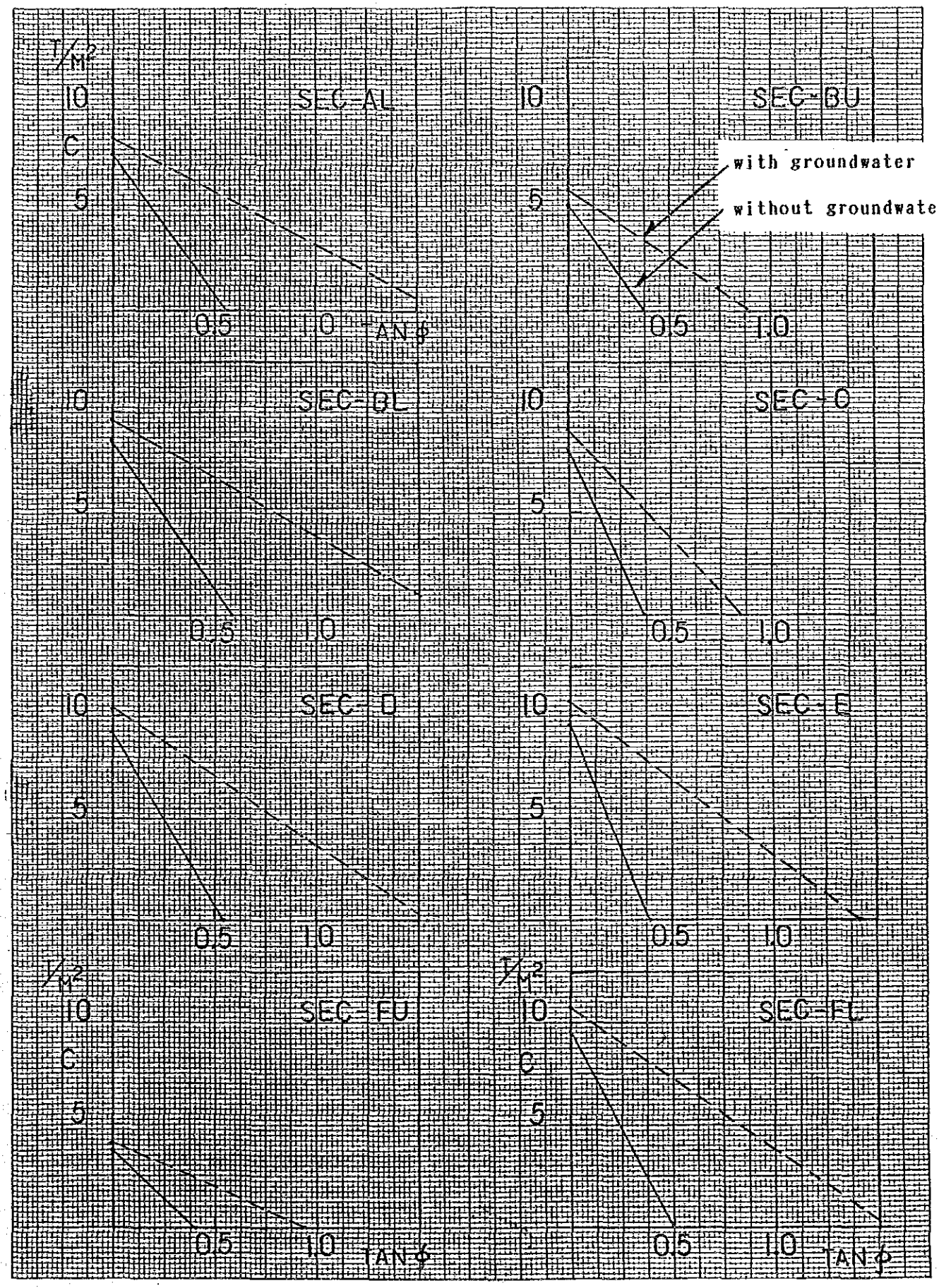

Table 4.2 C and ϕ Value of the Mountain Mass Obtained from the Back Analyses

		R	Without Ground Water			With Ground Water		
			$\phi = 0$	C = 0		$\phi = 0$	C = 0	
		m	ton/m²	tanϕ	° ' "	ton/m²	tanϕ	° ' "
UPPER	Sec-A	73.3	2.849	0.378	20 42 06	3.165	0.863	40 47 15
	Sec-B	102.20	5.348	0.370	20 17 44	5.952	0.897	41 53 16
	Sec-C	—						
	Sec-D	325.0	4.785	0.756	37 05 21	4.310	0.336	18 34 20
		210.0	6.061	0.733	36 13 35	5.345	0.327	18 06 28
	Sec-E	—						
	Sec-F	304.00	3.759	0.398	21 41 57	4.184	0.943	43 18 17
LOWER	Sec-A	238.53	7.752	0.555	29 01 39	8.621	1.618	58 17 02
	Sec-B	223.63	8.696	0.572	29 45 32	9.709	1.701	59 32 40
	Sec-C	113.66	8.264	0.355	19 31 30	9.174	0.845	40 11 03
	Sec-D	279.79	9.259	0.542	28 27 29	10.309	1.546	57 05 50
	Sec-E	247.78	9.709	0.385	39 51 09	10.753	1.422	54 53 34
	Sec-F	58.26	9.615	0.496	26 21 37	10.753	1.543	37 03 24

Table 4.3 Relation Between C and ϕ Values of the Mountain Mass Obtained from the Back Analyses (ϕ as Parameters)

Assumption	Upper		Lower	
	ϕ	C kg/cm²	ϕ	C kg/cm²
Landslide would occur under condition with no groundwater.	10 °	0.15～0.30	10 °	0.54～0.65
	20 °	0.02～0.05	20 °	0.08～0.34
	—	—	30 °	0 ～0.05
Landslide would occur under condition with groundwater up to the surface.	10 °	0.25～0.50	10 °	0.77～0.96
	20 °	0.19～0.36	20 °	0.67～0.84
	30 °	0.10～0.20	30 °	0.55～0.67

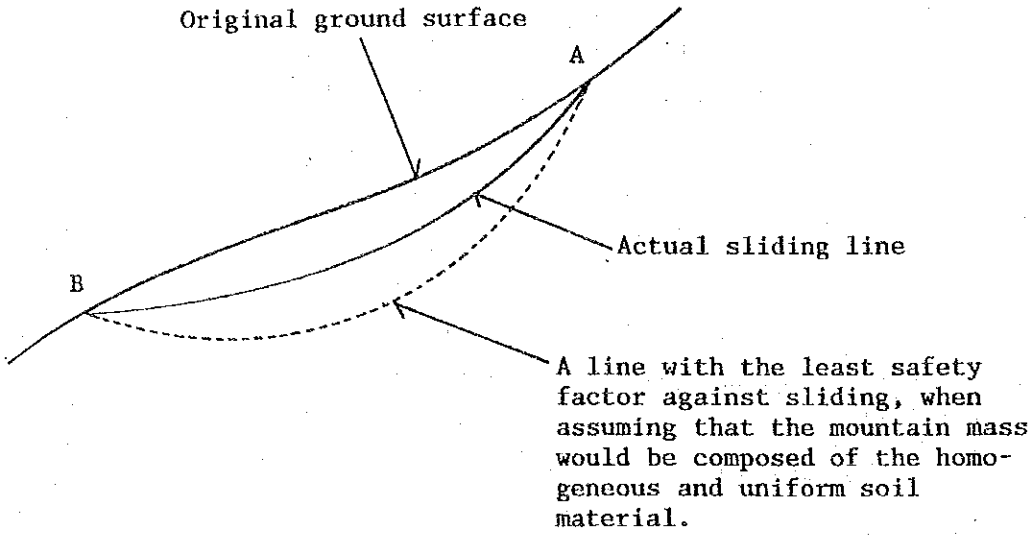

If the actual sliding line is such the one shown as the solid line, it may be attributable to either of the following two assumptions:

i) Precipitation infiltration into the mountain mass still remains to the depth close to the ground surface, and does not reach to the depth deeper than the solid line as shown.

ii) The physical properties (C and ϕ) of the mountain mass are dissimilar by depth from the ground surface, and become greater as a depth becomes deeper into the mountain.

Assuming that the C and ϕ values of the mountain mass would become greater as a depth from the surface becomes deeper, and accordingly, the actual sliding line would be such the one shown as the solid ACB line, while a line with the least safety factor would be such the one shown as the dotted AC'B line, as illustrated below, the least safety factor of the AC'B line must be greater than 1.0, since there occured no landsliding along the AC'B line in actuality.

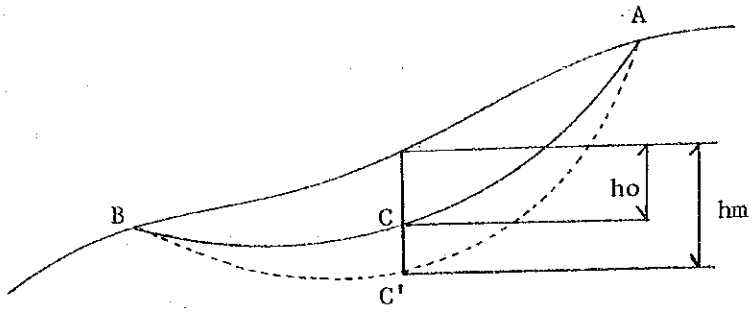

Shown in Table 4.4 are the minimum required C and ϕ values at Point C' obtained by back calculations made from the above-mentioned viewpoints.

4.4. Geological Survey at the Ex-Batcher Plant Site

4.4.1. N Values by Standard Penetration Tests

Boring investigation has been conducted from September 1987 at 12 points within the ex-batcher plant site. The locations of these points are shown in Fig.4.2, and the geology identified by the investigation is as shown in Table A4.1 attached to the Appendix.

Table 4.5 shows the results of the standard penetration tests conducted as part of the geological survey. The N values in the Table are the number of times of hammering to drive a test cone into the depth of 30 cm. As is seen in the Table, there were cases where the N values became irregularly high. These may be attributable to the encounter with obstacles such as cobble-stones during the penetration tests.

Table 4.4 Physical Properties at Deeper Mountain Mass

Longitudinal profile	hm	C Values (ton/m^2)		
		ϕ = 10°	ϕ = 15°	ϕ = 20°
A	13 m	11.7	9.4	7.3
B	15	11.8	9.2	7.2
D	7	9.8	7.0	5.3
E	5	12.6	9.8	7.7
F	8	12.4	9.8	7.3
Average	10	12.0	9.0	7.0

hm : The depth from the ground surface of a sliding line with the least safety factor, assuming that the mountain mass would be composed of the same and uniform soil material.

c : Cohesion of the mountain mass.

ϕ : Internal friction angle of the mountain mass.

Table 4.5 Results of the Standard Penetration Tests (N Values)

No. 1			No. 2			No. 3			No. 4		
Depth	Ave.	Adjusted	Depth	Ave.	Adjusted	Depth	Ave.	Adjusted	Depth	Ave.	Adjusted
m			m			m			m		
1.05 – 1.50	12	9	1.05 – 1.50	2.0	2.0	1.05 – 1.50	6.0	6.0	1.05 – 1.50	18.7	14.0
2.55 – 2.93	71	43	2.55 – 3.00	6.0	6.0	2.55 – 3.00	8.7	8.7	2.05 – 2.18	> 50	
			4.05 – 4.50	6.7	6.7	4.05 – 4.50	11.3	11.3			
			5.50 – 6.00	16.6	16.6	4.90 – 5.05	> 50				
			7.05 – 7.50	19.3	19.3						
			8.55 – 9.00	12.7	12.7						
			9.70	> 50							

(Table 4.5 continued)

No. 5			No. 6			No. 7			No. 8		
Depth	Ave.	Adjusted	Depth	Ave.	Adjusted	Depth	Ave.	Adjusted	Depth	Ave.	Adjusted
m			m			m			m		
1.05 – 1.50	4.7	4.7	1.05 – 1.50	4.7	4.7	1.05 – 1.50	19.3	15.0	1.05 – 1.50	4.0	4.0
2.55 – 3.00	13.3	13.3	2.55 – 3.00	6.0	6.0	2.55 – 3.00	27.3	27.3	2.55 – 3.00	8.0	8.0
4.05 – 4.50	11.3	11.3	4.05 – 4.50	10.0	10.0	4.05 – 4.50	5.3	5.3	4.05 – 4.50	17.3	17.3
5.55 – 6.00	8.0	8.0	5.55 – 6.00	13.3	13.3	5.55 – 6.00	6.7	6.7	5.55 – 6.00	45.3	45.3
7.05 – 7.50	14.0	14.0	7.05 – 7.50	20.7	20.7	7.05 – 7.50	10.0	10.0	7.05 – 7.50	71.3	63.0
8.55 – 9.00	26.0	12.0	8.55 – 9.00	53.3	20.0	8.55 – 9.00	8.0	8.0	8.55 – 9.00	87.0	70.0
10.05 –10.50	51.3	14.0	9.64	> 50		10.05 –10.50	8.7	8.7			
11.00 –11.45	38.6	38.6				11.55 –12.00	24.7	24.7			
11.75 –11.90	> 50	> 50				13.05 – 13.50	48.0	32.0			
						13.5<	> 50				

(Table 4.5 continued)

No. 9			No. 10			No. 11			No. 12		
Depth	Ave.	Adjusted	Depth	Ave.	Adjusted	Depth	Ave.	Adjusted	Depth	Ave.	Adjusted
m			m								
1.05 – 1.50	4.0	4.0	1.05 – 1.50	3.3	3.3						
2.55 – 3.00	8.0	5.0	2.55 – 2.93	85.0	85.0						

Shown in Table 4.6 are the average data of the N values by depth, after excluding such irregularly high values. Data on the deeper elevations with the N values greater than 50 are not shown in the Table, for reason that the mountain mass at those elevations is believed to be hard enough and not to be prone to landsliding. The numbers in brackets are irregularly high as compared with those in their vicinity, and these were not taken into account for studies in the following subsections.

Table 4.7 shows the data on the standard penetration tests done by NAPOCOR in September 1987, specifically for those portions at the elevations with the N values greater than 50. The depth from the ground surface and the respective elevation are shown therein.

As is seen in the Table, the elevations with the N values greater than 50 can be classified into the following two groups, except No.10 hole:

Group 1: Elevations of the boundary line beyond which N is greater than 50 are in the vicinity of EL.215 m. (Nos. 1, 2, 4, 6 and 7 holes)

Group 2: Elevations of the boundary line beyond which N is greater than 50 are in the vicinity of EL.200 m. (Nos. 3, 5 and 8 holes)

From the above classification, the average elevations by group can be assumed to be as follows:

Average Elevation	Group 1	Group 2
Ground surface	EL.224 m	EL.216 m
Boundary line beyond which N is greater than 50	EL.210 m	EL.203 m

Table 4.6 N Values by Depth of the Penetration Tests at the Ex-Batcher Plant Site

Depth (m) / Hole No.	1.0	2.5	4.0	5.5	7.0	8.5	10.0	11.5
	1.05-1.50	2.55-3.00	4.05 4.50	5.50-6.00	7.05-7.50	8.55-9.00	10.05-10.50	11.75-11.90
1	9	(43)	-	-	-	-	-	-
2	2	6	6.7	16.7	19.3	12.7	-	-
3	6	8.7	11.3	-	-	-	-	-
4	14	-	-	-	-	-	-	-
5	4.7	13.3	11.3	8.0	14.0	12.0	14.0	38.6
6	4.7	6	10.0	13.3	20.7	20.0	-	-
7	15	(27.3)	5.3	6.7	10.0	8.0	8.7	24.7
8	4	8	17.3	(45.3)	-	-	-	-
9	4	5	-	-	-	-	-	-
10	3.3	-	-	-	-	-	-	-

Table 4.7 Elevations with N Values Greater Than 50

(m)

Hole	Depth from Ground Surface	Elevation at Ground Surface	Elevation with N Values Greater Than 50
1	2.5	217.0	214.5
2	9.7	227.1	217.4
3	5.0	208.1	203.1
4	2.0	218.5	216.5
5	11.5	212.3	200.8
6	9.0	223.5	214.5
7	13.5	233.0	219.5
8	6.5	212.0	205.5
9		172.5	
10	2.5	182.5	180.0

The corresponding elevations for hole No.10 are as follows:

Elevation of the ground surface: EL.182.5 m

Elevation of the boundary line beyond which N is greater than 50 : EL.180 m

It is therefore considered reasonable from the above studies to assume that the elevations lower than EL.180 m of the mountain mass at and around the ex-batcher plant site would be of the N value greater than 50.

Shown in Table 4.8 are the average N values and the standard deviations by depth, using the data given in Table 4.6.

4.4.2. Examination of Physical Properties

(1) Examination Based on N Values

The relation between the N values of the standard penetration tests for the sandy ground and the internal friction angles of sandy soils in a drain condition can be determined using the equations prepared by Dunhum, Meyerhof, and Peck, etc. For this report, however, it was obtained by using the equation currently employed by the Ministry of Construction of Japan, as given below:

$$\phi = \sqrt{15N} + 15$$

Shown in Table 4.9 are the ϕ values by depth thus obtained.

The relation between the N values of the penetration tests for the cohesive soils and the cohesion strength (C) can be expressed, according to the practice of the Japan Highway Association, as:

$$C = (0.06 - 0.1)N \quad (kg/cm^2)$$

Table 4.8 Average N Value and the Standard Deviation by Depth

Depth (m)	Average N Value	σ	N+σ	N-σ
1.0	6.67	4.29	10.96	2.38
2.5	7.83	2.75	10.58	5.08
4.0	10.32	3.85	14.17	6.47
5.5	11.15	4.00	15.15	7.15
7.0	16.00	4.27	20.27	11.73
8.5	13.18	4.33	17.51	8.85
10.0	11.35	2.65	14.00	8.70
11.5	31.65	6.95	38.60	24.70
7.0 - 10.0 Average(*)	13.94	4.41	18.35	9.53

* N Values between the depths of 7.0m and 10.0m being resemble one another, the averages taken from the data given in Table 4.6 are shown herein.

Table 4.9 Internal Friction Angle Estimated from N Values
(In Case of Sandy Ground)

Depth (m)	Average	Upper Limit	Lower Limit
1.0	25°	27.8°	21.0°
2.5	25.8°	27.6°	23.7°
4.0	27.4°	29.6°	24.9°
5.5	27.9°	30.1°	25.3°
7.0 - 10	29.5°	31.6°	27.0°
11.5	36.8°	39.1°	34.2°

Given that the above is 0.08 N (kg/cm^2), taking an average, the cohesion strength (C) of such soils by depth can be as shown in Table 4.10.

(2) C and ϕ Values for Analyses on Possibility of Landsliding

The relation between the C and ϕ values given in Tables 4.9 and 4.10 is plotted on Fig. 4.9, with the ϕ values (Table 4.9) estimated from the average N values shown on the abscissa, while the C values (Table 4.10) estimated in similar manner on the ordinate.

The round marks in the Figure are the C values (Table 4.3) with the ϕ values assumed at 10° and 20°, obtained by back analyses on the basis of the actual landslide lines. The C values thus derived are all those on the assumption that the ground would have been impregnate with water to the surface, since the landsliding should have occurred in the midst of a heavy rainfall. A portion shadowed with oblique lines shows a range of the physical properties obtained by back calculations.

It is not considered probable that the actual landsliding would have occurred deep into the ground. It is very likely that the ϕ values in the ground where the landslide did occur would not be so large, but be at most between 10° and 20°, judging from the relation given in the Figure.

The field survey indicates the landslide to have occurred at the elevations higher than EL.180 m. The mountain mass at the elevations lower than EL.180 m has a steep gradient on the slope, but as mentioned in Section 4.4.1, it is considered unlikely that landsliding took place at these elevations where higher values of C and ϕ are presumed. Analyses on the possibility of landsliding in the future

Table 4.10 Cohesion Strength Estimated from N Values

(In Case of Cohesive Soil)

(ton/m^2)

Depth	Average	Upper Limit	Lower Limit
1.0	5.3	8.8	1.9
2.5	6.3	8.5	4.1
4.0	8.3	11.3	5.2
5.5	8.9	12.1	5.7
7.0 ~ 10	11.2	14.7	7.6
11.5	25.3	30.9	19.8

Fig. 4.9 Relation Between C and ϕ Values for Analyses on the Possibility of Landsliding

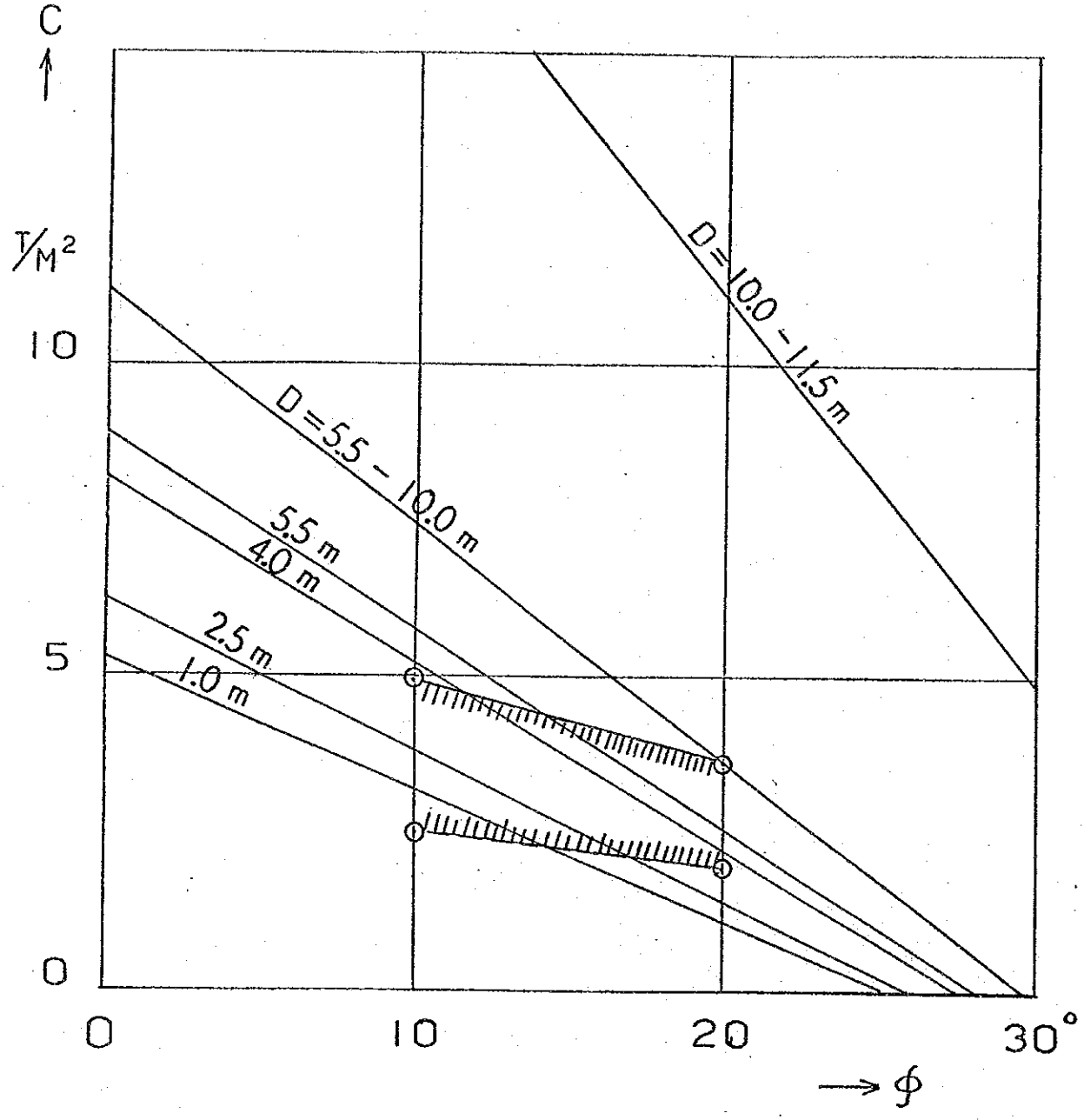

were, therefore, made of two separate sections, one at the elevations higher than EL.180 m, and the other at the elevations lower than EL.180 m.

i) Minimum Limit of C and ϕ Values in the Ground at Elevations Lower Than EL.180 m

Since no landslide occurred at elevations lower than EL.180 m, any conceivable sliding lines of the existing topography at these elevations must all be of the safety factor of greater than 1.0 at least. If it were less than 1.0, the landslide should have occurred at these elevations, too.

The actual safety factor against sliding at these elevations is not known, though it should be greater than 1.0. But, should it be assumed to be 1.0 or the marginal limit to cause a landslide, the corresponding physical properties of the mountain mass can be estimated therefrom. If these values are called the hypothetical minimum limits, the actual mountain mass at these elevations should be of the physical properties equal to or higher than these minimum limits, since no landslide did occur at these elevations.

Shown in Table 4.11 are the results of calculation of the hypothetical minimum limits of C and ϕ values in the ground at the elevations lower than EL.180 m.

Suppose the ground at the elevations lower than EL.180 m be composed of the homogeneous and uniform soil material, then the D profile would be most critical to landsliding. Hence, the physical properties of the mountain mass at the elevations lower than EL.180 m have to meet the following requirements:

Table 4.11 Hypothetical Minimum Limit of C & ϕ in the Ground at EL 180m or Lower Elevations
(In case where the ground is impregnate with water to the surface)

Longitudinal Profiles	C Values (ton/m^2)			
	ϕ = 10°	ϕ = 20°	ϕ = 30°	ϕ = 40°
A	24.4	14.6	9.9	6.2
B	22.8	14.3	10.5	6.7
D	30.0	20.5	12.3	6.6
E	29.2	19.8	11.8	5.4
F	27.1	17.9	9.5	5.5
f	18.6	12.2	7.8	4.5
g	17.6	11.9	7.0	3.6
Average	24.2	15.9	9.8	5.5
σ	4.5	3.3	1.8	1.1
Average- σ	19.7	12.6	8.0	4.4
Average+ σ	28.7	19.2	11.6	6.7

When ϕ = 10°, then C > 30 ton/m^2
When ϕ = 20°, then C > 20.5 ton/m^2
When ϕ = 30°, then C > 12.5 ton/m^2
When ϕ = 40°, then C > 6.7 ton/m^2

According to the results of the boring investigation, the N values in the ground at elevations lower than EL.180 m are believed to be greater than 50. Suppose these values be equal to 50, then ϕ must be greater than 42° if C is zero, and C must be greater than 40 ton/m^2 if ϕ is zero. These C and ϕ values are consistent with the physical properties of the ground on the D profile with the safety factor of 1.0 against sliding.

It is considered reasonable from the above discussions to assume that the ϕ value of the mountain mass at the elevations lower than EL.180 m would be 30°, while the C value would be at least 15 tons/m^2, somewhat greater than the hypothetic minimum limits.

ii) C and ϕ Values in the Ground at Elevations Higher than EL.180 m

Table 4.12 shows the C values in the ground by depth at the elevations higher than EL.180 m on two different cases, one with the ϕ Value assumed at 10° and the other with the ϕ value at 20°, which are as plotted on Fig.4.9.

In order to simplify the process of calculations, it was assumed that, for the case with the ϕ value set at 10°, the C values would be 3 tons/m^2 at the ground surface, 8 tons/m^2 at a depth of 6 m, and 12 tons/m^2 at a depth of 10 m, and at any other depths, they can be obtained from any points on a line connecting the above three base points one after another.

Table 4.12 Physical Properties of the Mountain Mass by Depth (at Elevations Higher Than EL 180m)

Depth from the Ground Surface	C Values (ton/m^2)	
	In case of $\phi = 10°$	In case of $\phi = 20°$
1.0	3.2	1.0
2.5	3.8	1.4
4.0	5.2	2.2
5.5	5.6	2.5
5.5 - 10.0	7.3	3.5
11.5	18.0	11.2

Similarly, for the case with the ϕ value set at 20°, it was assumed that the C values would be 1 ton/m^2 at the ground surface, 4.0 tons/m^2 at a depth of 6 m and 7 tons/m^2 at a depth of 10 m, and at any other depths, they can be obtained from any points on a line connecting the three base points one after another.

Table 4.12 indicates that the C values at depths of 10 to 11.5 m are considerably large, while those at depths of 5.5 to 10 m are relatively small, particularly for the case with the ϕ value assumed at 20°.

4.5. Possibility of Recurrence of Landsliding

Fig. 4.10 shows the probable sliding lines of possible landslides on the topography identified by the field survey made for this Study.

The probable sliding line Nos. 1 through 9 are all at the elevations higher than EL.180 m. The ground at these elevations is more or less poor, and is believed to be the fill-up for preparation of the batcher plant site. The probable sliding line Nos. 10 through 14 are all at the elevations lower than EL.180 m. The ground at these elevations is believed to be the original mountain mass.

The topography at the elevations lower than EL.180 m is rather steep in the slope, but there are no traces of landslides, and outcrops of bed rocks are seen in some places. It is therefore believed that a shallow landslide of any weathered surface layers, if happened, may not cause any serious subsequent landslide.

The purpose of the examination of the line Nos. 10 through 14 was, therefore, not to investigate the possibility of landslide recurrences, but to determine the physical properties of the mountain mass that are required for assurance of the safety for long.

Fig. 4.10 Probable Sliding Lines of Possible Landslides

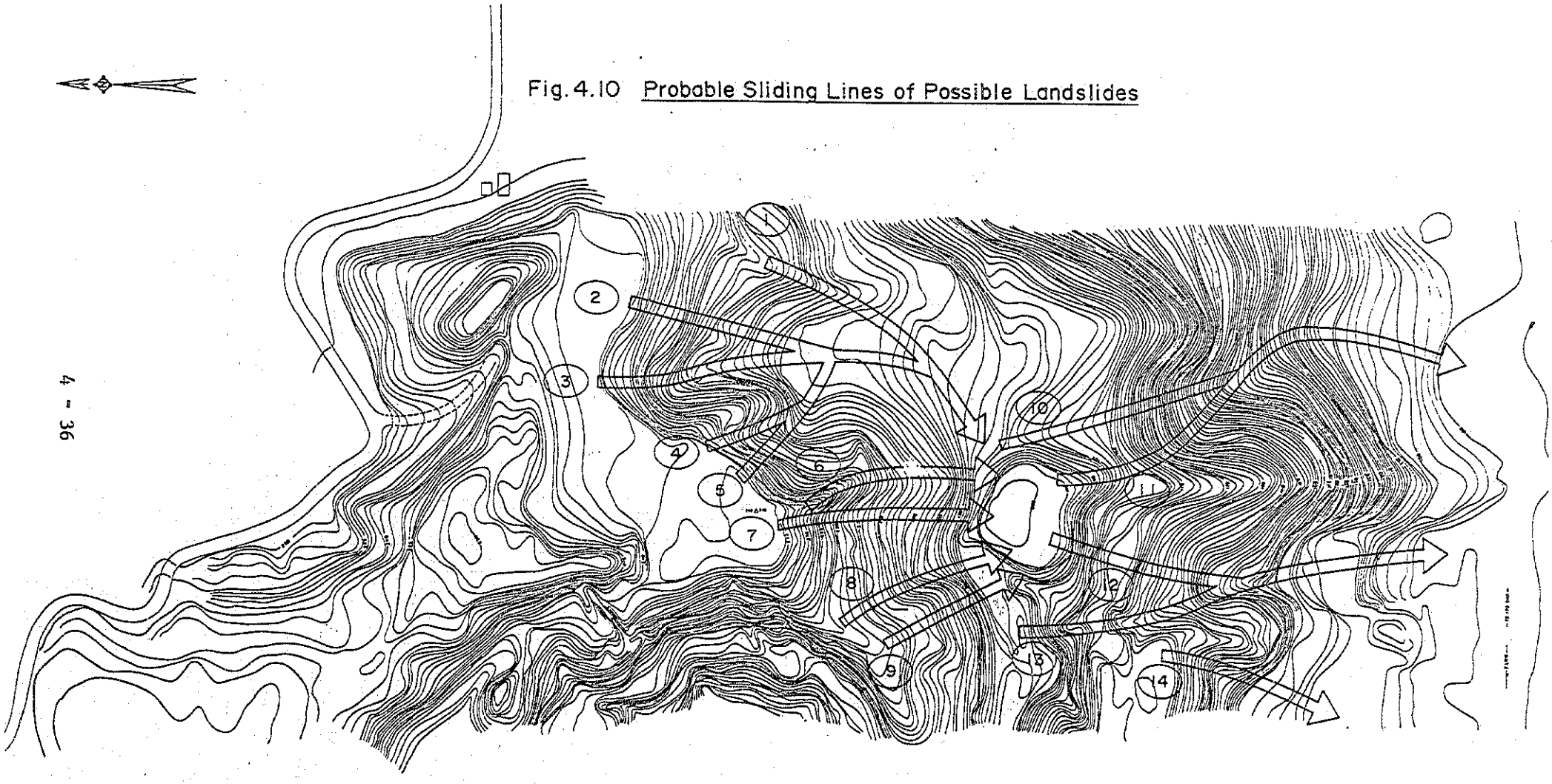

4.5.1. Supposed Physical Properties of the Mountain Mass

As discussed in the foregoing subsection, the mountain mass for analyses on the landsliding possibility can be grouped into two. One is the group (A) consisting of poor subsoil which is considered to be within the bounds of the landsliding possibility. The other is the group (B) made up of the original mountain mass with the N values of greater than 50 (by the penetration tests) which is considered to be out of the bounds of the landsliding possibility. The elevation EL.180 m was made a boundary line dividing the mountain mass into two groups.

Analyses on the possibility of landsliding in group A were made of the following two cases of physical properties:

Case	ϕ	C (ton/m^2)		
		Ground Surface	At a Depth of 6 m	At a Depth of 10 m
Case 1	10°	3	8	12
Case 2	20°	1	4	7

4.5.2. Calculations for Analyses

Calculations for the analyses on the possibility of landsliding were made of the following three cases.

	Ground Water Table	Seismic Force
Case A	Up to the ground surface	None
Case B	None	0.15 g
Case C	Up to the ground surface	0.15 g

The probable sliding line Nos. 1 through 9 at the elevations higher than EL.180 m can be represented by the typical five lines, Nos. 2, 3, 5, 7 and 9, when compared in detail. Similarly, the probable sliding line Nos. 10 through 14 at the elevations lower than EL.180 m can be represented by the typical two lines Nos. 12 and 14.

The analyses on the possibility of landsliding were, therefore, made only on Nos. 2, 3, 5, 7 and 9 for the elevations higher than EL.180 m, and Nos. 12 and 14 for the elevations lower than EL.180 m.

Fig.4.11 shows the longitudinal profiles of these probable sliding lines.

4.5.3. Method of Calculations

Since the established conventional method was used for the calculations, no particular explanations for the methodology are given in this Report.

4.5.4. Results of Calculations

(For Elevations Higher Than EL.180 m)

Tabulated in Tables 4.13.1 through 4.13.3 are the results of calculations for the analyses on the possibility of landsliding. Data given in the Tables are on the sliding line with the least safety factor by probable sliding line. The line with the least safety factor was selected among a large number of possible sliding lines passing through each of given node points on the respective probable sliding line. The node points are shown in Fig.4.11. These points were set up at an equal interval of one to two meters between turning points of the gradient of the slope.

Fig. 4.11 Longitudinal Profiles of the Probable Sliding Lines

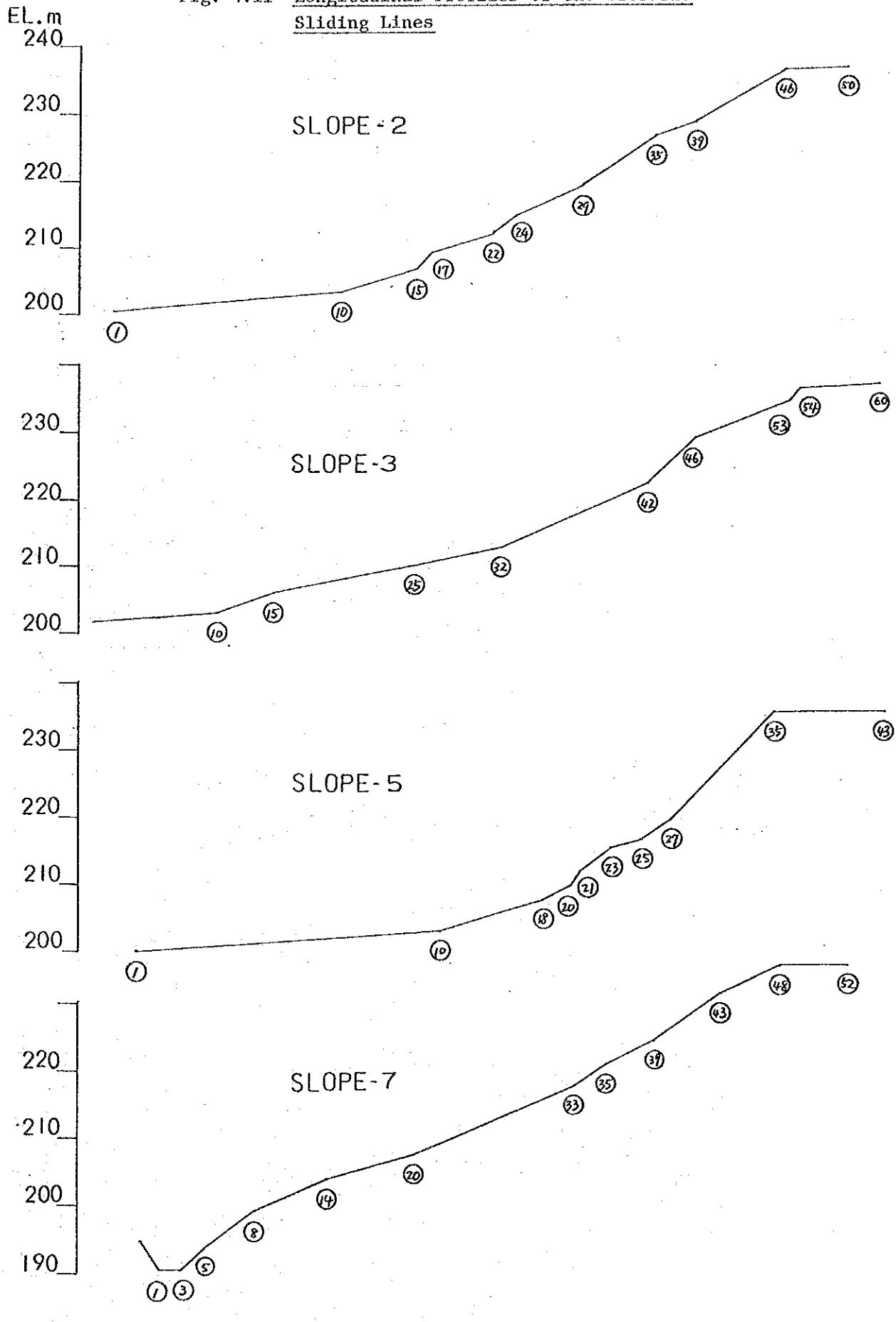

Longitudinal Profiles of the Probable Sliding Lines (Fig. 4.11 continued)

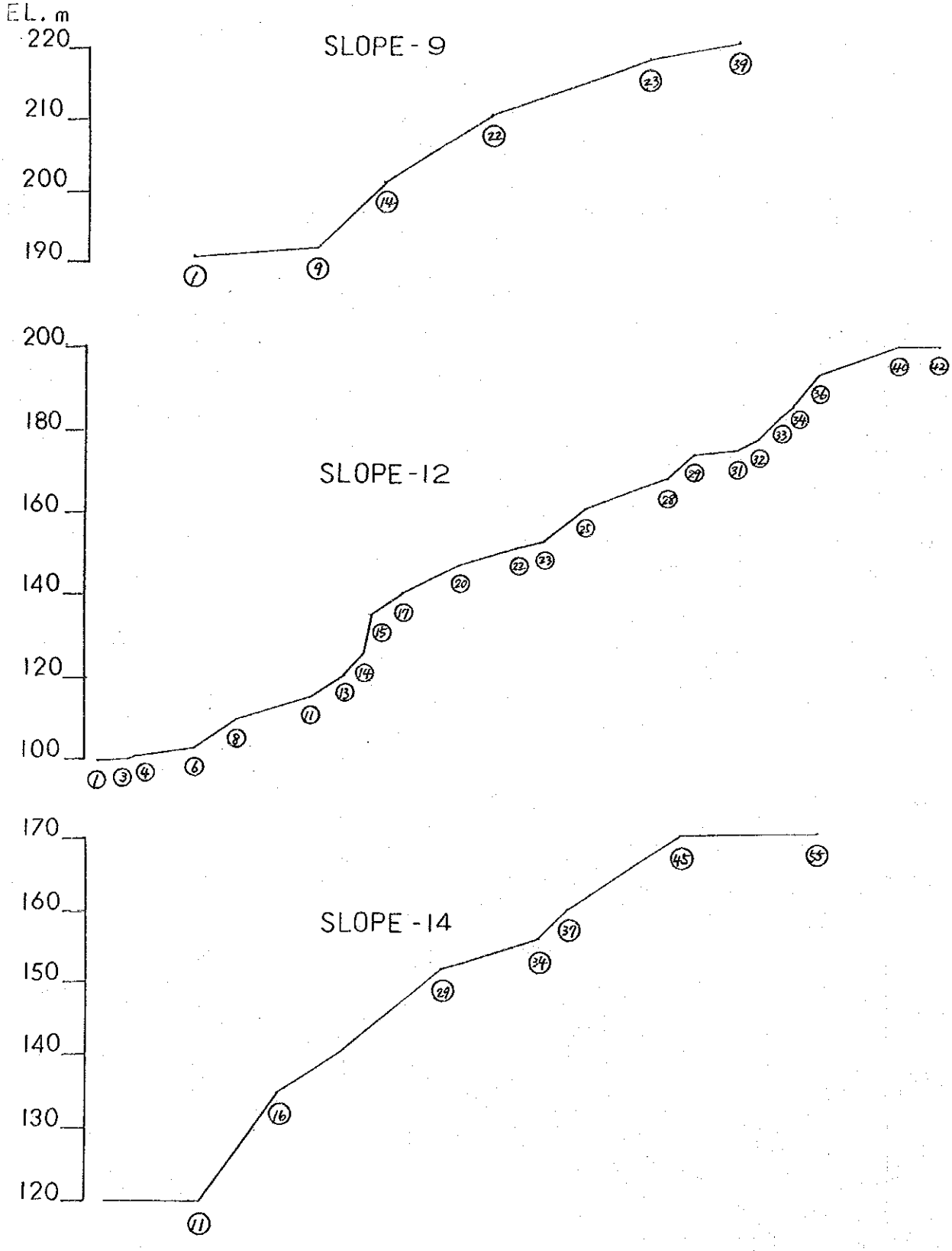

Table 4.13.1 Results of Analysis on Possibilities of Landsliding Calculations in Case A (Underground Water: Up to the Ground Surface; Seismic Force: Zero)

		(1)	(2)	(3)	(4)	(5)	(6)
	Probable Sliding Line	Least Safety Factor Against Sliding	Starting & Ending Points of the Sliding Line	Radius of the Sliding Line (m)	Sliding Resistance of the Sliding Surface (ton)	Sliding Force of the Sliding Line (ton)	Short Shearing Resistance of the Sliding Line (ton)
In case of ϕ = 10°	No. 2	1.781	48 - 22	67.67	442.17	248.20	-193.96
	No. 3	1.748	60 - 32	76.05	517.81	296.24	-221.57
	No. 5	1.344	40 - 19	61.92	388.81	289.30	-99.51
	No. 7	1.871	53 - 1	72.63	2684.73	1434.72	-1250.02
	No. 9	1.866	25 - 9	90.24	212.30	113.77	-98.53
	No.12	1.075	42 - 5	145.49	5974.05	5555.86	-418.20
	No.14	1.454	50 - 6	70.65	2199.69	1512.49	-687.20
In case of ϕ = 20°	No. 2	0.997	48 - 22	67.67	247.43	248.20	+0.77
	No. 3	1.003	56 - 33	44.83	251.57	250.73	-0.84
	No. 5	0.711	40 - 19	52.36	205.61	289.30	+83.69
	No. 7	1.075	49 - 8	143.77	272.60	253.64	-18.95
	No. 9	0.846	25 - 9	90.24	96.23	133.77	+17.53
	No.12	1.073	42 - 5	145.49	5959.09	5555.86	-403.24
	No.14	1.440	50 - 6	70.65	2178.33	1512.49	-665.84

Table 4.13.2 Analysis on Possibilities of Landsliding Calculations in Case B (Underground Water: None; Seismic Force: 0.15g)

		(1)	(2)	(3)	(4)	(5)	(6)
	Probable Sliding Line	Least Safety Factor Against Sliding	Starting & Ending Points of the Sliding Line	Radius of the Sliding Line (m)	Sliding Resistance of the Sliding Surface (ton)	Sliding Force of the Sliding Line (ton)	Short Shearing Resistance of the Sliding Line (ton)
In case of ϕ = 10°	No. 2	1.680	50 - 22	95.10	514.82	306.46	-208.37
	No. 3	1.624	60 - 32	76.05	566.43	348.76	-217.67
	No. 5	1.366	40 - 19	61.92	429.28	314.19	-115.09
	No. 7	1.750	53 - 12	142.60	765.53	437.45	-328.08
	No. 9	1.824	25 - 9	90.24	228.27	125.14	-103.13
	No.12	1.432	42 - 5	160.42	8314.90	5807.47	-2507.43
	No.14	1.754	51 - 11	95.83	2504.03	1427.74	-1076.29
In case of ϕ = 20°	No. 2	1.154	48 - 22	67.67	329.25	285.23	-44.02
	No. 3	1.160	56 - 33	44.83	335.26	288.90	-46.36
	No. 5	0.920	40 - 19	61.92	289.16	314.19	+25.03
	No. 7	1.206	50 - 4	243.83	463.04	383.84	-79.20
	No. 9	1.032	25 - 9	90.24	129.21	125.14	-4.06
	No.12	1.429	42 - 5	160.42	8301.02	5807.47	-2493.55
	No.14	1.744	51 - 11	95.83	2490.51	1427.74	-1062.77

Table 4.13.3 Analysis on Possibilities of Landsliding Calculations in Case C (Underground Water: Up to the Ground Surface; Seismic Force: 0.15g)

		(1)	(2)	(3)	(4)	(5)	(6)
	Probable Sliding Line	Least Safety Factor Against Sliding	Starting & Ending Points of the Sliding Line	Radius of the Sliding Line (m)	Sliding Resistance of the Sliding Surface (ton)	Sliding Force of the Sliding Line (ton)	Short Shearing Resistance of the Sliding Line (ton)
In case of ϕ = 10°	No. 2	1.366	50 - 22	95.10	465.08	340.51	-124.57
	No. 3	1.317	60 - 32	76.05	510.24	387.51	-122.73
	No. 5	1.094	40 - 19	61.92	382.04	349.10	-32.94
	No. 7	1.350	53 - 1	72.63	2563.62	1898.63	-664.99
	No. 9	1.505	25 - 9	90.24	209.29	139.05	-70.24
	No.12	0.803	42 - 4	150.07	5757.37	7173.84	+1416.47
	No.14	1.113	50 - 7	70.75	2158.15	1939.36	-218.78
In case of ϕ = 20°	No. 2	0.738	48 - 22	67.67	233.88	316.92	+83.05
	No. 3	0.742	56 - 33	44.83	238.30	321.00	+82.70
	No. 5	0.549	40 - 19	61.92	191.64	349.10	+157.46
	No. 7	0.774	49 - 8	143.77	258.75	334.44	+75.70
	No. 9	0.647	25 - 9	90.24	90.02	139.05	+49.03
	No.12	0.800	42 - 4	150.07	5742.57	7173.84	+1431.27
	No.14	1.099	51 - 4	82.06	2008.72	1828.53	-180.20

Column (1) in the Table shows the least safety factor against sliding. Column (2) shows the starting and ending points of the sliding line with the least safety factor. The numbers in the column are the respective node point Nos. as given in Fig.4.11. Column (3) shows the radius of such sliding line.

Column (4) in the Table shows the sliding resistance force along the sliding line with the least safety factor. Column (5) shows a sum of the sliding force of such sliding line. Column (6) shows the short shearing resistance of such sliding line. The negative shows the surplus of shearing resistance against the safety factor of 1.0, while the positive shows the shortage of shearing resistance against the safety factor of 1.0.

Shown in the upper right of Fig.4.12 is the distribution curve of the least safety factors. Each point in the curve indicates the least safety factor among numbers of possible sliding lines, each starting from the corresponding nodal point. Shown in the upper left of the Figure is also the distribution curve of the least safety factors. In this curve, each point indicates the least safety factor among numbers of possible sliding lines, each ending at the corresponding nodal point. The sliding line connecting the lowest points of both curves shows the most probable sliding line with the least safety factor of all probable sliding lines.

Table 4.14 shows a comparison of the short shearing resistance of the sliding line with the least safety factor with the ϕ value assumed at 20° among three different cases (Case A: ground water up to the ground surface but no seismic force taken into account, Case B: no underground water in existence but a seismic force of 0.15 g to be taken into account, and Case C: underground water up to the ground surface and a seismic force of 0.15 g to be taken into account).

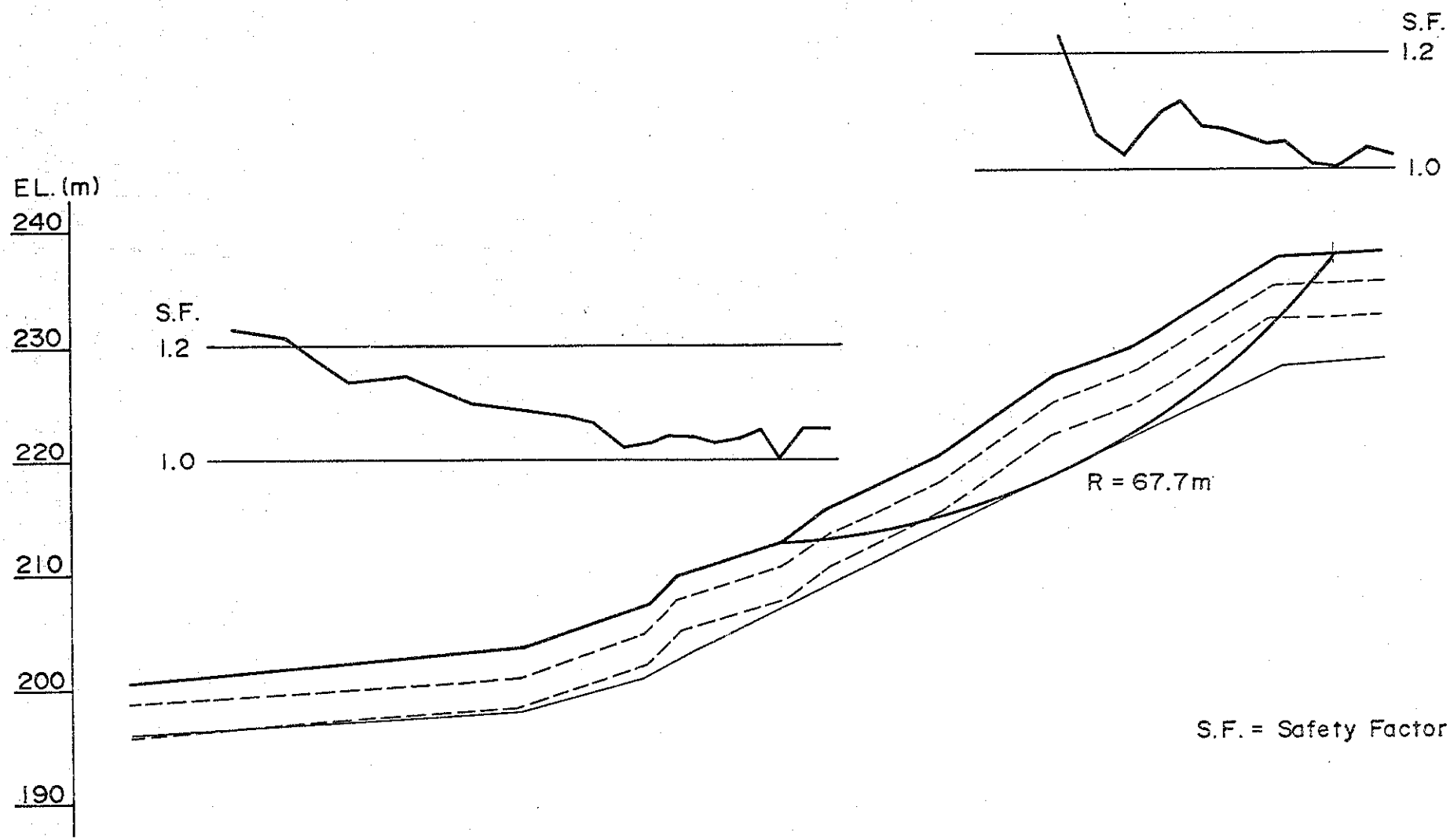

Fig. 4.12.1 Analyses on Possible Sliding Lines
(Line No. 2, Case A)

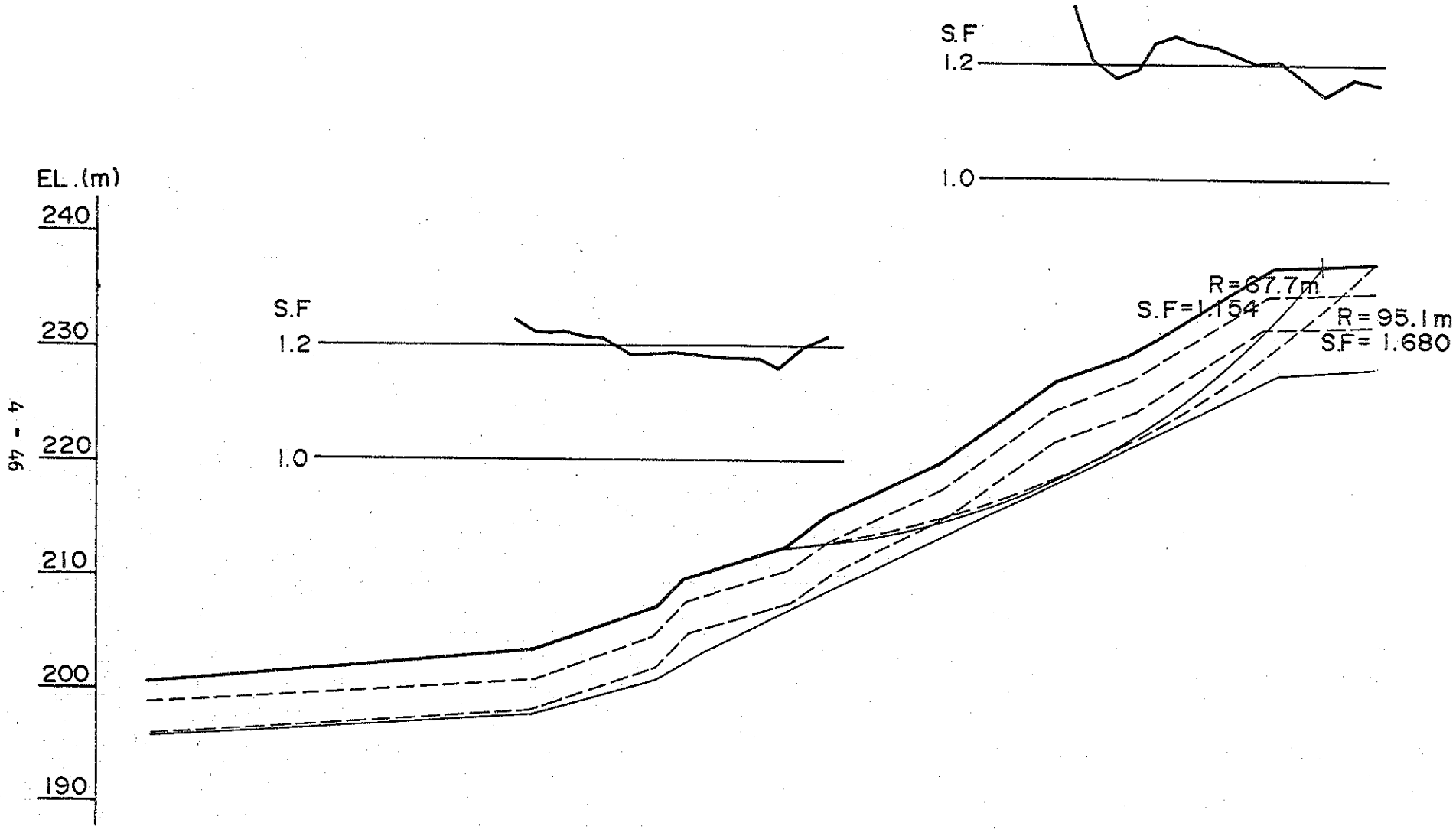

Fig. 4.12.2 Analyses on Possible Sliding Lines
(Line No. 2 Case B)

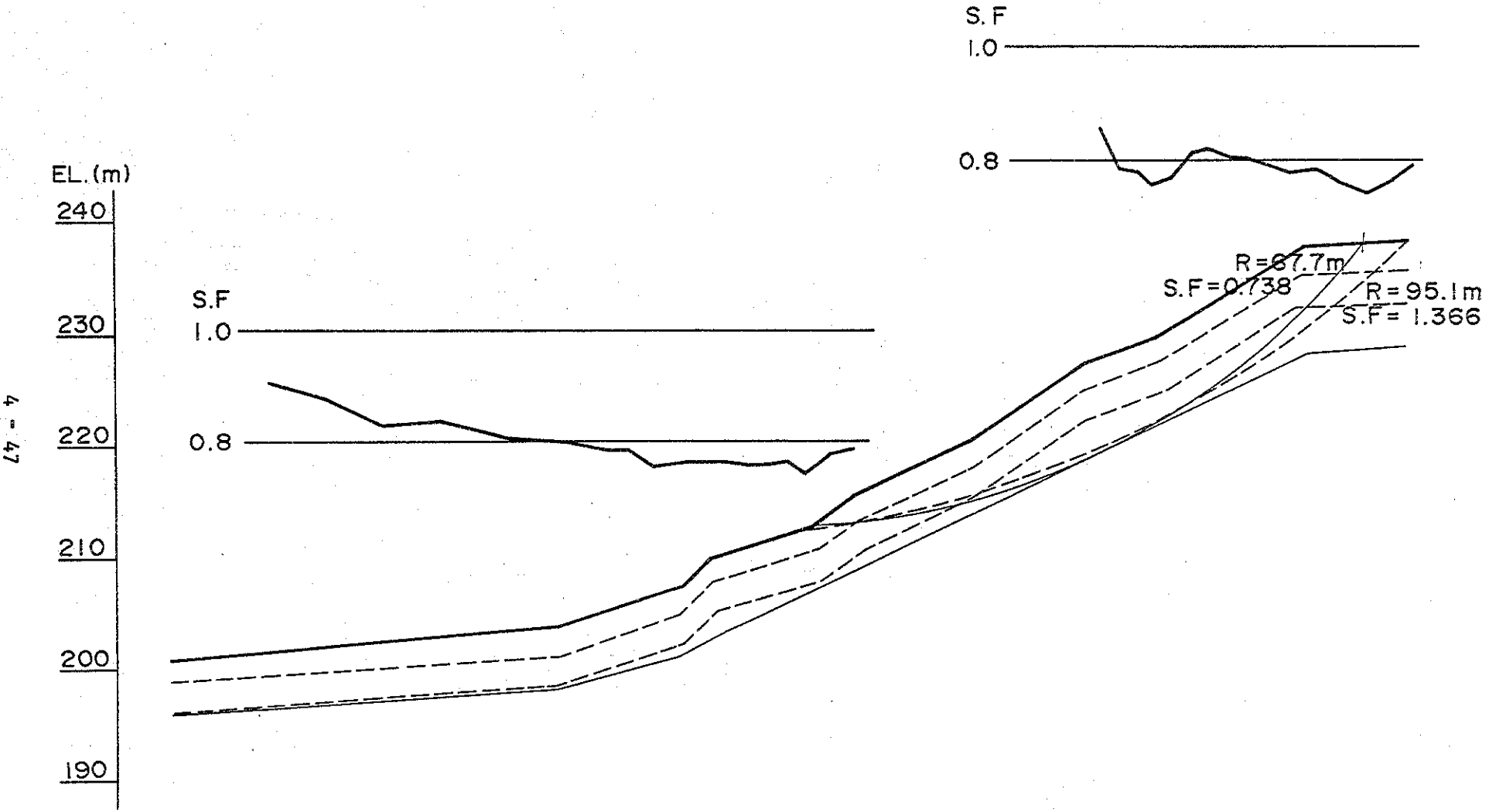

Fig. 4.12.3 Analyses on Possible Sliding Lines
(Line No. 2 Case C)

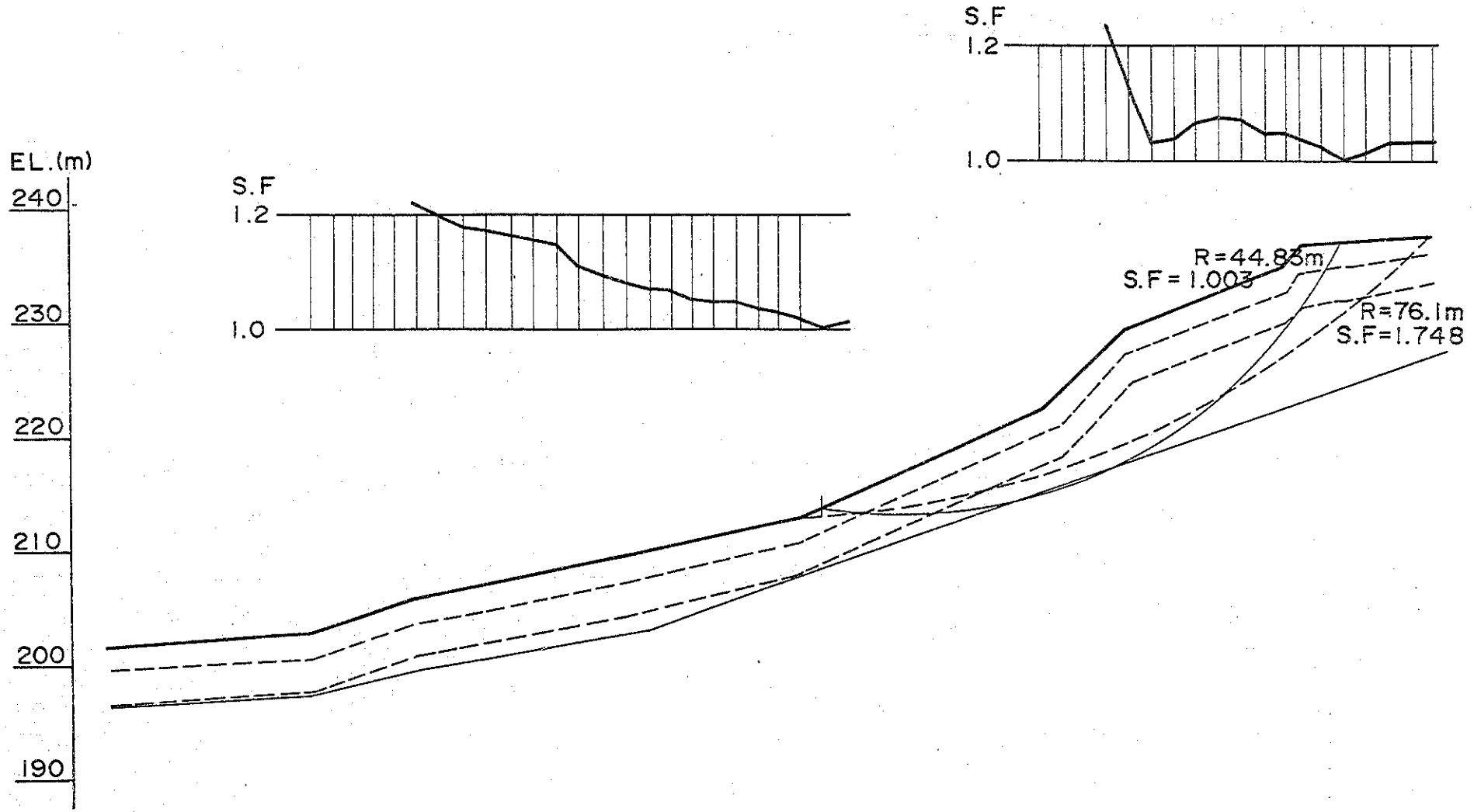

Fig. 4.12.4 Analyses on Possible Sliding Lines
(Line No.3 Case A)

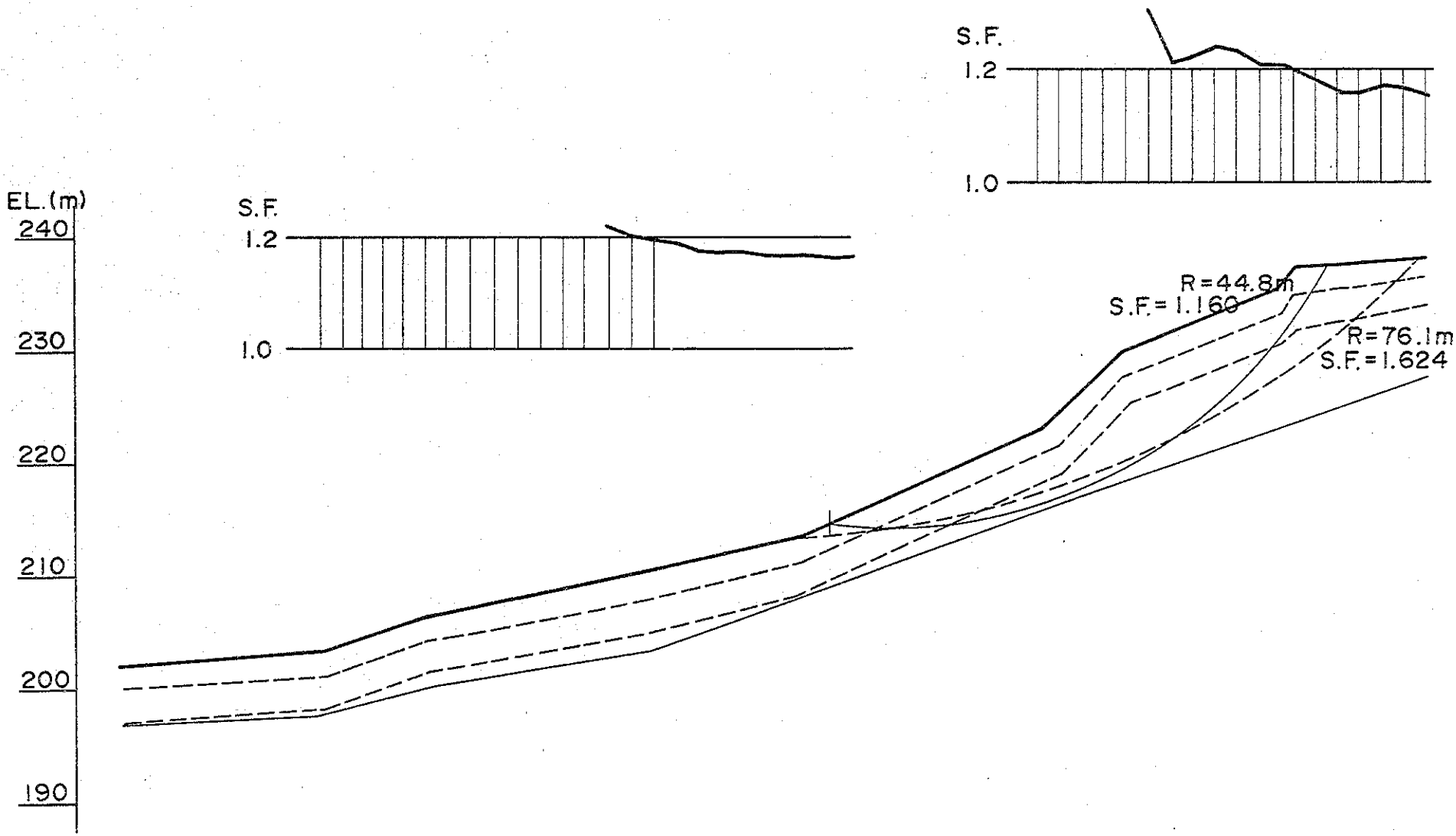

Fig. 4.12.5 Analyses on Possible Sliding Lines
(Line No.3 Case B)

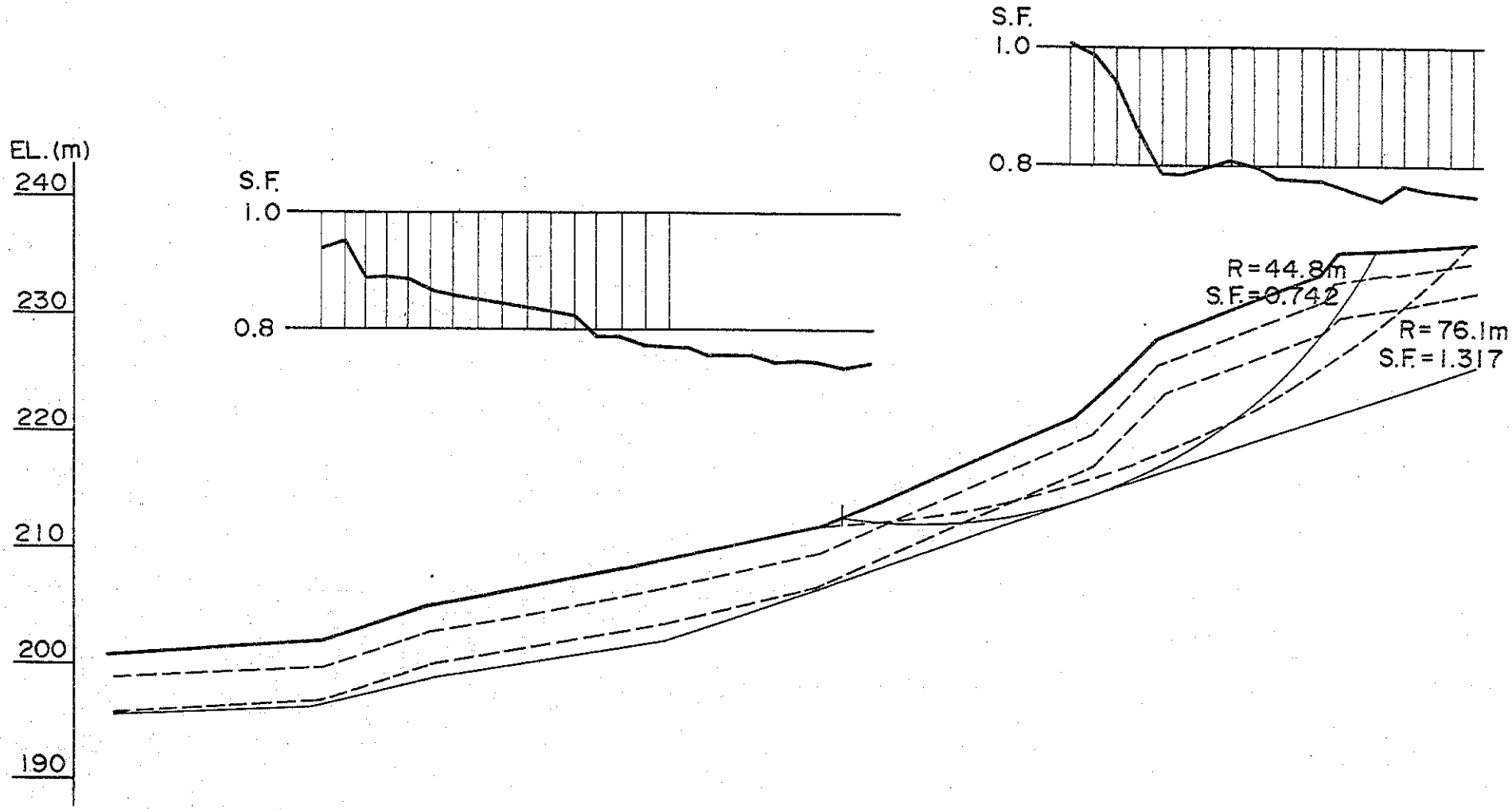

Fig. 4.12.6 Analyses on Possible Sliding Lines
(Line No.3 Case C)

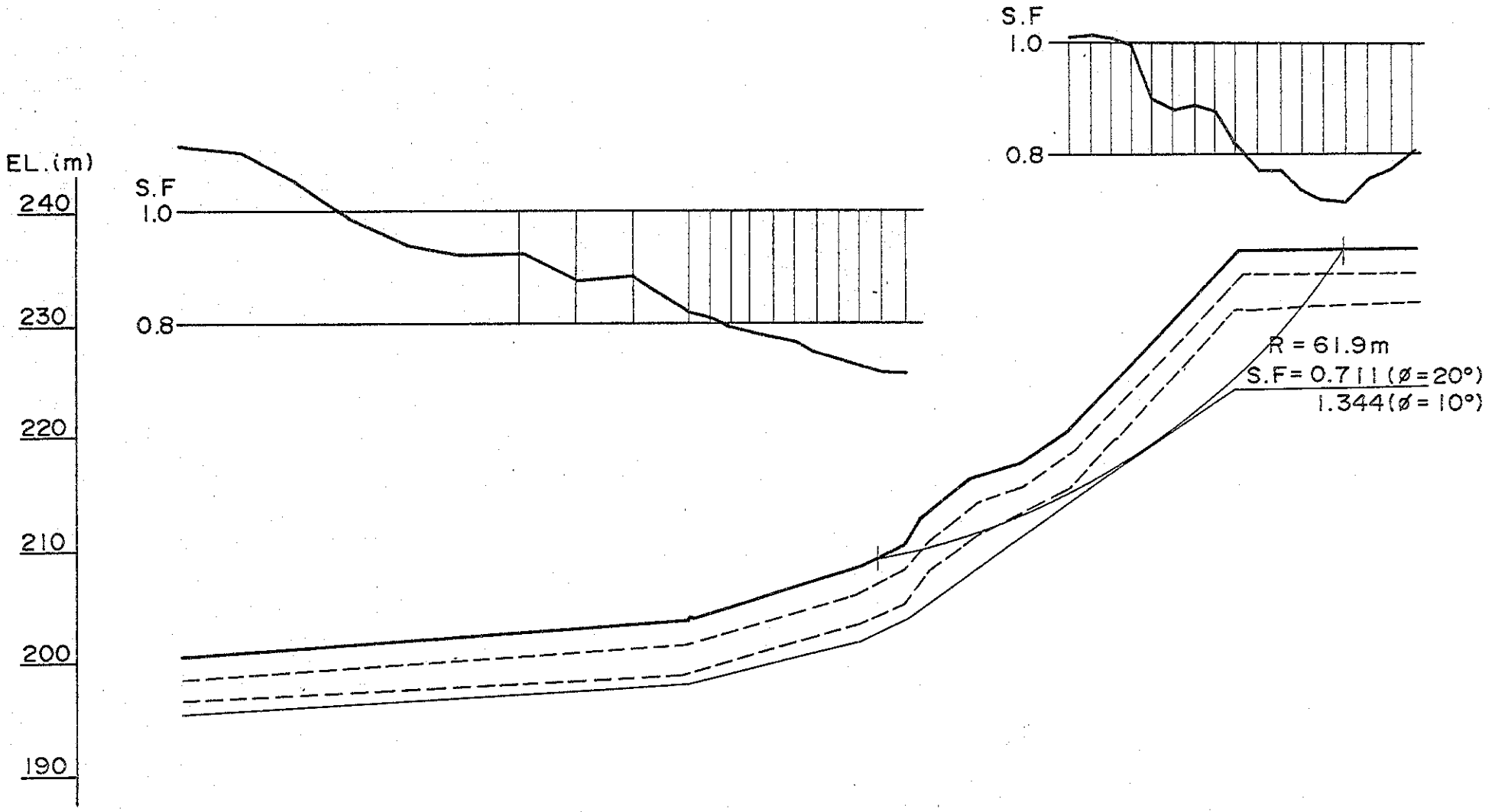

Fig. 4.12.7 Analyses on Possible Sliding Lines
(Line No 5, Case A)

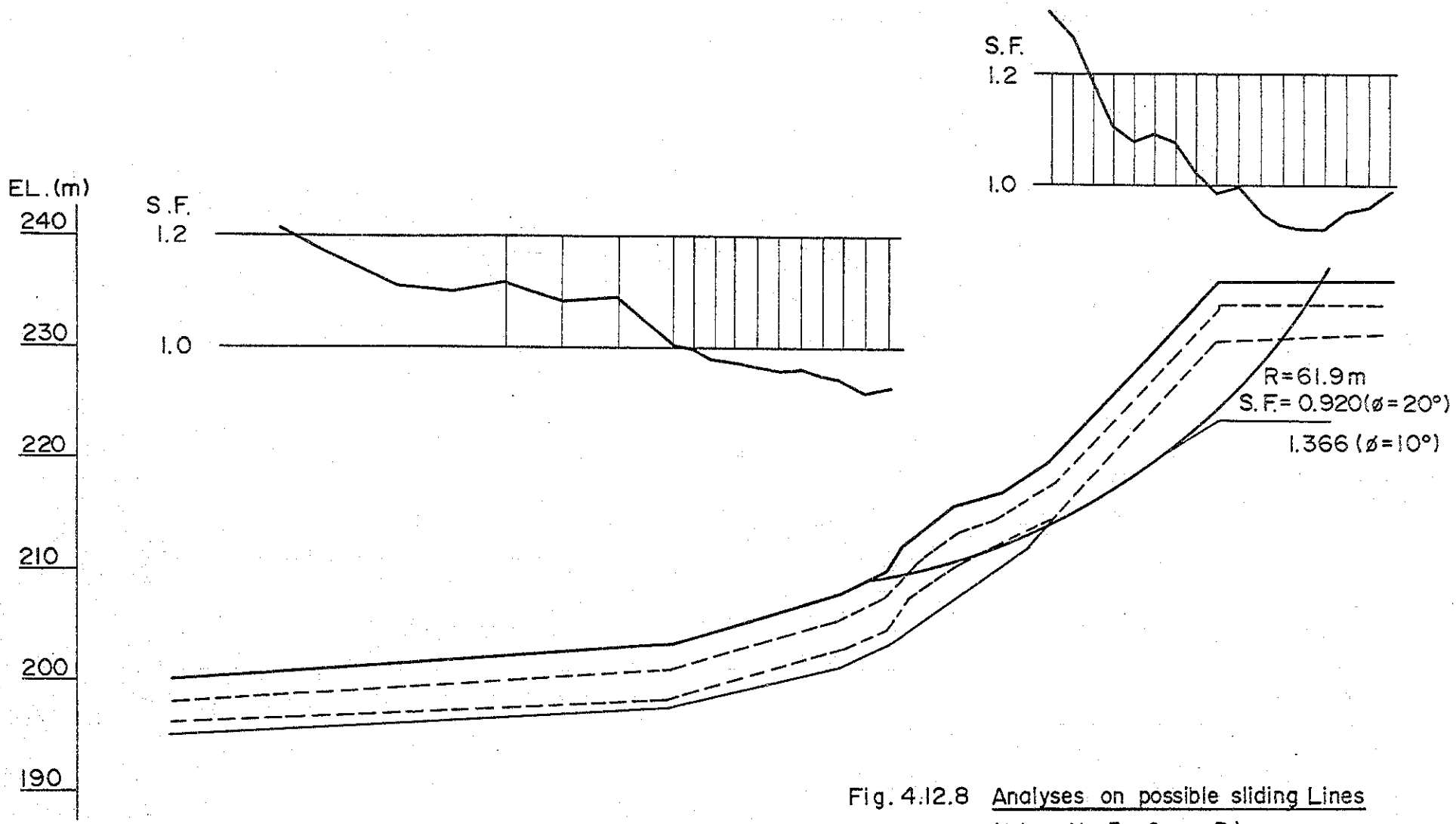

Fig. 4.12.8 Analyses on possible sliding Lines
(Line No.5, Case B)

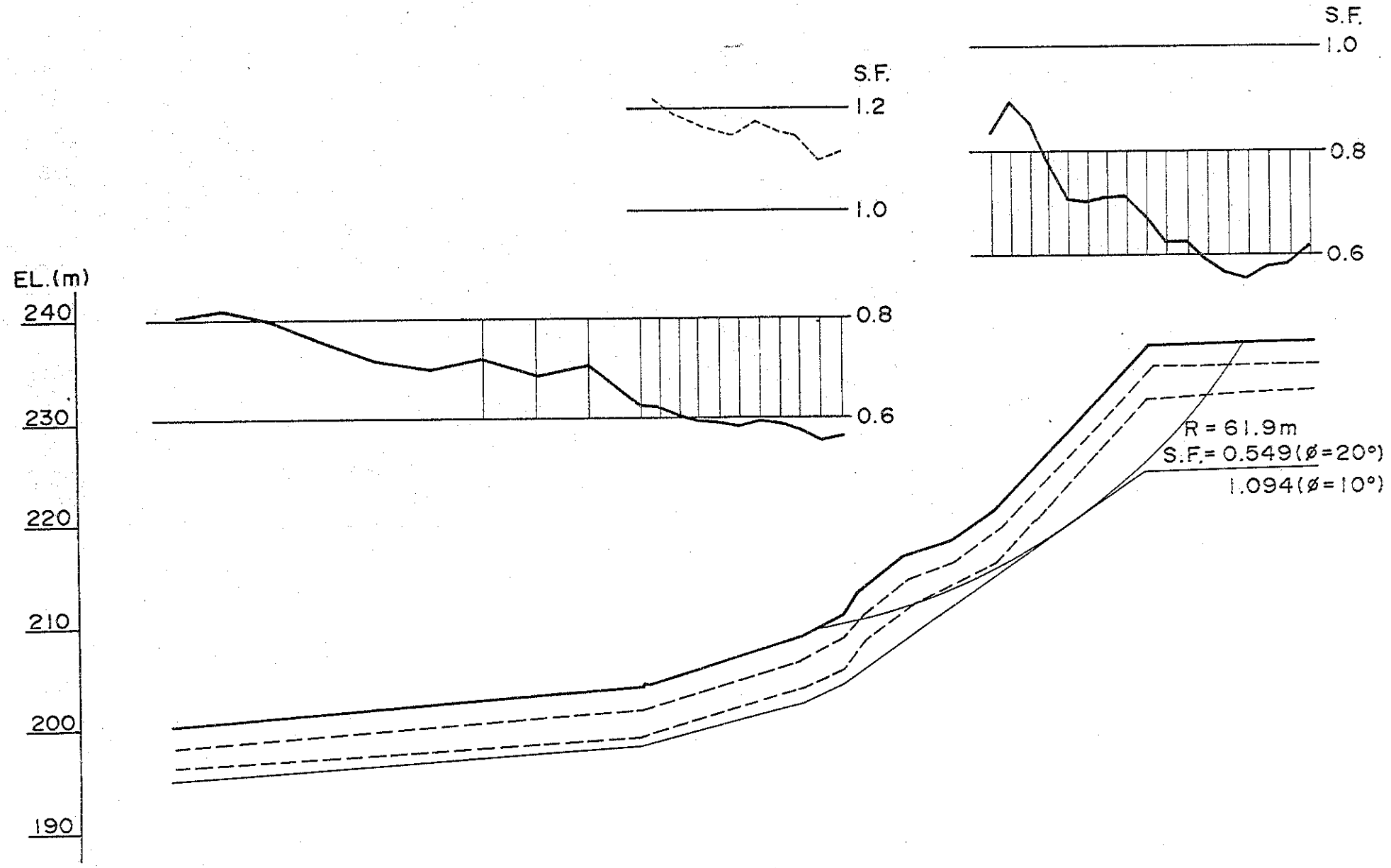

Fig. 4.12.9 Analyses on Possible Sliding Lines
(Line No 5 , Case C)

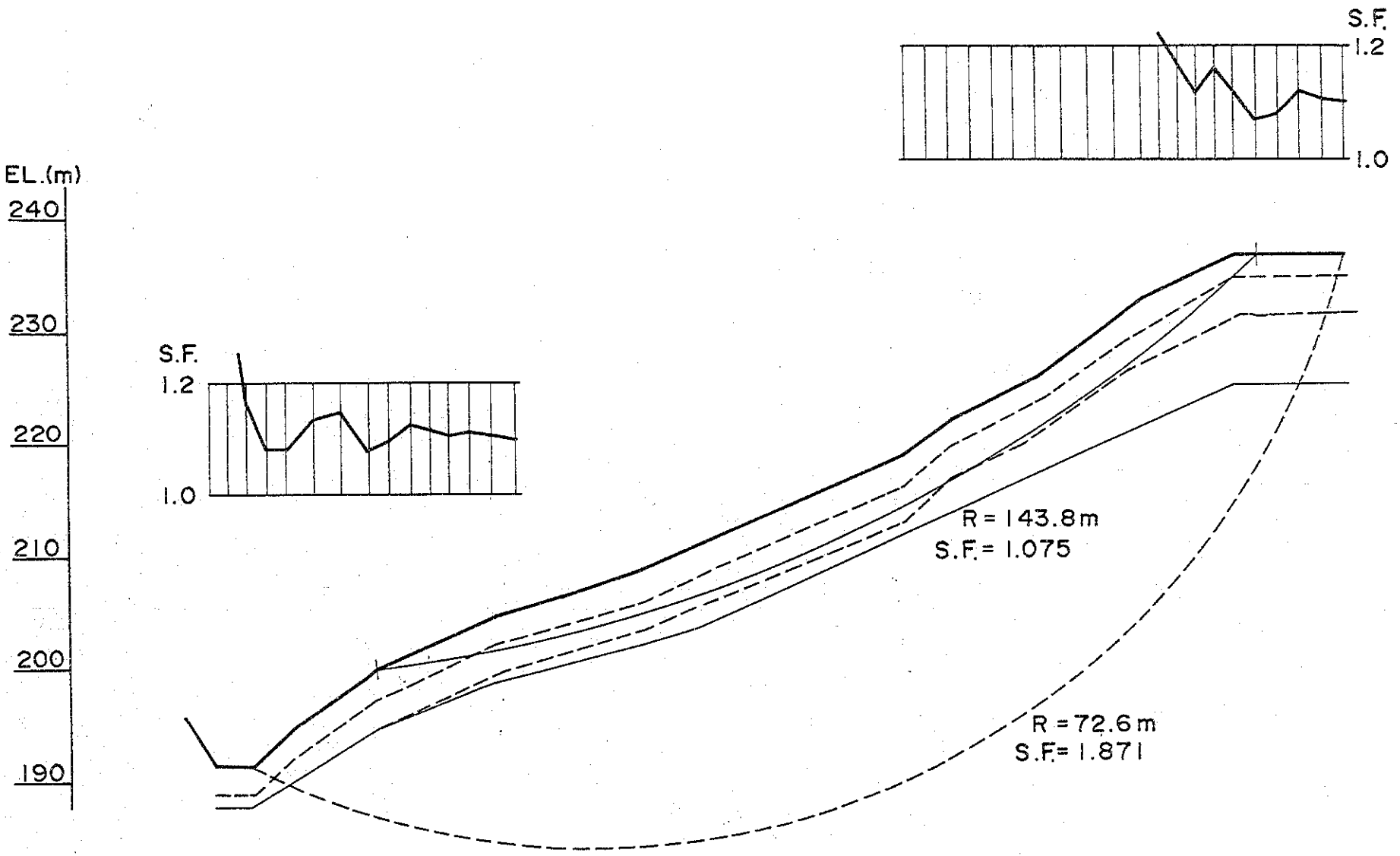

Fig. 4.12.10 Analyses on Possible Sliding Lines
(Line No. 7, Case A)

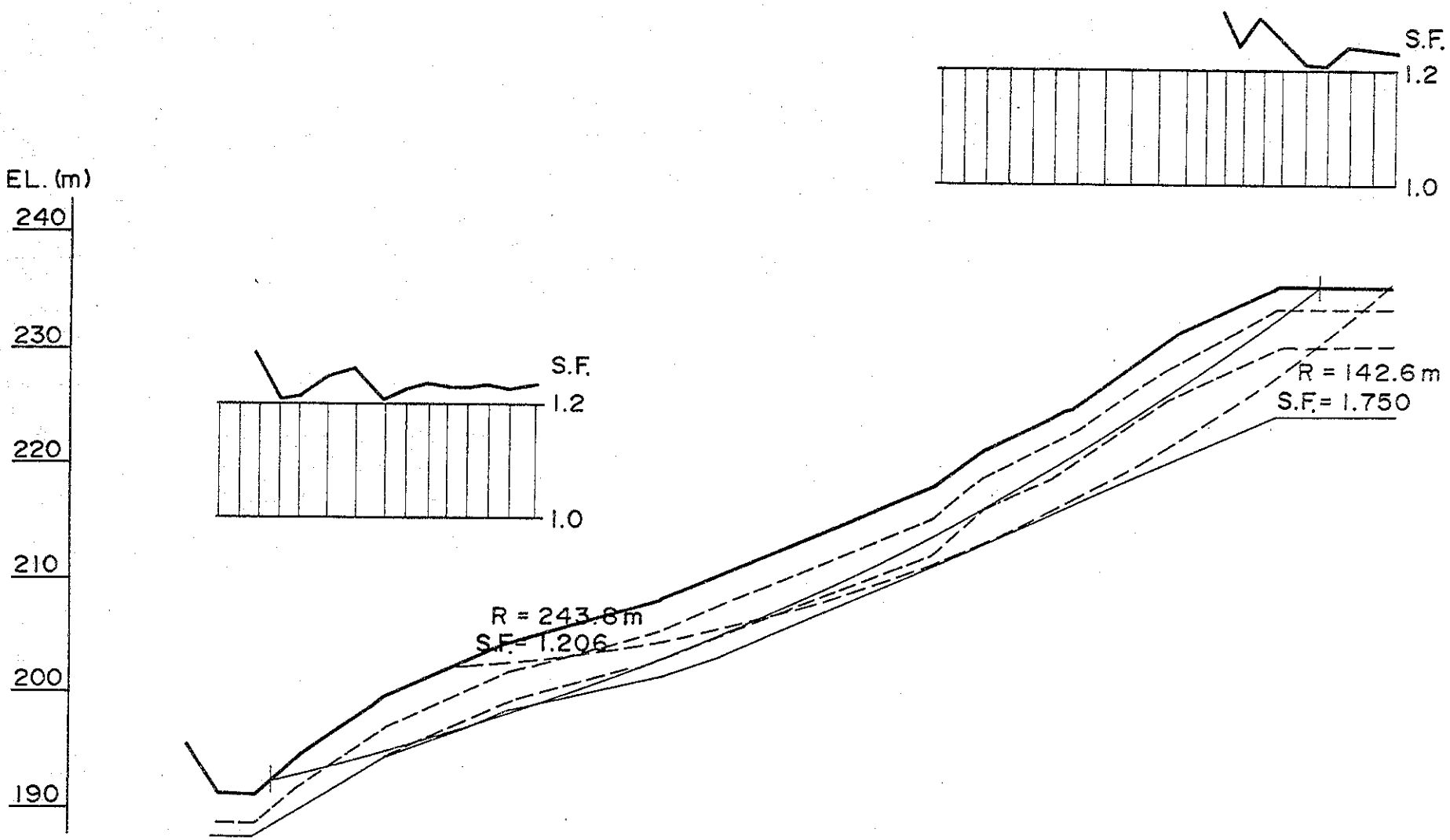

Fig. 4.12.11 Analyses on Possible Sliding Lines
(Line No 7, Case B)

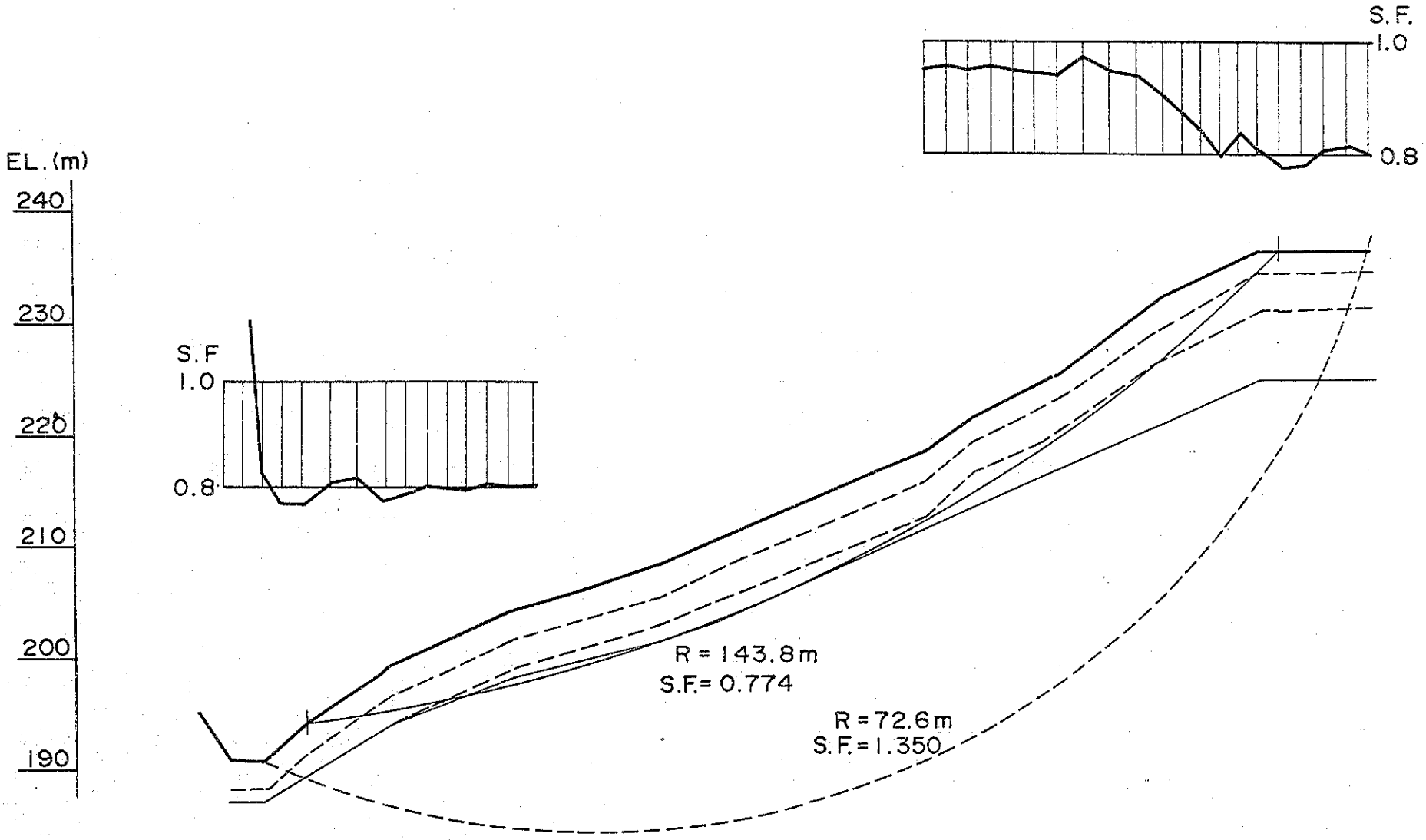

Fig. 4.12.12 Analyses on Possible Sliding Lines
(Line No.7, Case C)

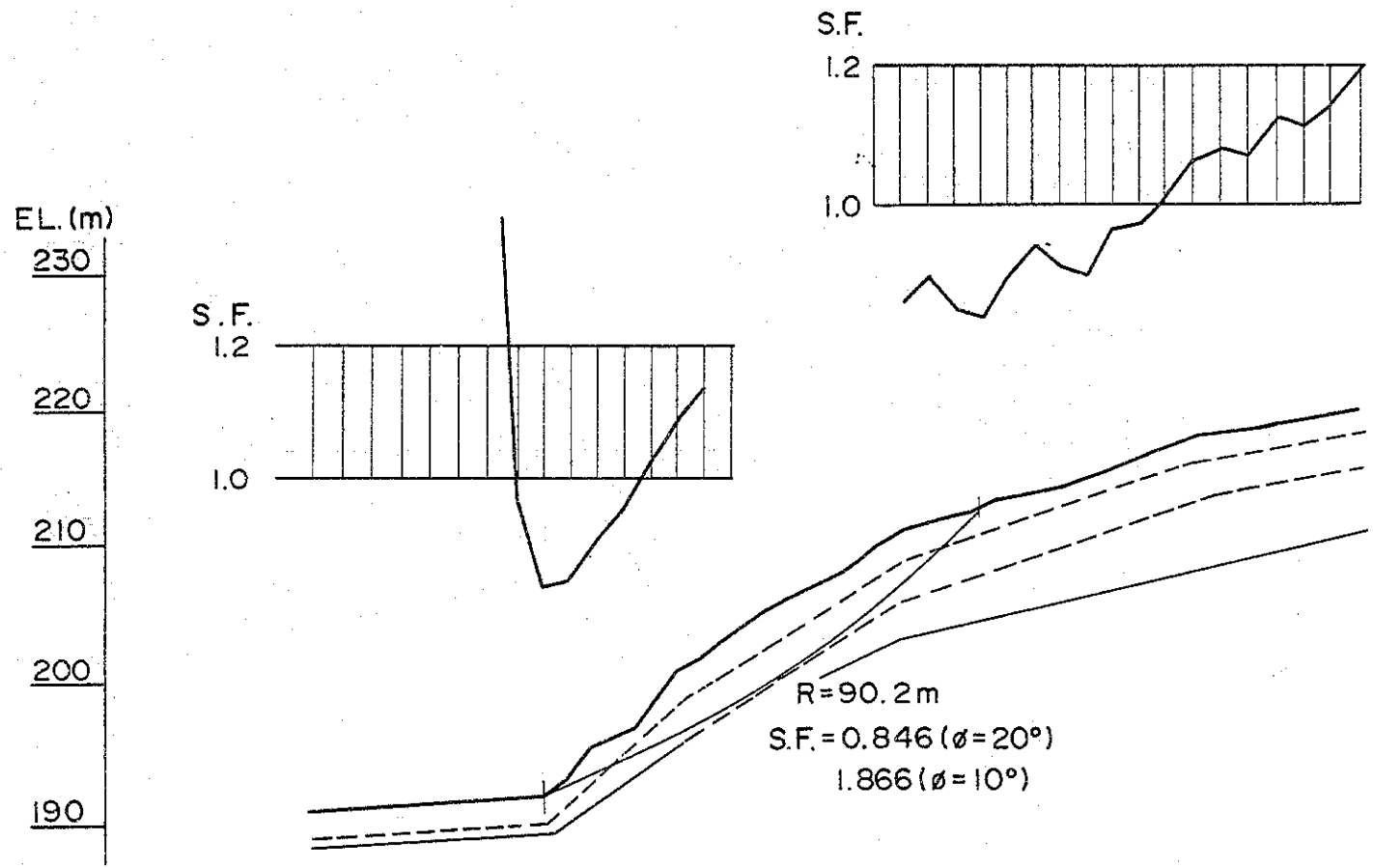

Fig. 4.12.13 Analyses on Possible Sliding Lines
(Line No. 9, Case A)

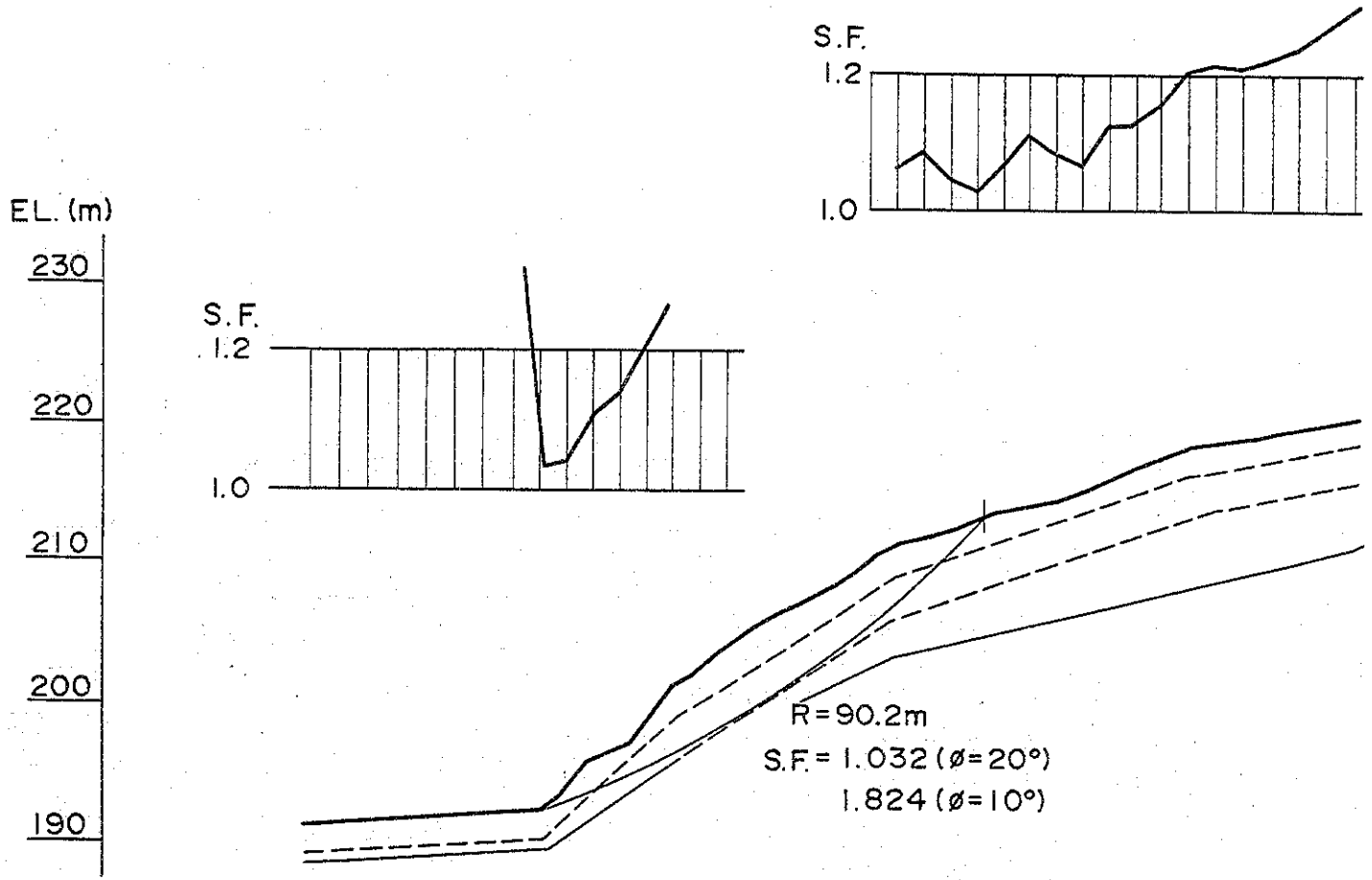

Fig. 4.12.14 Analyses on Possible Sliding Lines
(Line No. 9, Case B)

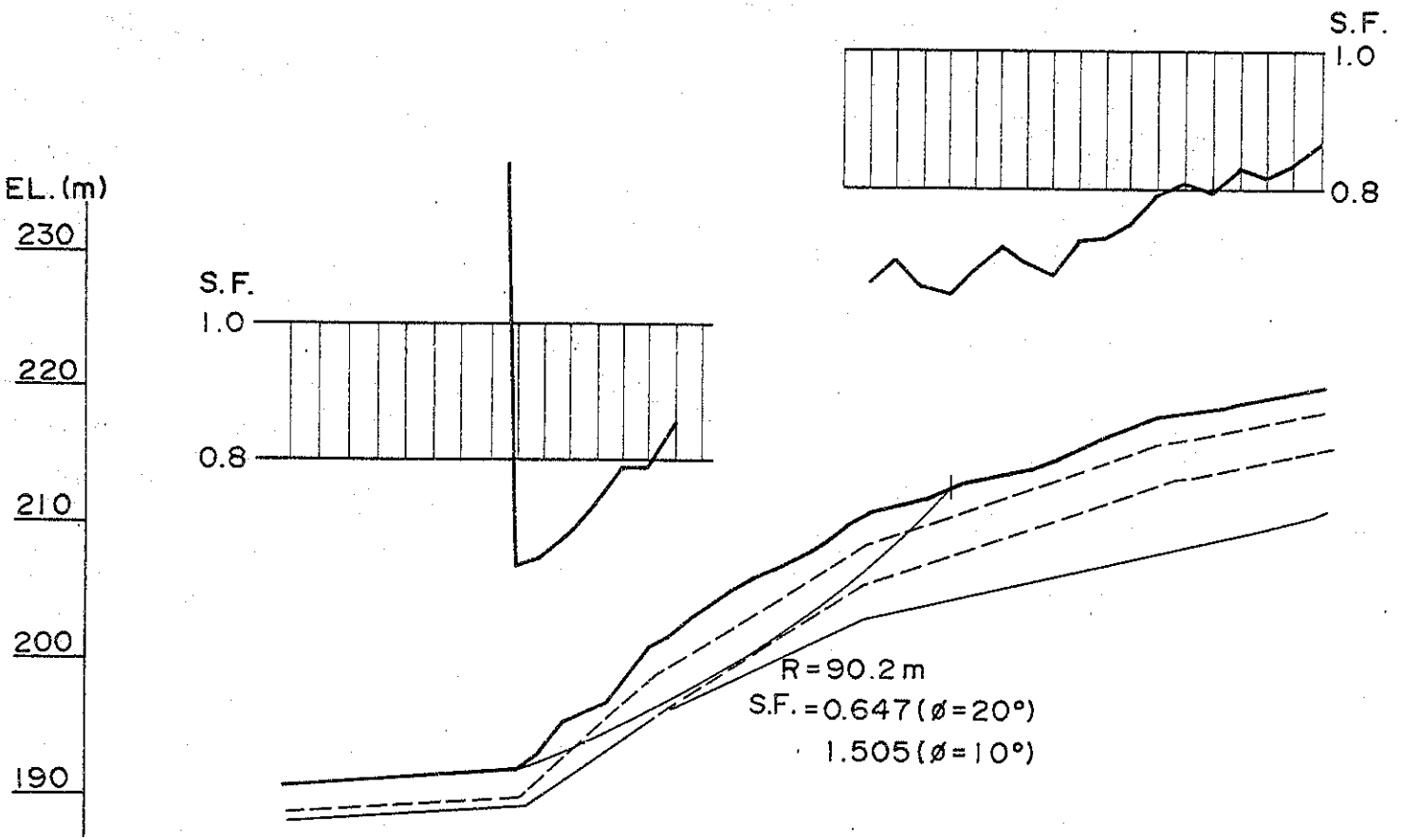

Fig. 4.12.15 Analyses on Possible Sliding Lines
(Line No. 9, Case C)

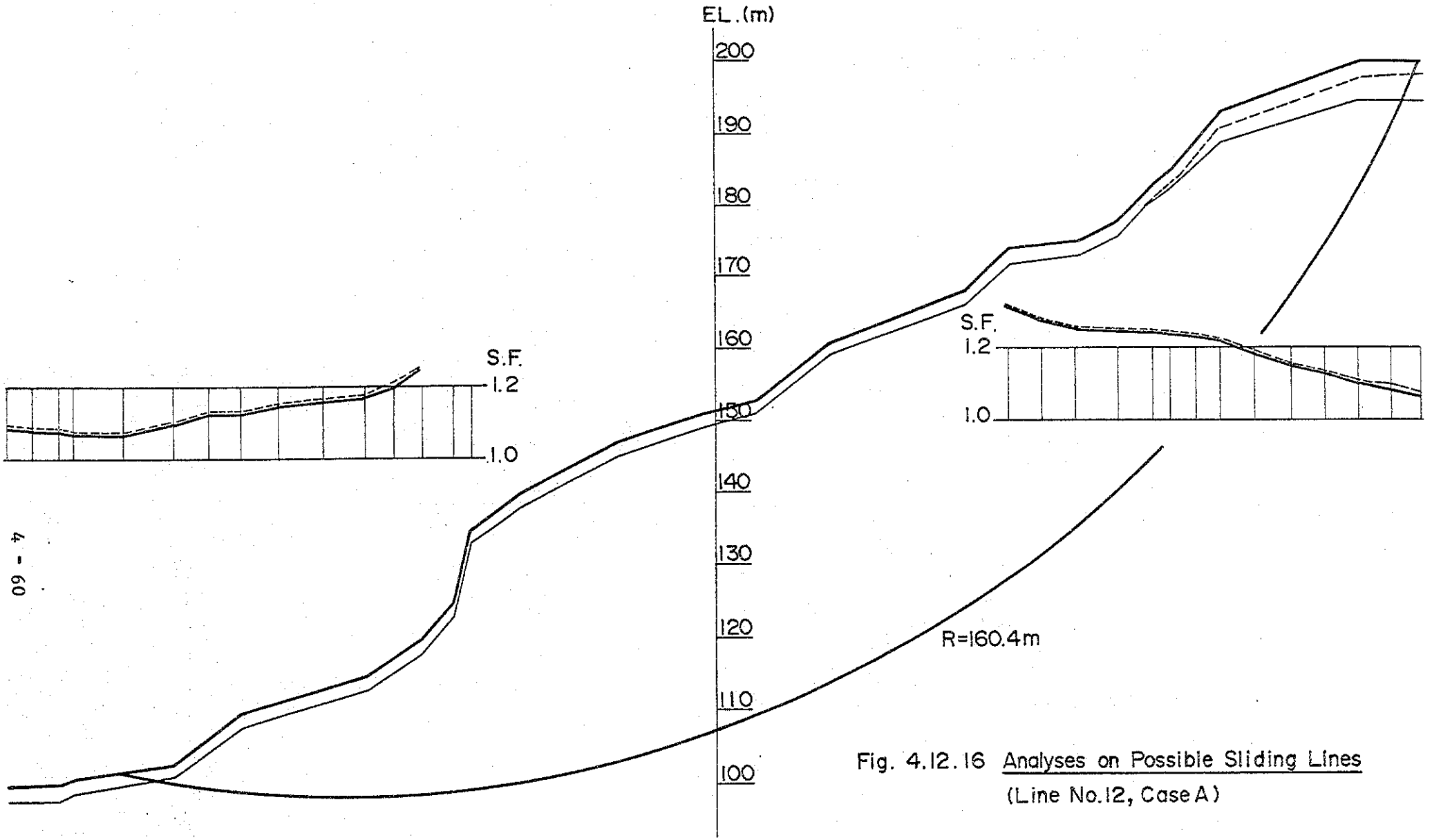

Fig. 4.12.16 Analyses on Possible Sliding Lines
(Line No.12, Case A)

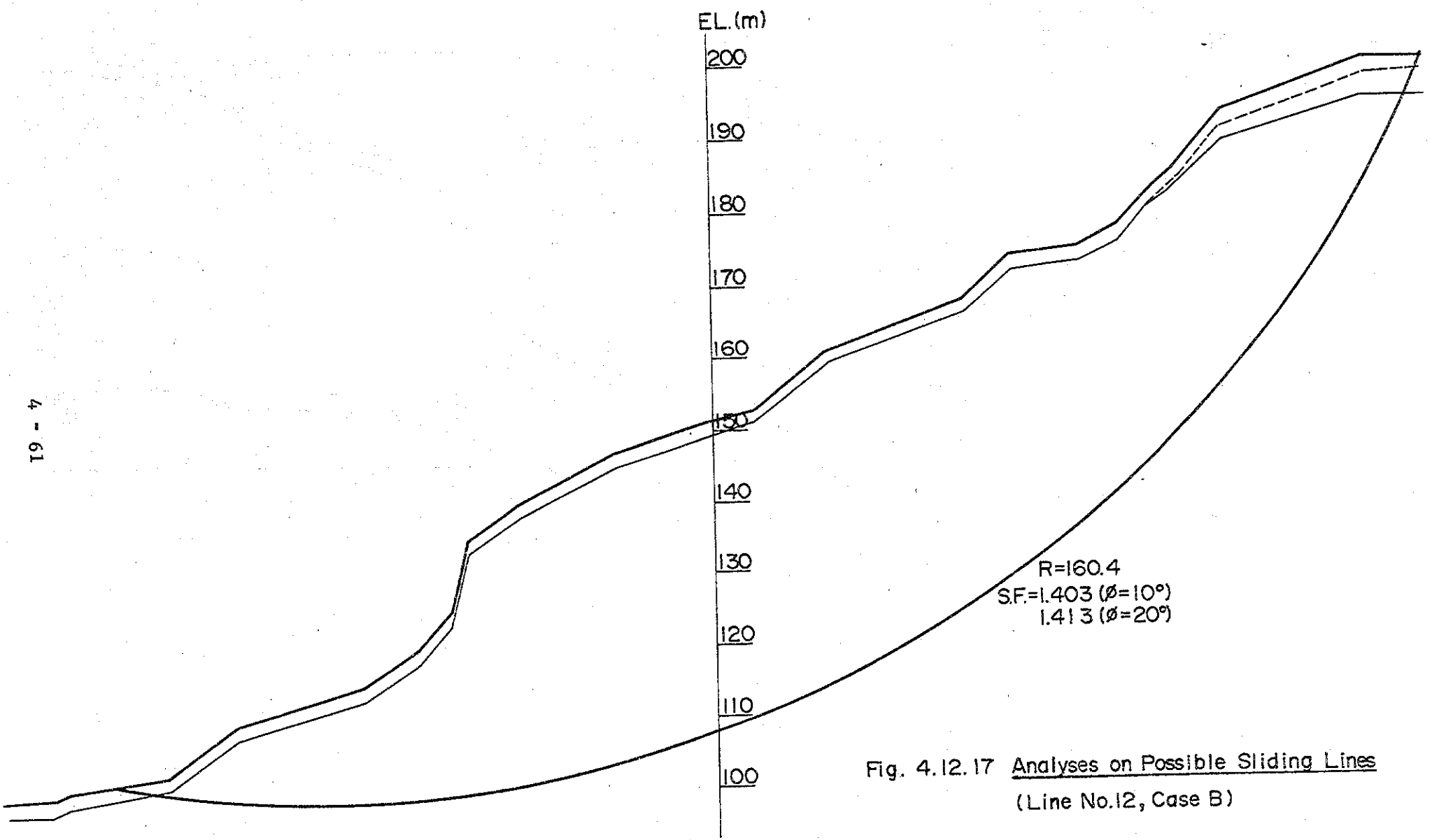

Fig. 4.12.17 Analyses on Possible Sliding Lines
(Line No.12, Case B)

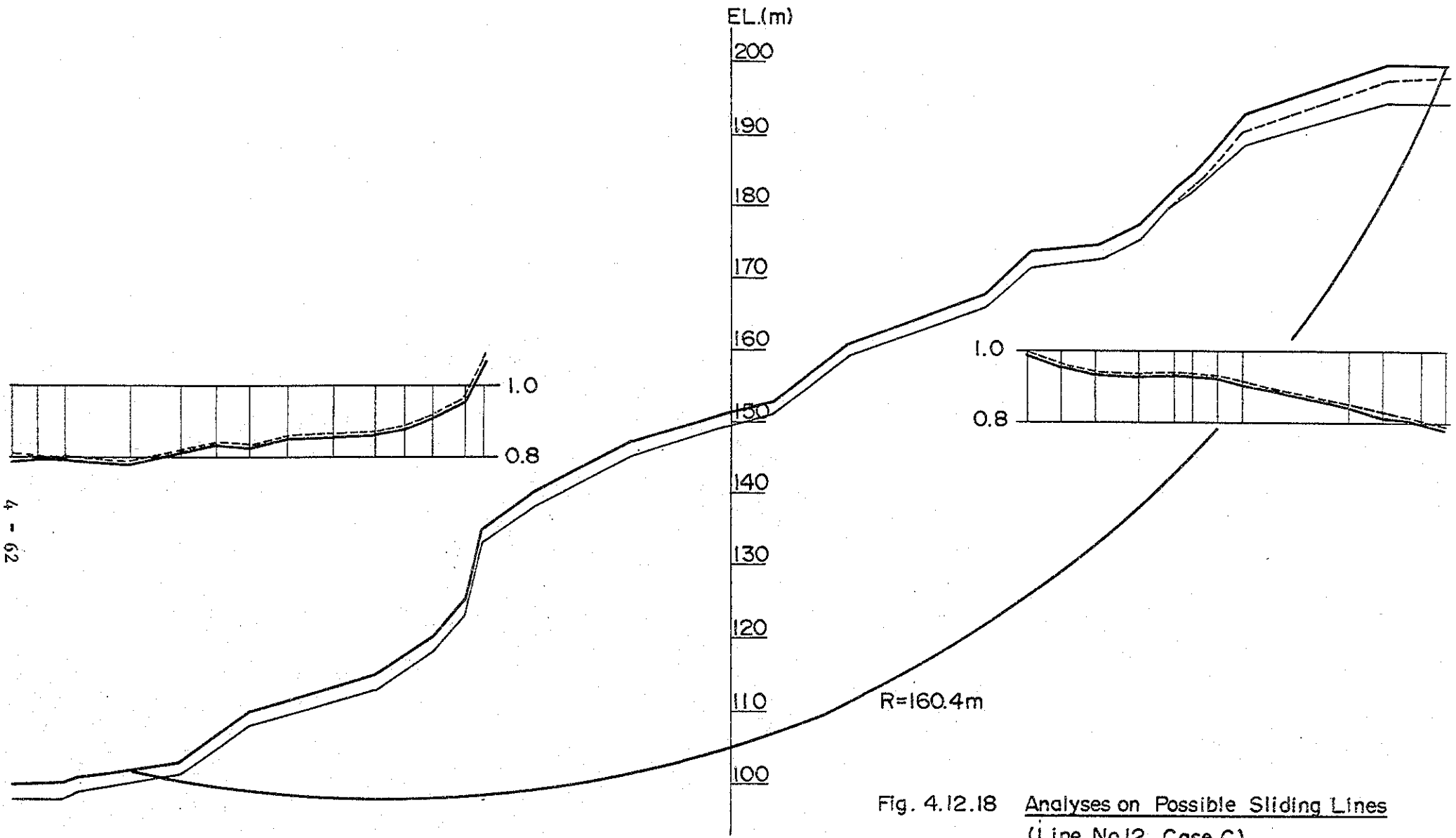

Fig. 4.12.18 Analyses on Possible Sliding Lines
(Line No.12, Case C)

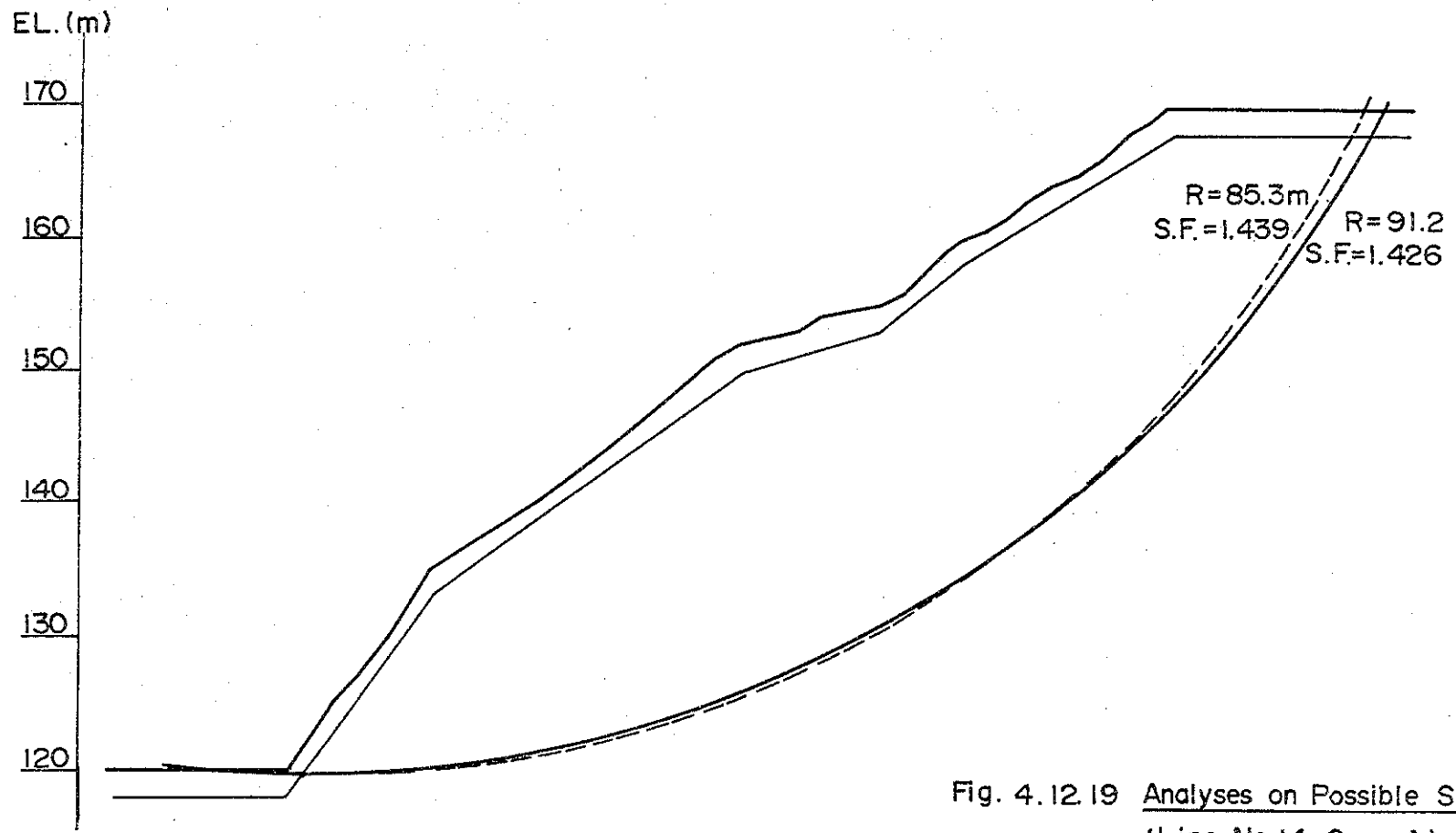

Fig. 4.12.19 Analyses on Possible Sliding Lines
(Line No.14, Case A)

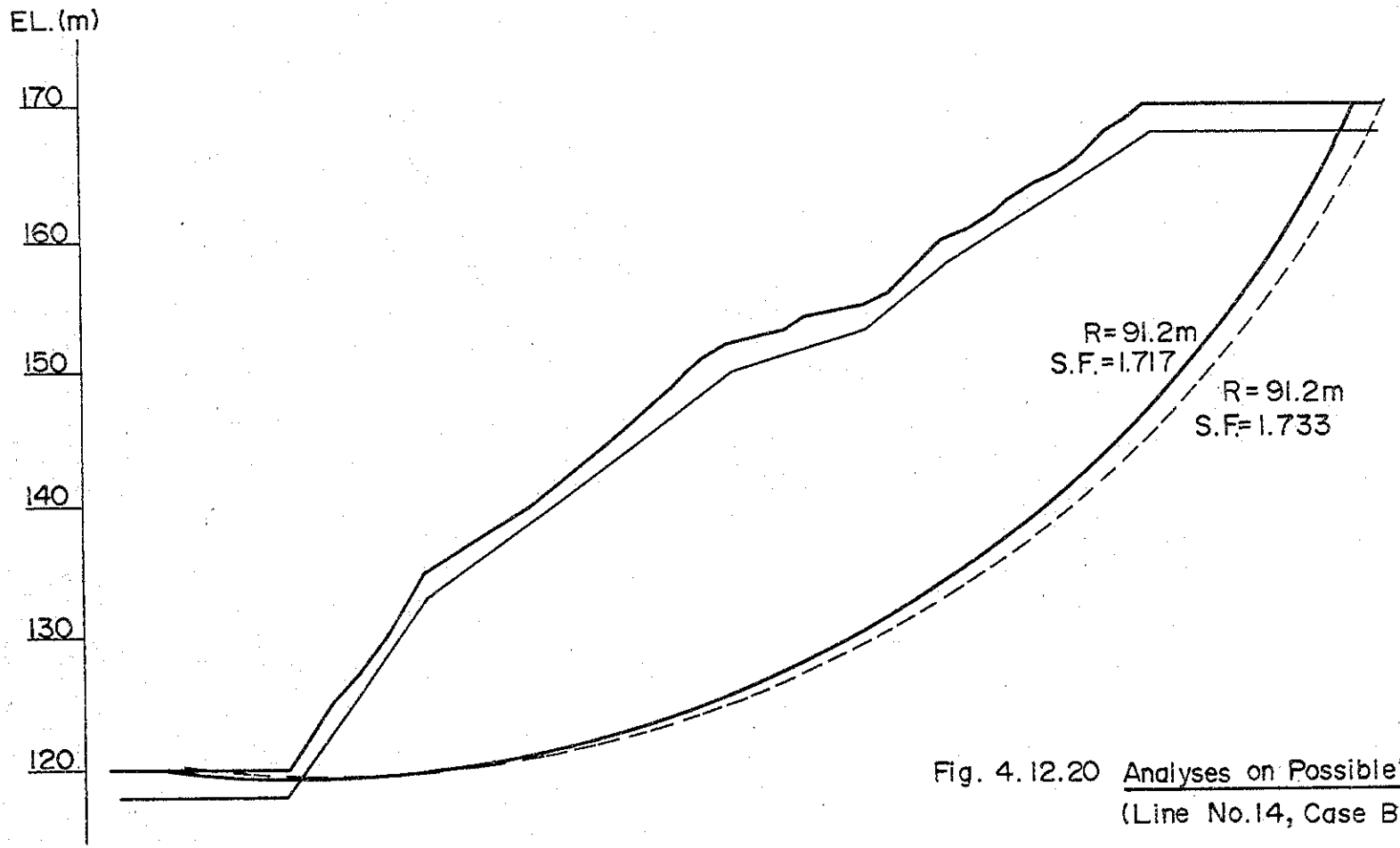

Fig. 4.12.20 Analyses on Possible Sliding Lines
(Line No.14, Case B)

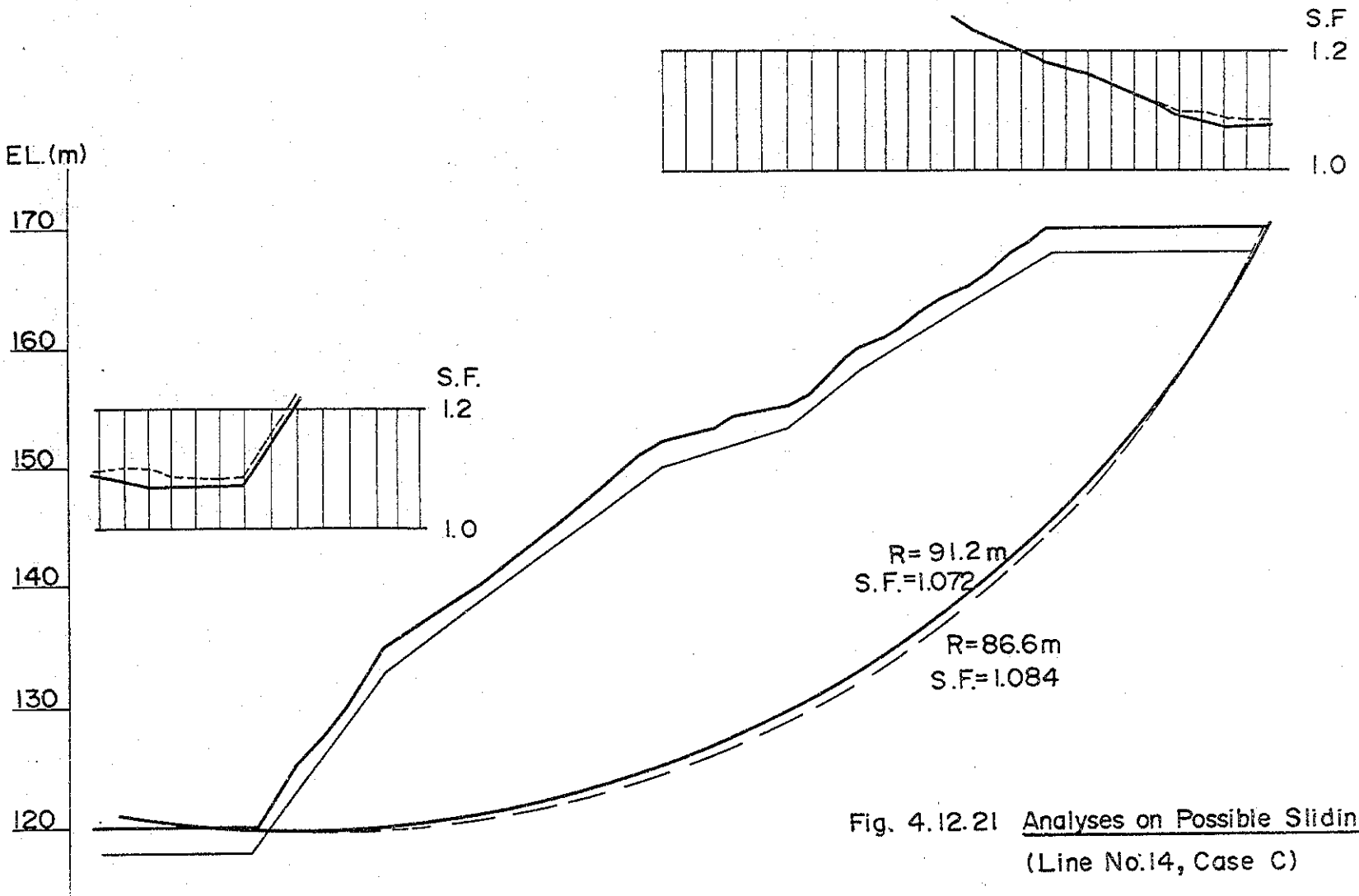

Fig. 4.12.21 Analyses on Possible Sliding Lines
(Line No.14, Case C)

Table 4.14 Comparison Among Cases (A, B and C) of Shearing Resistance Against Sliding Under Condition of $\phi = 20°$

(ton)

Hypothetic Sliding Line	CASE A		CASE B		CASE C	
	SF=1.0	SF.1.2	SF=1.0	SF=1.2	SF=1.0	SF=1.2
No.2	-0.77	50.4	-44.0	13.0	83.05	146.4
No.3	-0.84	49.3	-46.4	11.4	82.7	146.9
No.5	83.69	141.6	25.0	87.9	157.5	227.28
No.7	-18.95	31.8	-79.2	-2.4	75.7	142.6
No.9	17.53	40.3	-4.1	20.9	49.0	76.8
No.12	-403.24	707.9	-2493.6	-1332.0	1431.3	2866.0
No.14	-665.84	-363.3	-1062.8	-777.2	-180.2	185.5

Note: The negative shows the surplus of shearing resistance.

From the data shown in Table 4.14, the following conclusions can be made:

i) The safety factor against sliding for the case with the ϕ value assumed at 20° is smaller than that for the case with the ϕ value set at 10°, irrespective of the Calculation Cases (A, B and C).

ii) The safety factor against sliding for the case with the ϕ value assumed at 10° is greater than 1.2 in all Cases of A, B and C, except the one (1.1) of the hypothetic sliding line No.5 in Case C.

iii) The safety factor against sliding at the elevations higher than EL 180 m for the case with the ϕ value assumed at 20° is in the range of 0.7 to 1.1 in Case A, 0.9 to 1.2 in Case B, and 0.5 to 0.8 in Case C.

iv) Hence, the measure to be taken against possible landsliding should be focussed to a conservative assumption, i.e. the case with the ϕ value set at 20°.

The safety factor after implementation of the measure in Cases A and B should be aimed at 1.2 or greater. Case C is on the assumption that a heavy rainfall would occur simultaneously with an earthquake. Accordingly, it is considered more appropriate that the safety factor in this extremely rare case be set at 1.0 or greater. Under such condition, the probable sliding line No.5 is most critical against sliding. The short shearing resistance of this sliding line is as large as 157.5 tons/m^2 as shown in Table 4.13.

Solutions to be taken as protective measures against possible landsliding are considered as follows:

i) To excavate earth on the shoulder portion of the slope that is prone to landsliding (the portion in which landsliding would start), thereby decreasing a sliding force, and to pile the excavated earth on the portion in which landsliding would end, thereby increasing a shearing resistance against sliding.

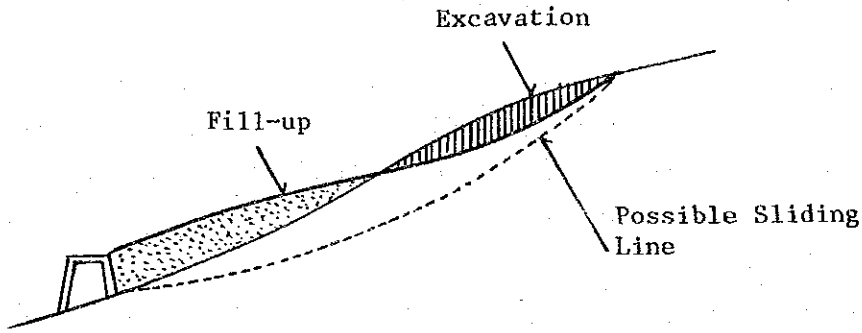

ii) To provide a retaining structure by driving piles into ground, or the like, thereby to increase a shearing resistance against sliding.

iii) To combine the above two measures to make doubly sure of the stabilization effect.

Itemized below are the summary of the results of calculations of the safety factor of the reformed slope for the case with the ϕ value assumed at 20°:

i) In Case B where the seismic force only is taken into account as the design condition, the least safety factor of all probable sliding lines, except No.5, is, in general, higher than 1.2. This implies that the mountain mass would be safe against an earthquake unless it is accompanied with a heavy rainfall.

With regard to the sliding line No.5, too, the slope would be on the safest side in Case B, when comparing on the basis of the target least safety factor of greater than 1.2 for Cases A and B, and greater than 1.0 for Case C.

As the design condition, therefore, Case A or Case C should be considered.

ii) Occurrence of a deep seated landslide with such a magnitude as the maximum depth is greater than 10 m seems unlikely in any Cases of A, B or C. In other words, there would be no such a case that the sliding line passes through the ground with the N value greater than 50. Or, it is very likely that a landslide, if any, would take place at the ground of poorer subsoil closer to the ground surface.

iii) In Case A where the ground is impregnate with water to the ground surface due to rainfall, Nos. 5 and 9 sliding lines should become unsafe with the least safety factor against sliding down to less than 1.0. Most critical against sliding is No.5 line, and it is followed by No.9 line. Nos. 2, 3 and 7 lines should still be safe with the least safety factor against sliding still kept at 1.0 or very close to 1.0. This indicates that no large magnitude landslide would occur even in case where the ground water rises to the surface due to rainfall.

iv) In Case C where an earthquake with Kh of 0.15 g occurs at times when the ground is impregnate with water due to rainfall, all probable sliding lines become unsafe with the least safety factor against sliding coming down to smaller than 1.0. This implies that the slope would become unstable when an earthquake and rainfall occurs simultaneously.

The elevations that are prone to landsliding may not substantially differ from those in Case A, but the least safety factor against sliding is smaller than that in Case A by some 0.3 for Nos. 2, 3 and 7 sliding lines, and by some 0.2 for Nos. 5 and 9 sliding lines.

v) The calculations were made under an extremely unfavorable condition (ϕ=20°) against landsliding, and on the very severe assumptions such as simultaneous occurrence of an earthquake and a rainfall, and the resultant data are, as shown, very harsh. But, these data themselves indicate that it is essential to increase the safety factor of the slope against sliding to maintain stability.

4.5.5. Results of Calculations

(For Elevations Lower Than EL. 180 m)

The probable sliding line Nos. 12 and 14 are for analyses on the possibility of landsliding at the elevations lower than EL.180m.

No.14 sliding line is rather deep in circle, or large in scale, but the least safety factor against sliding would still keep 1.4 in Case A where the ground is impregnate with water to the ground surface due to heavy rainfall, and 1.07 even in Case C where an earthquake occurs simultaneously with a heavy rainfall.

As to No.12 sliding line, the least safety factor against sliding would still keep 1.1 in Case A, but would decrease to 0.8 in Case C. The sliding line with such least safety factor, however, would pass through a ground deep into the mountain mass, where the physical properties would be substantially larger than 15 ton/m^2 (C) and 30° (ϕ), as originally assumed (See Section 4.4.2). The relation of ϕ and C of the mountain mass when the least safety factor of No.12 sliding line should be 1.0 in Case C might be:

When $\phi = 45°$, $C \fallingdotseq 14$ ton/m^2, or
When $\phi = 35°$, $C \fallingdotseq 21$ ton/m^2

Such physical properties at the elevations lower than EL.180 m are the levels that can be reasonably expected from the result of the field survey.

It may therefore be given as a conclusion that there would be no possibility of landsliding in the mountain mass at the elevations lower than EL.180 m.

4.6. Protective Measures Against Possible Landsliding

4.6.1. Slope Reformation

As discussed in the foregoing subsection, the topography of the ex-batcher plant site is not stable against sliding at elevations higher than EL.180 m, if it remains unchanged. The stability analysis was made of the slope reformation measure to excavate earth on the slope at higher elevations, and fill up the slope at lower elevations with the excavated earth, as illustrated in Fig.4.13. In the analysis, the physical properties of the filled-up slope were assumed to be same as those of the surface layer ($C=3.0$ at $\phi=10°$, $C=1.0$ at $\phi=20°$). The analysis was made under the conditions of Case A and Case C only, because the safety factor against sliding in Case B (earthquake loading only taken into account) is higher than that in Case A (ground water only taken into account). The ϕ value was assumed on conservative side of 20°.

Shown below is the summary of the calculation results:

Probable Sliding Line	The Least Safety Factor Against Sliding	
	Case A	Case C
No.2	2.1	1.2
No.3	2.1	1.2
No.5	1.5	1.0
No.7	1.6	1.2
No.9	2.5	1.8

Fig. 4.13 Changes in Longitudinal Profiles by the Slope Stabilization Measure

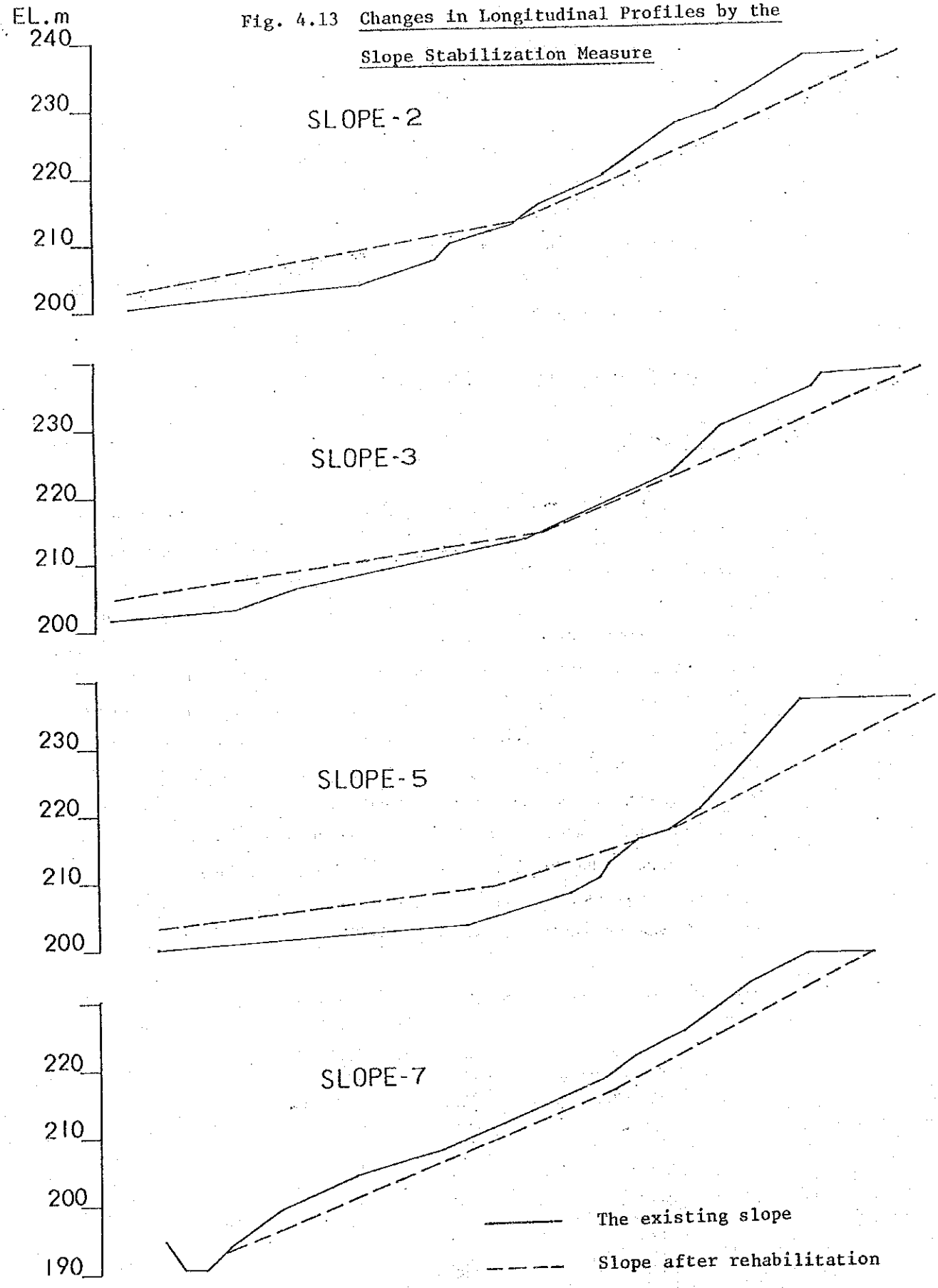

Changes in Longitudinal Profiles by the Slope Stabilization Measure (Fig. 4.13 continued)

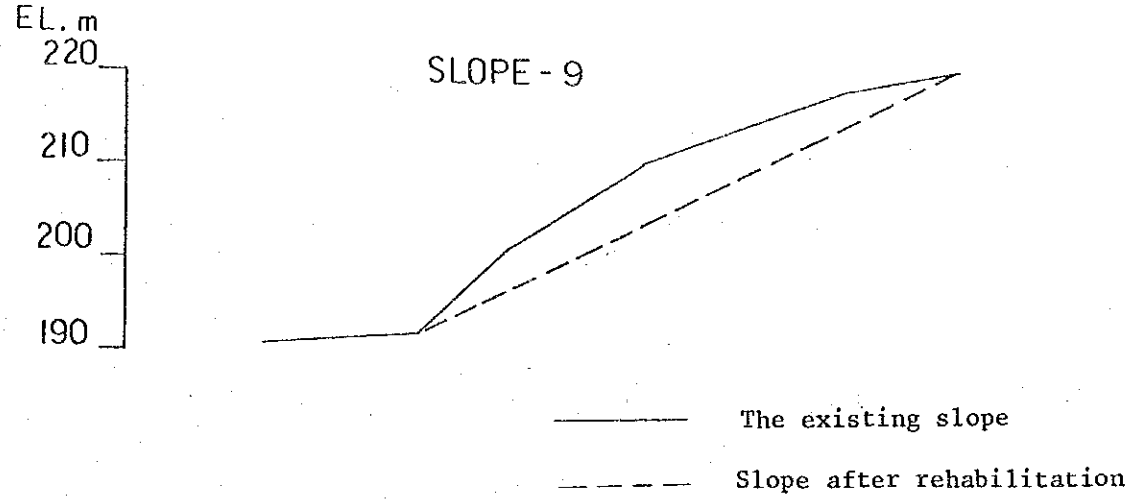

This table indicates that the reformation of the topography as mentioned above will ensure the safety of the slope without causing any large-scale sliding, even in an extreme case where an earthquake with Kh of 0.15 g would occur at times when the ground is impregnate with water up to the surface.

A plan of the protective measure worked out based on the above analysis is as given in Fig. 4.14. In this measure, the slope surface at elevations higher than EL.215 m is to be excavated and the slope surface at elevations lower than EL.215 m is to be filled up with the excavated earth, as illustrated in Figs. 4.15.1. and 4.15.2.

4.6.2. Provision of Drain Holes and Ditches

(1) Ground Water Level after Slope Reformation and Safety Factor against Sliding

Fig. 4.16 shows the relation between the safety factor against sliding and the ground water level for different level cases.

As is seen in the Figure, there may be cases where the safety factor against sliding comes down to a slightly lower than 1.0, when the ground water level is higher than EL.235 m, and under the condition of Case C (the earthquake loading with Kh of 0.15 g at times when the ground is impregnate with water up to the surface).

However, such spot as unstable against sliding is very local and limited only to a portion of the surface layer which may be left unremoved from the excavation work. As discussed in Subsection 4.6.1, the reformed slope is safe

Fig. 4.14 Rehabilitation Plan at the Ex-Batcher Plant Site

Fig. 4. 14

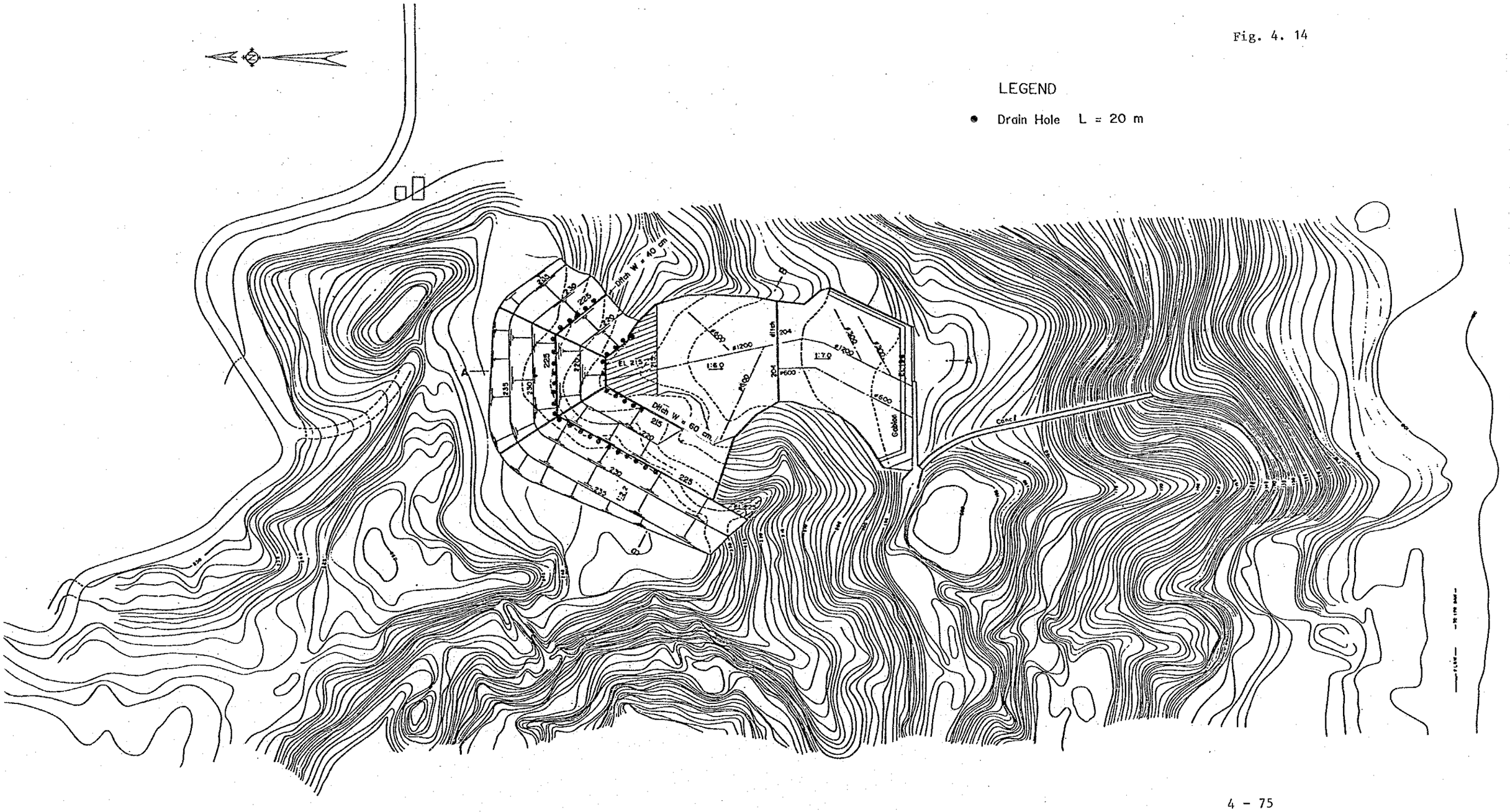

Fig. 4.15.1 Longitudinal Profile after Slope Reformation (Cross Section A-A)

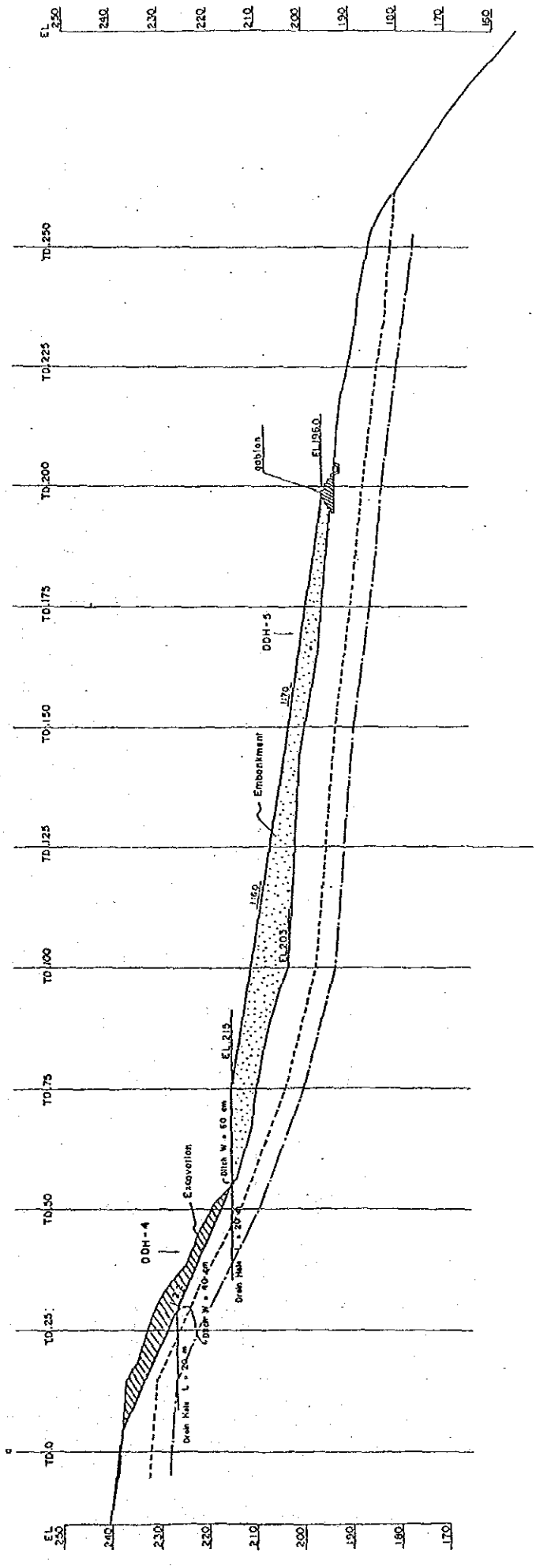

Fig. 4.15.2 Longitudinal Profile after Slope Reformation (Cross Section B-B)

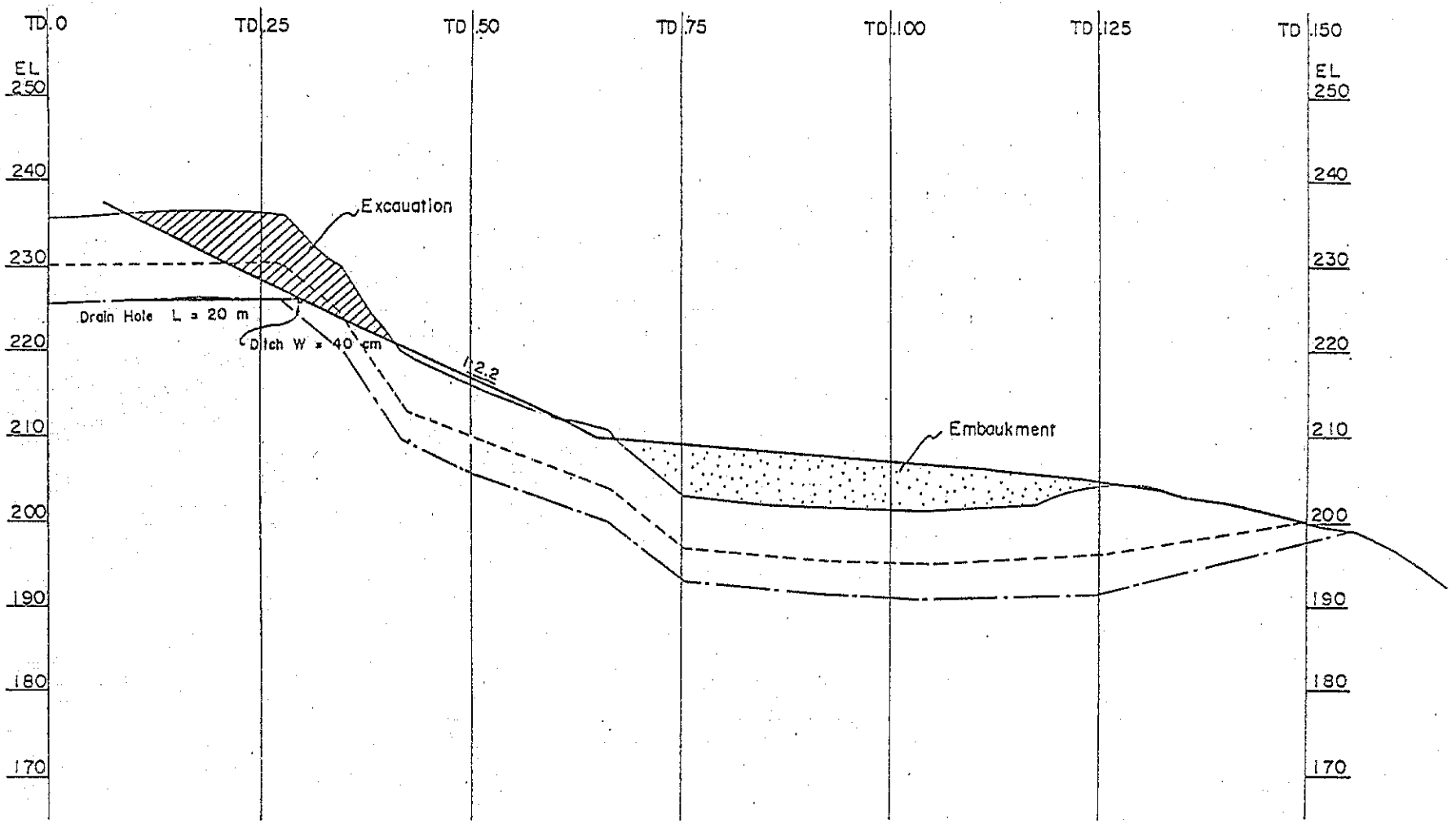

Fig. 4.16 Relation Between Ground Water Level and Safety Factor Against Sliding

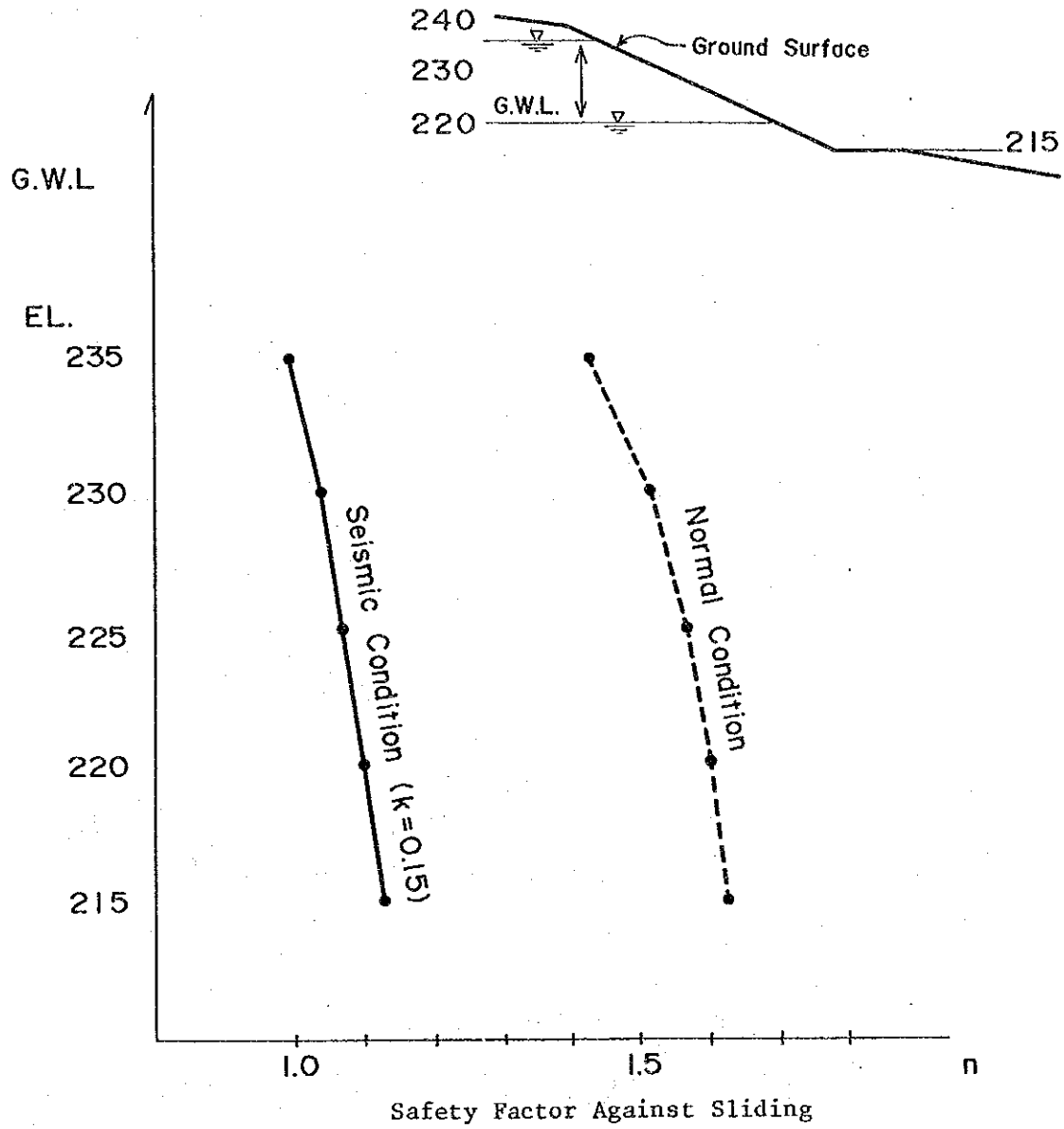

and stable against any large-scale sliding under any loading conditions.

The provision of drain holes in the mountain masses is to reduce the ground water level to lower than EL.235 m, thereby to increase the stability of the reformed slope. The effect of the provision of drain holes was ascertained by the following analysis.

(2) Arrangement of Drain Holes

i. Elevation of Drain Holes

In the Figure shown below, water flow per unit width in the same single direction can be expressed as:

$$q = k \cdot y \cdot \frac{dy}{dx} \quad \cdots\cdots\cdots (1)$$

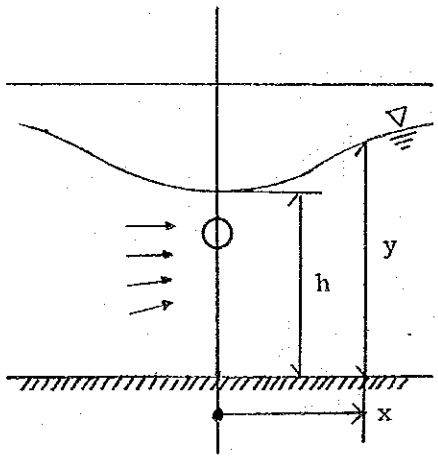

Where,

q = Water flow per unit width in the same single direction.
y = Height of ground water table from the impermeable layer underneath a drain hole.
k = Permeability coefficient of mountain masses.

When Eq.(1) is solved under the condition of y=h at x=0, then y at an arbitrary point x can be expresses as:

$$y^2 = 2\frac{q}{k} \cdot x + h^2 \quad \ldots\ldots\ldots \quad (2)$$

Eq.(2) can be replaced with:

$$q = k\frac{H^2 - h^2}{2R} \quad \ldots\ldots\ldots\ldots \quad (3)$$

Where,

R = A range of the effect of a drain.
H = Height of free ground water surface from the impermeable layer at x=R.

To eliminate q from Eq.(2) and Eq.(3) can create the following equation:

$$y = \sqrt{h^2 + \frac{x}{R}(H^2 - h^2)} \quad \ldots\ldots \quad (4)$$

When the ground water level at a point in between two drain holes, beyond which level no rise of water is required, is indicated in E_M as shown in the Figure, then the elevation of the center of drain holes should be established at the value as obtained by the following equation:

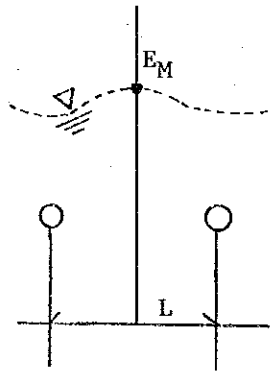

$$E_D \leq E_M - \left[\sqrt{h^2 + \frac{L}{2R}(H^2 - h^2)} - h\right] \quad \ldots\ldots\ldots (5)$$

Where,

E_D = Elevation of the center of drain holes.
L = Distance between drain holes.

Studies were made on the assumption that the impermeable layer would be at EL.180 m which is supposed to have the N value at greater than 50, and the ground water level at x=R would be at EL.230 m which is equivalent to the elevation of the upper plain portion of the existing topography.

The value R was assumed to be 250 m, taking an approximate average of 25-500 m, obtained through test results in the past of boring holes and wells using fine grain sands.

Since H and h are both heights of ground water table from the impermeable layer,

H = 230 - 180 = 50 m
$h = E_D - 180$

Hence, the value E_D can be expressed as:

$$E_D \leq 180 + \sqrt{\frac{m^2 - \frac{L}{2R}H^2}{1 - \frac{L}{2R}}} \quad \ldots\ldots\ldots (6)$$

Where,

$$m = E_M - 180$$

The value E_D with L assumed to be at 5, 10, 20 and 30 m can be given as follows:

In case L = 5 m,

$$E_D \leqq 180 + 1.005 \sqrt{(E_M - 180)^2 - 25}$$

In Case L = 10 m,

$$E_D \leqq 180 + 1.01 \sqrt{(E_M - 180)^2 - 50}$$

In case L = 20 m,

$$E_D \leqq 180 + 1.02 \sqrt{(E_M - 180)^2 - 100}$$

In case L = 30 m,

$$E_D \leqq 180 + 1.03 \sqrt{(E_M - 180)^2 - 150}$$

ii. Arrangement

It is recommended to provide drain holes at intervals of 5 m at the elevations of EL.215 m and 225 m, as shown in Figs. 4.14 and 4.15.

The provision of these drain holes is, as mentioned, to lower the ground water level of the mountain masses, because there is a slight possibility of local

landsliding of a portion of the surface layer left unremoved from the excavation work under the extreme condition (the earthquake loading with Kh of 0.15 g at times when the ground is impregnate with water up to the surface).

The arrangement of drain holes was determined in due consideration of the fact that the ground water level in the ridge by the side of the spillway is higher than that in other mountain masses, as evidenced by the field investigation made for this Study.

5. SEEPAGE THROUGH THE DYKE

5. Seepage through the Dyke

Seepage has been observed at the dyke adjacent to the left bank of the main dam since completion of the Angat Project. To control this seepage, drain tunnels were provided at EL.175 m on both banks downstream of the dyke. The drain tunnel, 1.0 m wide and 1.8 m high, extends for 610 m on the left bank and 290 m on the right bank. These drain tunnels were first used for executing the watertight grouting, and then have been serving as the drainage facilities of seepage water.

The plan and typical cross section of the dyke are shown in Figs.5.1 and 5.2. It has a total crest length of 475 m and the maximum height of 52 m.

According to the record, seepage was first observed at both abutments and the center of the dyke with the maximum height, but soon, no seepage came out from the right bank abutment. At present, seepage is being observed at the left bank abutment and the center of the dyke as shown in Fig.5.3.

There is a record that in 1974 cement grouting from the ground surface was carried out at the left bank of the dyke to stop the seepage. The grout takes were heavier in volume at higher elevations. It is reported, however, that no substantial change in the amount of seepage was noticed after the grouting work.

In September, 1987, JICA study team inspected the drain tunnels to look into the state of seepage. The water level of the reservoir on that occasion was EL.187 m, higher than the elevation of the tunnel of EL.175 m. There was, nonetheless, no substantial seepage in the drain tunnels. From this fact, it can be assumed that, even if seepage were passing through the mountain masses, the ground water level around the tunnel would be lower than EL.187 m.

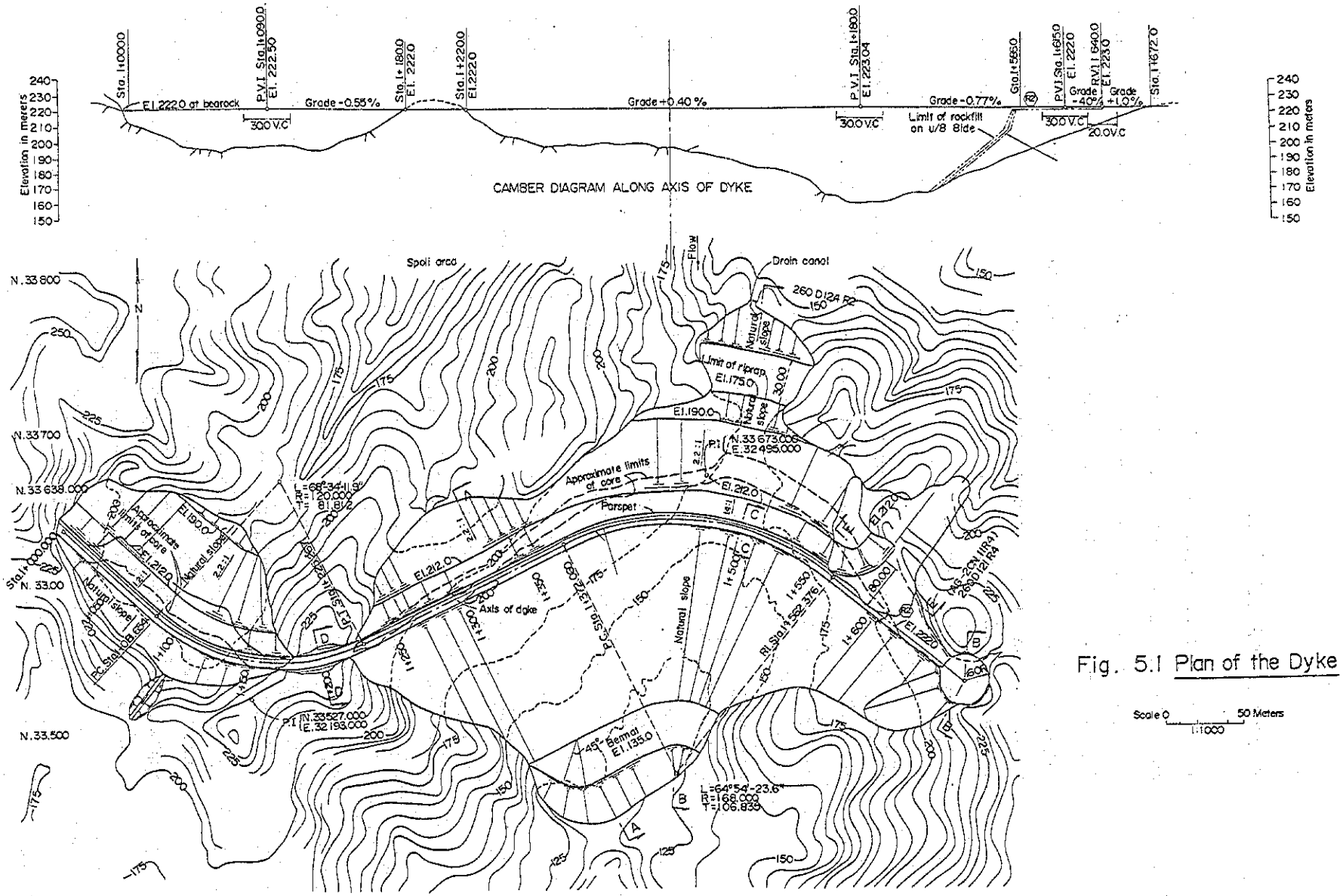
CAMBER DIAGRAM ALONG AXIS OF DYKE
Elevation in meters
Sta. 1+0000
E.I. 222.0 at bearock
P.V.I. Sta.1+0900
El. 222.50
Grade -0.55%
30.0 V.C
Sta.1+1800
El. 222.0
Sta.1+2200
El.2220
Grade +0.40 %
P.V.I. Sta.1+1800
E.I. 223.04
30.0 V.C
Grade -0.77%
Sta.1+5850
P.V.I.Sta.1+6150
El. 2220
Grade -.40% +1.0%
R.V.I. 6400
El. 223.0
30.0 V.C
20.0 V.C
Limit of rockfill on u/s side
Sta.1+6720
Spoil area
Flow
Drain canal
260 D 124 R2
Natural slope
Limit of riprap El.175.0
30.00
El.190.0
N.33800
N.33700
N.33638.000
N.33.00
N.33.500
Sta.1+000.000
P.I N.33 673.000 E.32 495.000
Approximate limits of core
El.212.0
Parapet
Axis of dyke
P.I Sta.1+582.376
L=68°34-11.9"
R=120.000
T=81.814
L=64°54-23.6"
R=168.000
T=106.839
45° Berm at El.135.0
P.I N.33527.000 E.32193.000
Approximate limits of core
El.190.0
El.212.0
Natural slope
2.2:1
2.5:1
3:1
Sta.1+100
Sta.1+150
Sta.1+350
Sta.1+500
Sta.1+550
Sta.1+600
El.220
El.232.0
A
B
C
D
Fig. 5.1 Plan of the Dyke
Scale 0 50 Meters
1:1000

Fig. 5.2 Typical Cross Section of the Dyke

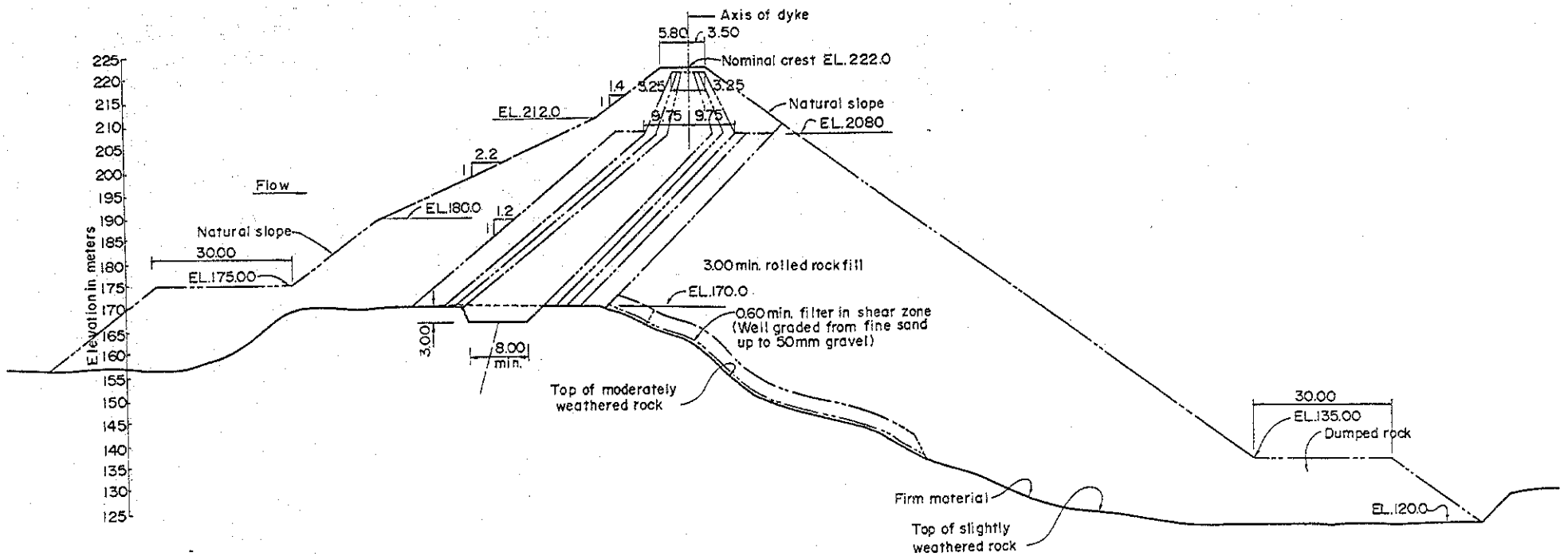

Fig. 5.3 Location of Measurement Weir
SW - 1, SW - 2, SW - 3

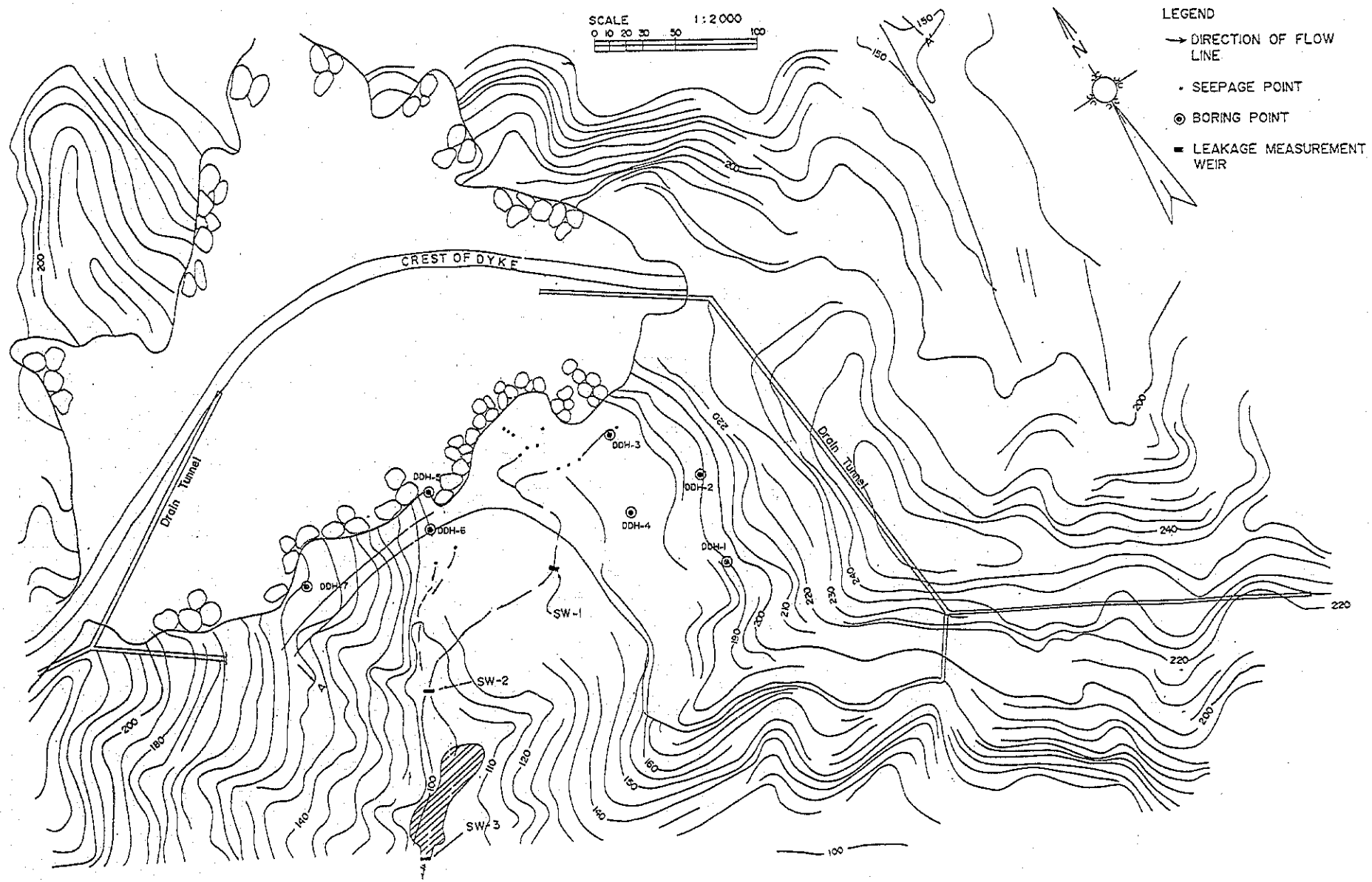

From the result of analysis on the amount of seepage through the dyke that was measured throughout 1987, it is believed that water impregnation from the reservoir into the mountain masses would be predominantly when the reservoir water level is at elevations higher than EL.190 - 195 m as described in the subsequent subsections. No substantial seepage in the drain tunnel observed during the field inspection by JICA study team was, therefore, attributable to the fact that the reservoir water level then stood at EL.187 m.

On the other hand, the fact that cement grouting from the ground surface was not remarkably effective in reducing the amount of seepage may indicate that it would originate not only from the reservoir, but also from other sources such as rainfall. If so, grouting into the mountain masses to whatever extent may not produce any substantial effect on the reduction of seepage.

From the above standpoints, the result of seepage measurement conducted so far at three measurement weirs installed downstream of the dyke was analyzed to study the seepage problem.

5.1. Result of Seepage Measurement

Since January, 1987, the seepage measurement has been continued at the three measurement weirs (SW-1, SW-2 and SW-3) installed downstream of the dyke. The location of each weir is shown in Fig.5.3. SW-1, installed at EL.138 m, is to measure seepage through the left bank side of the dyke. SW-2, installed at EL.114 m, is to measure seepage through the center of the dyke with the maximum height. SW-3 is installed approximately 80 m downstream of SW-2 at EL. 110 m.

Tables A5.1.1 through A5.1.22 as attached to the Appendix comprise the data on seepage measurements conducted during the period of January, 1987 through October, 1988. Also shown in these tables are the data on daily rainfalls at the Angat dam site during the same period.

The measurement data collected from the three weirs were processed to obtain the net amount of seepage through the dyke in the following manner:

1) To apply the Numachi-Kurokawa-Fuchizawa formula to the SW-1 data.

2) To apply the Govinda Rao formula to the SW-2 data.

3) To apply the Numachi-Kurokawa-Fuchizawa formula to the SW-3 data with h > 7 cm, and to apply a coefficient of discharge (C) based on the actual measurement data to the SW-3 data with h<7 cm.

The Numachi-Kurokawa-Fuchizawa formula is for a right-angled triangular weir and the discharge passing through the triangular weir (Q) is expressed as follows:

$$Q = Ch^{5/2} \ (m^3/sec.)$$

$$C = 1.354 + \frac{0.004}{h} + (0.14 + \frac{0.2}{\sqrt{D}})(\frac{h}{B} - 0.09)^2$$

where,

h is an overflow depth at the weir (m)
B is a width of the weir (m)
D is a depth from the lowest point of V-notch opening to the bottom of the weir (m)

The Govinda Rao formula is for a rectangular weir, and the discharge through the weir is expressed as follows:

$$Q = C_1 Bh^{3/2} \ (m^3/sec.)$$

$$C_1 = 1.552 + 0.083\,(h/L), \ 0.1 \leqq h/L \leqq 4$$
$$= 1.642\,(h/L)^{0.022}, \ 0 < h/L \leqq 0.1$$